REPORT DOCUMENTATION PAGE

Form Approved
OMB No. 0704-0188

1. REPORT DATE *(DD-MM-YYYY)*	2. REPORT TYPE	3. DATES COVERED *(From - To)*
September 30, 2006	Quarterly Report	1 Jan. to 31 July 2006

4. TITLE AND SUBTITLE
Advanced Wireless Integrated Navy Network (AWINN)

5a. CONTRACT NUMBER
N00014-05-1-0179

5b. GRANT NUMBER
N00014-05-1-0179

5c. PROGRAM ELEMENT NUMBER

6. AUTHOR(S)
Warren Stutzman and Rick Habayeb

5d. PROJECT NUMBER

5e. TASK NUMBER

5f. WORK UNIT NUMBER

7. PERFORMING ORGANIZATION NAME(S) AND ADDRESS(ES)
Virginia Polytechnic Institute and State University
Electrical and Computer Engineering Department
302 Whittemore Hall (0111)
Blacksburg, VA 24061

8. PERFORMING ORGANIZATION REPORT NUMBER
6

9. SPONSORING/MONITORING AGENCY NAME(S) AND ADDRESS(ES)
Office of Naval Research
ONR 313
875 N. Randolph St.
Arlington, VA 22203-1995

10. SPONSOR/MONITOR'S ACRONYM(S)

11. SPONSOR/MONITOR'S REPORT NUMBER(S)

12. DISTRIBUTION/AVAILABILITY STATEMENT
Approved for public release; distribution unlimited.

13. SUPPLEMENTARY NOTES
The views, opinions and/or findings contained in this report are those of the author(s) and should not be constructed as an official Department of the Navy position, policy or decision, unless so designated by other documentation.

14. ABSTRACT
Final progress report on AWINN hardware and software configurations of smart, wideband, multi-function antennas, secure configurable platform, close-in command and control for Sea Basing visualization of wireless technologies, Ad Hoc networks, network protocols, real-time resource allocation, Ultra Wideband (UWB) communications network and ranging sensors, cross layer optimization and network interoperability.

15. SUBJECT TERMS

16. SECURITY CLASSIFICATION OF:			17. LIMITATION OF ABSTRACT	18. NUMBER OF PAGES	19a. NAME OF RESPONSIBLE PERSON
a. REPORT	b. ABSTRACT	c. THIS PAGE			Rick Habayeb
U	U	U	UL		19b. TELEPHONE NUMBER *(Include area code)* 540-231-4353

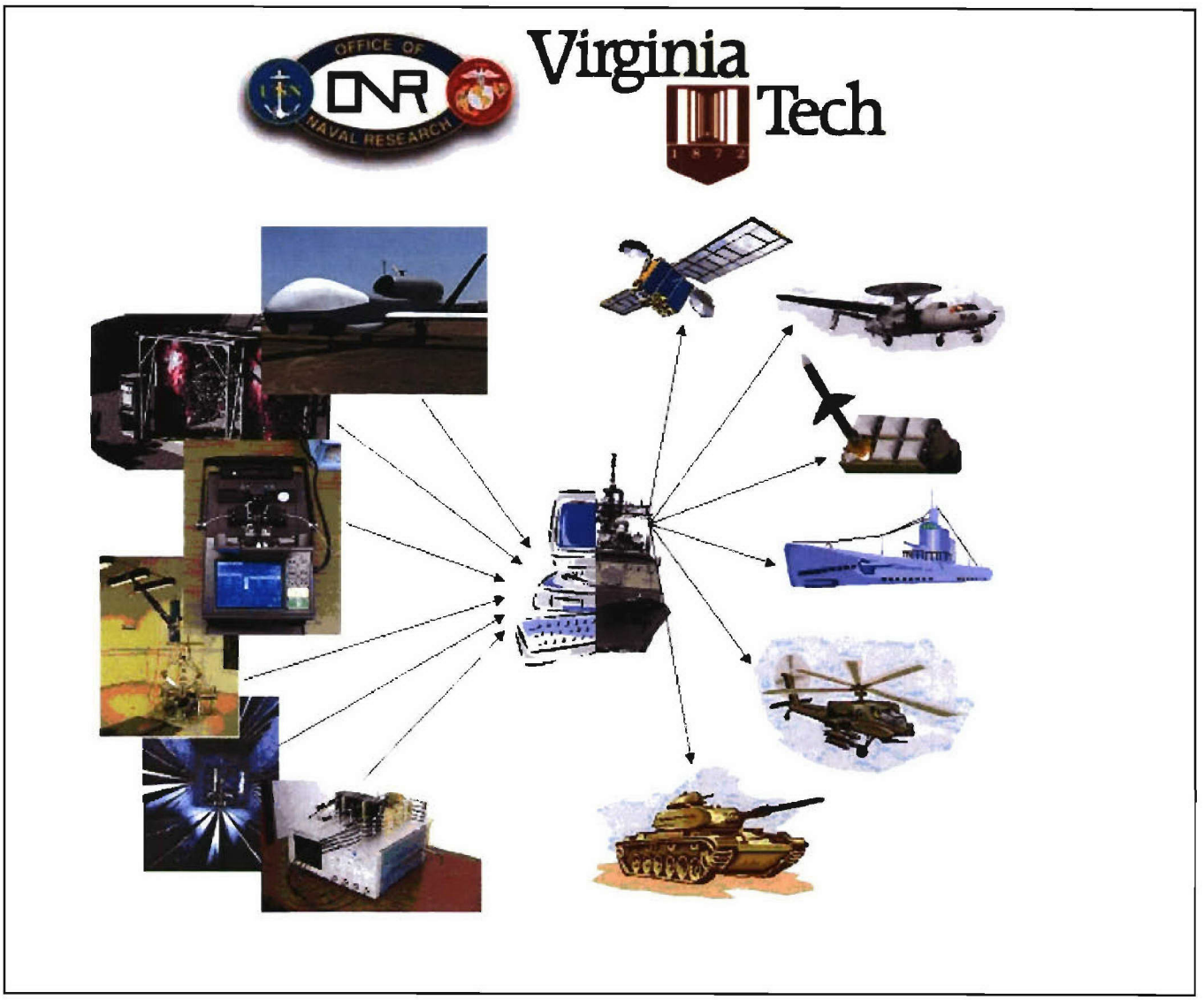

Advanced Wireless Integrated Navy Network – AWINN

Final Report

Virginia Tech

January 1,2005 – July 31, 2006

TABLE OF CONTENTS

Executive Summary

The AWINN project had its beginnings with the NAVCIITI (NAVy Collaborative Integrated Information Technology Initiative) project. The combined NAVCIITI/AWINN effort, which spanned eight years from 1998 to 2006, passed through several phases. In beginning several technologies were examined were explored, followed by a focusing of direction and coordination of technologies toward a common goal. Finally the technologies were refined and integrated. This final report provides cumulative summaries of the activities and productivity of the AWINN team at Virginia Tech. The highlights of our progress in compact form follow. Also see:

awinn.ece.vt.edu

1. Advanced Wireless Technology

1.1 Advanced Antennas

- Designed, constructed, and tested (in frequency and time domains) the following new antennas:
  - Top-loaded and folded-notch ultra-wideband (UWB) antennas for dual band operation with band reject characteristics to avoid interference in an internal band
  - Wearable antennas made of copper wire woven into fabric to cover the 3.1 to 10.6 GHz UWB band.
  - A UWB tape helix antenna for moderate gain, omnidirectional handheld and mobile terminals
- Designed, constructed, and tested (in frequency and time domains) the following antennas in support of integrated demonstrations:
  - UWB sensing antennas
  - Balance dipoles for mobile robot demo
  - Directive UWB antennas for the container crane (Sea Basing) demo
- Theoretical and experimental investigation of the fundamental limits on the size of omni-directional and directive antennas
- Characterized wideband antennas in the time and frequency domains with a simple and general model using only a few poles and zeros.
- Developed wideband baluns for wideband arrays
- Created propagation models for indoor scattering in support of UWB sensing and communications supplemented with testing that represents ship interiors.

1.2 Advanced Software Radio

- Developed a software radio platform that includes:
  - Cross-layer optimization
  - Ad hoc networking
  - Communications capability, including UWB
  - Data capture mode
- Constructed a UWB transceiver testbed and accomplished the following with it:
  - Achieved an effective 8-GHz sampling rate using four 2-GHz ADCs
  - Monitored human breathing rate
  - Estimated range distance accurately
- Demonstrated and evaluated distributed MIMO techniques – See TIP #1
- Integrated with crane demonstration hardware to support cargo position location – See TIP #2

1.3 Collaborative and Secure Wireless Communications

- Developed a collaborative communications scheme called ensemble synchronization that allows many nodes, including mobile nodes in a battlefield, to communicate with a base

station using low power. The low power level at each node leads to long battery life and low probability of signal interception.

- Examined three modulation schemes for ensemble synchronization.
- Demonstrated ensemble synchronization with hardware and software in test beds with both wired and wireless communications and synchronization.

2. Secure and Robust Networks

2.1 Ad Hoc Networks and 2.3 Network Interoperability and Quality of Service

- Investigated various protocols for QoS, security, mobile routing, and cross-layer optimization
- Integrated routing and MAC protocols for ad hoc networks to support multiple channel operation and implemented support for both IPv4 and IPv6 with IPsec
- Designed and implemented a topology control mechanism to dynamically adjust node transmission power levels to decrease interference and increase effective network capacity

2.2 Real-Time Resource Management

- Developed real-time scheduling algorithms for distributable threads in ad hoc networks
- Contributed to Sun Microsystems' Distributed Real-Time Specification for Java (DRTSJ) that is likely to transition into Sun's Java Specification Request 50 through Mitre Corp.
- Created a comprehensive demonstration using a Coastal Air Defense example that has been shown to several Navy and industrial units.

2.4 Cross-Layer Optimization

- The effort of the Cross-Layer Optimization group is focused on cross-layer design of UWB for position location networks PoLoNet and collaborative radio networks.

3. Visualization of Wireless Technology and Ad Hoc Networks

- The Visualization of Wireless Technology team is completed an investigation of UWB contact-less sensors for close-in operations

4. Technology Integration Projects (TIPs)

TIP#1 Distributed MIMO UWB Sensor Networks Incorporating Software Radio

- Showed that distributed MIMO provides higher capacity than SISO based communication
- Showed that cooperative communication based on distributed OSTBC performs better than SISO and can provide a doubling of range
- Calculations showed that air-to-ground coordinated UAVs with cooperative beamforming can extend over-the-horizon range 35 times.

TIP#2 Close-in UWB Wireless Applcation to Sea Basing

- Constructed and tested a pulsed UWB position location system for all weather, day-night, non-line-of-sight sensing
- Integrated the position location system with a $1/24^{th}$-scale model crane to simulate sea basing operations (see TIP #4).

TIP#3 Secure Ad Hoc Networks

- Demonstrated secure ad hoc networks in three tracks using the common hardware/software test bed network (see Task 2.1):
  - Core network services
  - Cross-layer approach to multiple description video routing
  - Real-time middleware in an ad hoc network.

TIP#4 Integration of Close-in UWB Wireless with a Crane Model for Sea Basing

- Performed demonstrations and experiments with the $1/24^{th}$-scale crane simulation system employing a nonlinear control system and UWB range sensing subsystem.

- The hardware has 1-mm resolution and 16 updates per second.
- In the first experiment, the cargo crate was lowered onto a stationary floor using antennas on only one side of the crate. The maximum position error was 2 mm and the mechanical positioning distance was 0.25 m, which scales to over 6 m.
- In a second experiment, the crate with two ranging antennas on each corner was lowered onto an oscillating platform simulating a ship deck in rough seas. Accuracy results were similar to the first experiment.

Advanced Wireless Integrated Navy Network (AWINN)

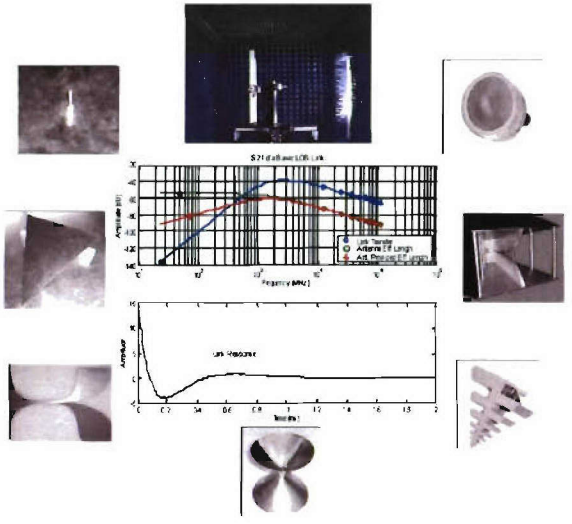

Technical Significance

- **To support the design and implementation of a flexible, reconfigurable wireless network with multiple frequency requirements, including the capabilities of ultra-wideband (UWB) radio technology and indoor/topside propagation**
- **The modeling and design techniques will improve the time to production of antennas to meet the Navy mission for a multitude of needs**

Major Performers

Virginia Polytechnic Inst. and St. U.,
Dr. William Davis
Dr. Warren Stutzman

TASK 1 Advanced Wireless Technologies

New antenna technologies applicable to Navy missions & hardware for AWINN integration projects.

Task 1.1 Advanced Antennas

- Investigation of compact antennas for handheld and mobile terminals
- Antenna Characterization – transient & wideband to provide improved prediction and design for system design
- UWB antenna design (support of AWINN demonstrations)
- Antenna and Propagation modeling for wideband and MIMO applications
- Wideband balanced antenna/array feed networks

Impact

New techniques for design of antennas and propagation channels to more effectively use the mission environment, particularly for applications requiring small antennas for frequency flexibility. The techniques also offer the potential of simplifying the topside design of the electromagnetic environment.

AWINN Task #1.2
Advanced Software Radio

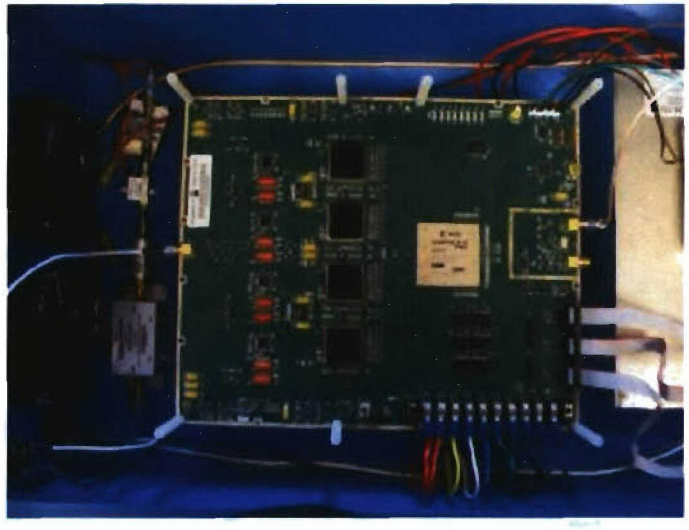

Task Objectives

- Develop an Advanced Software Defined Radio optimized for Impulse UWB signals.
- Evaluate range extension via collaborative networks using UWB signals.
- Demonstrate the ability of UWB signals to provide precision position location and precision ranging.
- Apply Markov Models to more accurately model real-world wireless channels.

Task Description

- Develop an Advanced Software Radio capable of supporting cross-layer optimization, ad-hoc networking, ranging/imaging and collaborative systems.
- Investigate novel algorithms for Ultra Wideband communications, with emphasis on ad-hoc networks, distributed MIMO, and ranging/position location.
- Integrate the use of the Software Radio and algorithms into Sea Basing.

Experiments and Demonstrations

- Demonstrate UWB communication in a laboratory environment using Advanced SDR Receiver.
- Demonstrate 3-D crane cargo container ranging using laboratory equipment.
- Demonstrate precision ranging using Advanced SDR Receiver.

Team

Dr. Jeffrey H. Reed, Task Leader

Dr. R. Michael Buehrer

Dr. William H. Tranter

Advanced Wireless Integrated Navy Network (AWINN)

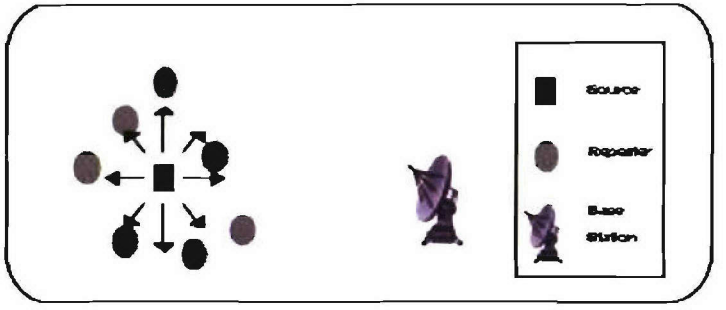

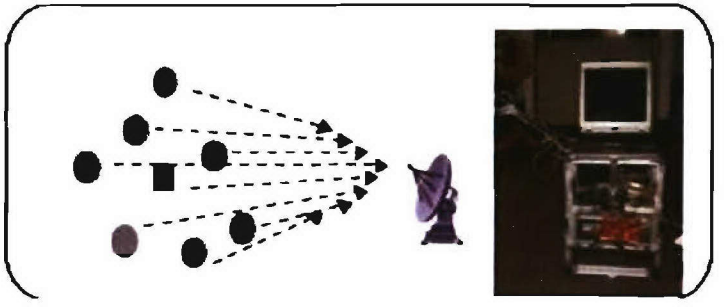

Task 1.3 Collaborative and Secure Wireless Communications

- A cluster of mobile, independent, interchangeable nodes collaborates to send a message to a distant base station
  - No single node is powerful enough to reach base station
  - Nearby nodes reinforce the signal
  - Nodes are very loosely synchronized
- The method offers reliability, fault tolerance, power efficiency, fairness, and simple, low-cost nodes.

Approach

- Create two or more multi-mode radio prototypes that can be deployed in a meaningful way on the campus to demonstrate the communications modes.
- In cooperation with Task 2.1, perform a simulation that illustrates the network being transformed into an ad hoc network using a node model.
- Demonstrate a multi-node system comprised of commodity robotic devices to emulate behavior of a loosely coupled mobile sensor network

Task 1.3 Benefits

- Extended Range and/or Battery Life
- Computationally Simple
- Emergency Early Response
- Homogenous Network
- Fault Tolerant Remote Sensing
- Economy of Scale

Principal Investigator:. *P. Athanas*

AWINN Task 2.1/2.3: Secure and Robust Networks
(Ad hoc networks / Network Interoperability and Quality of Service)

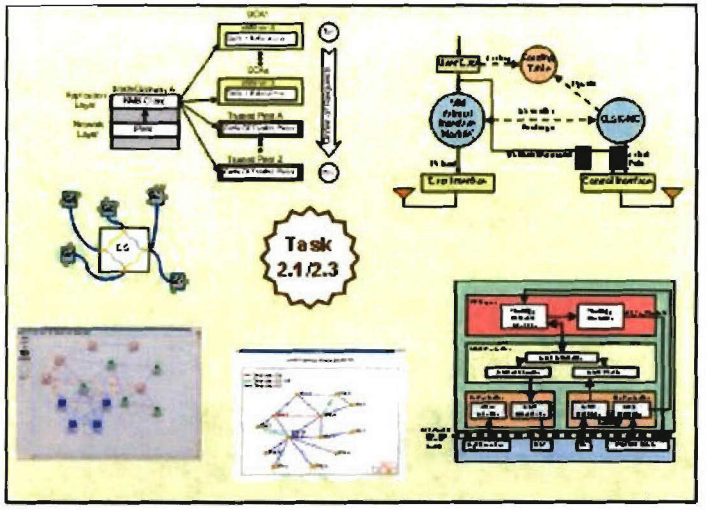

Objectives

- To investigate core network capabilities for quality of service (QoS), security, and routing in ad hoc networks
- To integrate network services with real-time middleware (as investigated in Task 2.2)

Team

Dr. S. F. Midkiff, Leader
Dr. L. A. DaSilva
Dr. Y. T. Hou
Dr. G. Hadjichristofi
Dr. U. Lee
W. M. de Sousa

Description

- Decentralized key management
  - Increase service availability
  - Integrate with existing IPsec implementation
- Multi-channel routing
  - Increase network capacity
- Topology control mechanism
  - Decrease interference and increase network capacity
- Network Management
  - Provide topology views via NRL OLSR extensions and SNMP
- Mobile ad hoc network emulation (via Dynamic Switch)
  - Repeatable ad hoc network testing environment
- MD Video
  - Increase resilience of MD video

Experiments and Demonstrations

- TopoView and OLSR-TV for topology and status monitoring
- Improved security associations and a distributed key management scheme using IPv4 and IPv6
- Multichannel MANET routing
- Multi-path route optimization for multiple description video
- Topology control for reducing radio interference

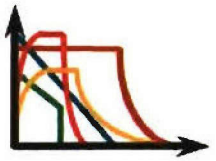

AWINN Task 2.2

Real-Time Resource Management, Communication, and Middleware

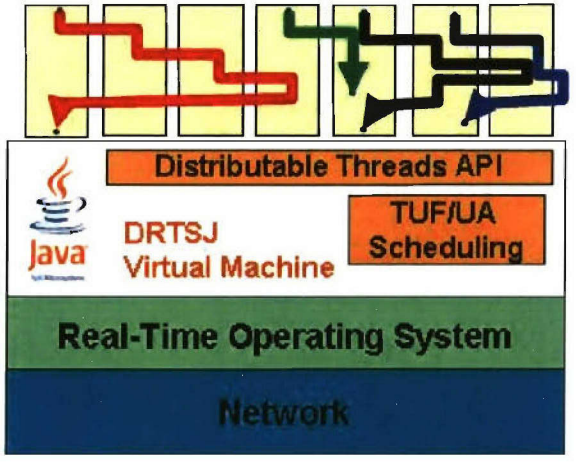

Task Objectives

- Develop TUF/UA Algorithms for RT-CORBA's distributable threads
- Develop TUF/UA non-blocking synchronization algorithms for distributable threads
- Develop Distributed Real-Time Specification for Java (DRTSJ) under Sun's JCP

Team

Dr. Binoy Ravindran — Hyeonjoong Cho

Umut Balli — Haisang Wu

Ed Curley — Jonathan Anderson

Collaboration on DRTSJ with the MITRE Corporation

Description and Motivation

Develop TUF/UA scheduling and synchronization algorithms and provide implementations of new real-time programming facilities appropriate to support construction of dynamic, distributed real-time systems as envisioned by the US Navy DD(X) program. This work will be done in the context of the Real-Time Specification for Java (RTSJ), the target platform for DD(X), and its extension, the Distributed Real-Time Specification for Java (DRTSJ).

Primary Accomplishments

- Distributed scheduling algorithms for distributable threads in the presence of application- and MANET-induced run-time uncertainties;
- Bounded-time distributable thread integrity protocols for dynamic networks and MANETs;
- TUF/UA real-time scheduling and synchronization algorithms for single and multiprocessors; and
- Early Draft Release of the DRTSJ standard
- Coastal Air Defense demonstration application

AWINN Task 2.4a

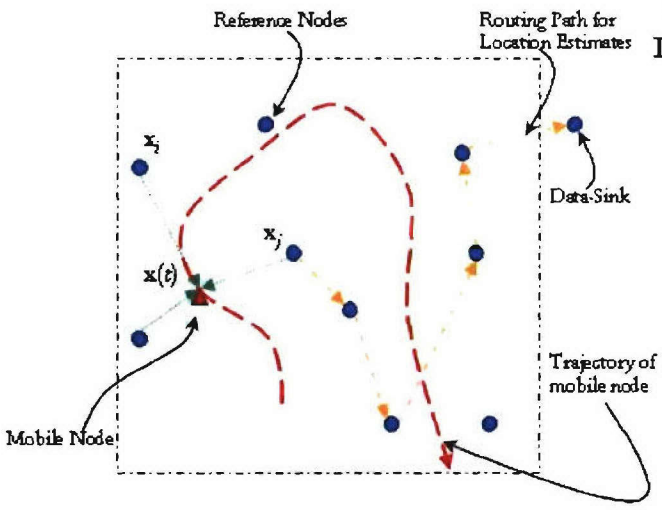

Cross-Layer Optimization
Position Location Networks

Team: Technical Lead: Dr. R. Michael Buehrer
GRA: Swaroop Venkatesh

Task Objectives

- Investigate the interaction between localization accuracy (application layer) and network design parameters (PHY, MAC and network layers) for UWB position location networks.
  - Investigate the relation between physical layer network parameters and the design of MAC protocols.
  - Investigate the impact of MAC protocol design on localization accuracy.
  - Investigate the efficacy of power control algorithms on localization accuracy.
- Investigate the NLOS problem in indoor position location networks.

Description and Motivation

Investigation of the interaction between different layers in UWB position-location network design. For emergency tracking applications, localization accuracies of below 1 m^2 are desired. Cross-layer interactions can be exploited to improve localization accuracy, e.g., using power-control, or increasing the throughput of the MAC protocol. Further, the NLOS nature of propagation in indoor environments represents a serious challenge in attaining the desired localization accuracy.

Primary Accomplishments

- Investigated the relation between MAC protocol performance and localization accuracy; showed that increasing throughput results in better localization accuracies.
- Proposed a spread-spectrum MAC scheme for UWB position location networks; showed that the scheme outperforms the CSMA protocol in terms of localization accuracy at any time.
- Investigated the use of power-control algorithms to improve localization accuracy in indoor position-location networks; Showed that power control which is driven by application layer is superior to power control driven by PHY
- Characterized the NLOS problem in indoor UWB position location networks; proposed a novel linear-programming technique for NLOS mitigation in indoor position-location networks.

AWINN Task 2.4b

Cross-Layer Optimization,
UWB-based Ad Hoc Networks

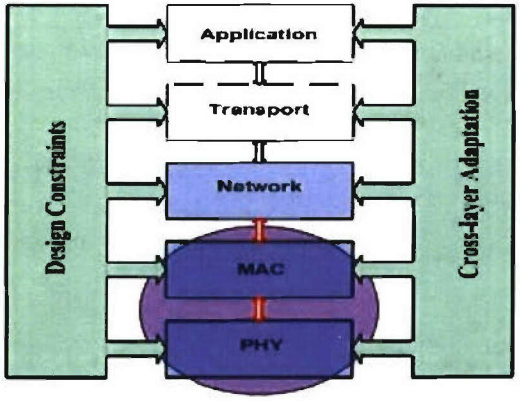

Task Objectives

- Optimize UWB PHY, MAC and NET in an ad-hoc wireless network to maximize total flow rates
- Employ sequence optimization techniques and an adaptive exclusion region with MMSE receivers to mitigate multi-access interference
- Develop a distributed UWB MAC protocol to realize the core cross-layer concepts

Team

Dr. R.M. Buehrer, Technical Lead
Qiao Chen, Graduate Assistant
JeongHeon Lee, Graduate Assistant

Description and Motivation

UWB technology has unique physical layer characteristics of which the higher layer protocols can take advantage. We take a cross-layer approach to optimize a UWB network through the interaction between physical, MAC and network protocols. Specifically, we examine network performance when combining sequence optimization techniques and MMSE receivers at the PHY, MAC design using an adaptive exclusion region along with direct and multihop routing.

Primary Accomplishments

- Analytical expressions and simulation results for sequence optimization techniques for both centralized and ad-hoc UWB networks
- Demonstrated that with proper PHY optimization a nearly pure CDMA MAC approach is viable which substantially reduces the required MAC coordination.
- Showed that waveform and MAC optimization mitigated the need for minimum energy routing (in favor of longer hops) in order to control interference and thus increase network flow.

AWINN Task 3 - Visualization of Wireless Technology and Network

Day Time Communication

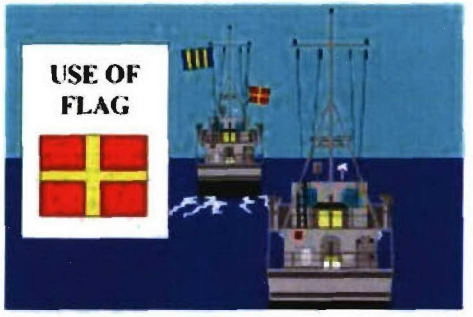

Technical Significance

To design and develop C3 using UWB sensors and Ad Hoc mesh networks
*Perform close-in ranging of cargo, ranging of ships during maneuver, and netting distributed sensors of a cluster of ships
•The close-in C3 will rely on the AWINN enabling technologies

Major Performers

Virginia Polytechnic Inst. and St. U.,
Dr. Rick Habayeb
Dr. Ali Nayfeh

Accomplishments and Approach

* Design and develop close-in C3
* Design and develop UWB cargo ranging sensors for soft pickup and landing of containers
*Design and develop UWB ship ranging Sensors and network
* Leverage and integrate AWINN wireless technologies and sensor networks to support the close-in Sea Basing missions

Impact

* Sea Basing missions require close-in C3 to transfer cargo and provide communication links. The AWINN provides the enabling technologies for the close-in sea basing missions.

AWINN TIP #4.1
Distributed MIMO Using UWB

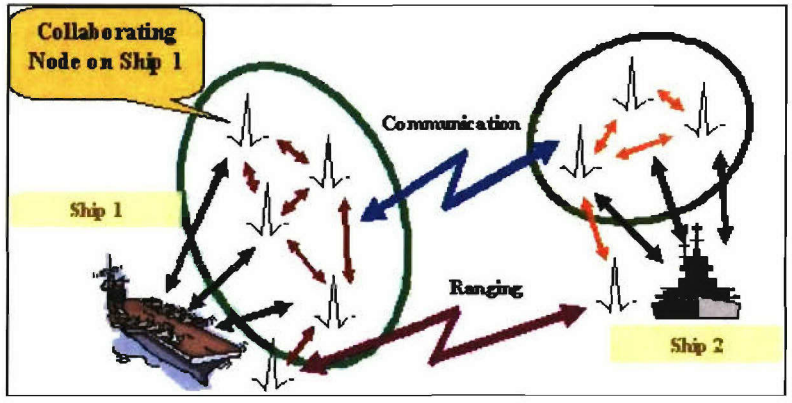

Task Description

- Develop an Advanced Software Radio capable of supporting cross-layer optimization, ad-hoc networking, ranging/imaging and collaborative systems.
- Investigate novel algorithms for Ultra Wideband communications, with emphasis on ad-hoc networks, distributed MIMO, and ranging/position location.

Task Objectives

- Develop an Advanced Software Defined Radio optimized for Impulse UWB signals.
- Demonstrate range extension via collaborative networks using UWB signals.
- Demonstrate the ability of UWB signals to provide precision position location and precision ranging.
- Apply Hidden Markov Models to more accurately model **real-world wireless channels.**

Experiments and Demonstrations

- Demonstrate UWB communication in a laboratory environment using Advanced SDR Receiver.
- Demonstrate 3-D crane cargo container ranging using laboratory equipment.
- Demonstrate precision ranging using Advanced SDR Receiver.

Team

Dr. Jeffrey H. Reed, Task Leader
Dr. William H. Tranter

AWINN TIP #4.2
Close-In UWB Applied to Sea Basing

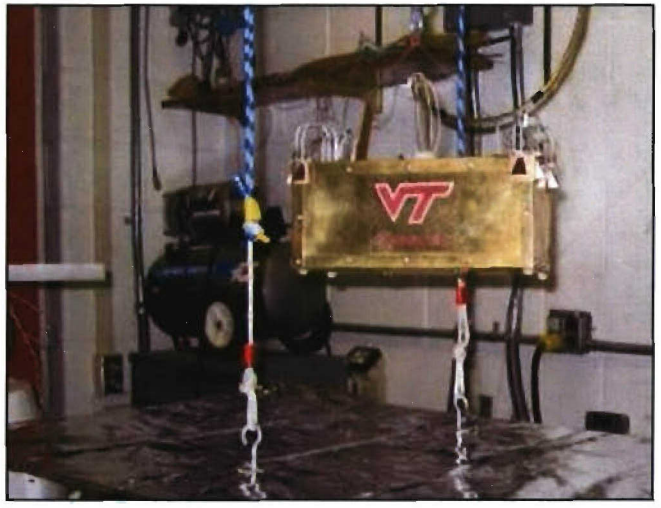

Task Objectives

- Develop a UWB precision ranging algorithm.
- Demonstrate the feasibility of the precision ranging algorithms by applying them to a scale model of the cargo container.
- Integrate the precision ranging system with the cargo container soft landing routine.

Task Description

- Develop algorithms that allow UWB signals to provide precision ranging and position location.
- Integrate these algorithms into the Advanced SDR Receiver.

Experiments and Demonstrations

- Demonstrate that D-MIMO provides higher capacity than SISO communication systems.
- Simulate the performance of Air-to-Ground D-MIMO communications and evaluate their performance relative to SISO systems.

Team

Dr. R. Michael Buehrer

Dr. Ali Nayfeh

1. TASK 1 Advanced Wireless Technologies

1.1 Task 1.1 Advanced Antennas

1.1.1 Overview

Task Goal: This task investigates new antenna technologies that are applicable to Navy missions and provides hardware for AWINN integration projects.

Organization: This task is managed by Director of Virginia Tech Antenna Group (VTAG) using the following personnel:

Bill Davis, Director
Warren Stutzman, Faculty
Randall Nealy, Engineer
Scott Bates, GRA
Gaurav Joshi, GRA
John Kim, GRA
Terry Vogler, GRA
Taeyoung Yang, GRA

Summary: During the term of this project, several aspects of antennas and propagation for potential use by the Navy were addressed, including:

1. Evaluation of antenna designs for bandwidth, size, and radiation performance. Major emphasis was placed on the relationship between fundamental limits of antennas and the ability to address specific design specifications.
2. UWB (ultra-wideband) designs both for small size antennas, omni-directional coverage and for directional requirements. The principles apply to a variety of needs, but the emphasis was on a basic understanding of the radiation mechanisms and near-field effects.
3. Review and development of wideband baluns (typically 2:1 desired) for use with the Four-Square array and other antenna systems.
4. Antenna design and construction to support the integrated demonstrations, including UWB sensing antennas, balanced dipoles for the robotics demo, and antenna designs for use in the sea-basing demo. The latter included designs for use on containers as well as for receiving reflections from support cables to provide feedback control of the container crane systems.
5. Propagation characterization of indoor channels in a UWB measurement environment. The emphasis was on scatterer contamination of the propagation environment. The results lead to models of the scattering mechanisms as well as to an investigation of UWB MIMO (multiple-input, multiple-output) concepts.

1.1.2 Task Activities for the Period

Subtask 1.1a: Investigation of compact antennas for handheld and mobile terminals

Task objective: Design compact planar UWB antennas for various applications and systems.

Accomplishments during the reporting period: Several new antenna designs were developed that have a potential for handheld and mobile applications. A new top-loaded ultra-wideband antenna covering both the 2.4 – 10.6 GHz band (VSWR < 2.5) and the 2.05 – 11.6 GHz UWB band with

nearly constant radiated power was designed and fabricated. The proposed antenna is a good candidate for backward compatibility of 802.11g in the 2.4 GHz ISM band, as well as providing an indoor/outdoor, ultra-wideband frequency range of 3.1 – 10.6 GHz. In addition, it can be used for both multi-band OFDM and impulse-UWB applications.

A variation of the top-loaded UWB antenna was created. The new folded-notch half-disk antenna supports the dual bands of 2.4-2.5 and 3.1-10.6 GHz without increasing the size of the original UWB half-disk antenna and covering only the UWB band. A parametric study demonstrated the effectiveness of controlling the location of a frequency notch and width of the additional operating band. The measured radiated power showed approximately 10 dB suppression at 2.6 GHz. The antenna has good impedance match over both bands and an omni-directional radiation pattern. The link response showed a linear phase response versus frequency and narrow, transient pulse width. This antenna structure is a good candidate to support both 802.11g, wireless LAN and indoor/outdoor, UWB-mobile applications.

Wearable antennas were considered by using both solid-copper and woven-copper versions of a wearable, half-disk antenna, designed to cover 3.1–10.6 GHz. These structures showed good measured characteristics of return loss, omni-directional patterns, and transient responses. The results showed the wearable half-disk is a good candidate for both multi-band OFDM and impulse-UWB applications. However, further study is required to improve the efficiency of the woven version.

Various planar, monopole-like, ultra-wideband antennas have been proposed in the literature. The antennas include monopoles of rectangular shape, inverted triangular forms similar to the bow-tie dipole, triangular disk, elliptical, half-disk, and inverted cone with holes. Typically, the ratio of height-to-width of these antennas is in the range of 2 to 1. However, the footprint for some portable UWB applications requires a higher ratio, making the width a more critical specification than height. To meet this need, several sample structures were constructed in a rolled form to create UWB antennas with a higher aspect ratio. The bi-arm, rolled monopole was created by wrapping the rectangular monopole to achieve about a 5.3:1 height-to-width ratio; it displayed good impulse response with a highly-damped ringing. The monopole with a twist was created by wrapping half of a triangular monopole to obtain about a 2:1 ratio. However, the metal patterns of both antennas are not located on the surface of the cylinder with fixed radius, which may cause some difficulties when trying to print those antennas on flexible printed circuit boards or on thin film for mass production. The manufacturing limitations motivated us to investigate a logarithmic tape helix with equiangular width, which has the metal pattern located on the surface of a cylinder with fixed radius.

A UWB tape helix was designed and characterized. The tape helix is a good candidate for UWB handheld and mobile terminals requiring directional radiation and a wideband in a monopole-type form factor. The metal pattern of the tape helix can be printed on flexible, printed-circuit board material, providing simple fabrication and mass production. In addition, an impulse-radiating antenna was designed and its performance was evaluated through simulations. The designed impulse-radiating antenna will be used for demonstrating some new aspects of the fundamental-limit theory on antennas, an emphasis of Subtask 1.1b.

Links to other tasks: This task supports the Tasks 1.2 and 4
Personnel: Taeyoung Yang, GRA

Subtask 1.1b: Antennas Characterization – transient & wideband

Task objective: Provide antenna characterization methods in both frequency and time domains

Accomplishments during the reporting period: A new effort in UWB antennas includes the characterization of the antennas for use in transient or wideband simulation and design. The characterization provides a minimal parameter description of the antenna properties that is also useful in frequency-domain antenna and propagation simulations. This work was a small extension of the effort in the previous contract on pole-zero antenna characterization, with additional characterization of impedance and patterns in the frequency realm. The UWB offers a large potential for channel modeling, as well as multipath mitigation over short distances.

The designed compact, planar, UWB antennas with top-loading and a frequency notch were characterized in both the frequency (radiation patterns, EIRP, and return loss) and time domain (link impulse response).

The relative permittivity and loss tangent for the camouflage cloth for wearable antennas were estimated using microwave measurements with a TRL calibration and the two-microstrip-line method. The results showed that camouflage cloth has $\varepsilon_r \sim 1.5$ and $tan\delta \sim 0.02$. The characterized information was used for the wearable UWB antenna design.

Some experimental and simulation results in both time and frequency domains were obtained to characterize the designed UWB tape-helix antenna. Using a HP 8720, the transient response and the group delay were determined. Two identical co-polarized antennas (both for the tape helix and the fat monopole) were separated by 40″ in order to be in the quasi far-field region. A Gaussian pulse, with a 50 ps, 50% pulse width, was used to excite the antenna. The group delay of the tape helix measured at four different azimuth angles was fairly constant to about 11 GHz, while the fat monopole had a constant group delay to about 8 GHz. A minor ringing for each transient response was observed in the late time response. The transient pulse shape of the tape helix varies with radiation angle because the tape helix does not have a symmetrical shape. This suggests that the radiation patterns are not omni-directional at all operating frequencies. The calculated axial ratio and realized gain show that as frequency increases, the realized gain increases through 7 GHz, which is about the frequency that the axial mode begins. After 7 GHz, the realized gain decreases.

Test antennas for the tape helix and a fat monopole supporting the indoor/ handheld UWB range (3.1-10.6 GHz) were fabricated, characterized, and compared in both the frequency and time domains using both measurements and simulations. Even though the test helix was not optimized, the measured results showed an impedance bandwidth (VSWR <3) over 2.5 – 12 GHz and a group delay fairly flat to 11 GHz. The measured impulse response was marginally directional in azimuth and had a narrow pulse width (less than 500 picoseconds for 50 ps Gaussian source) without dispersion.

Links to other tasks: This task supports the Tasks 1.2 and 4
Personnel: Taeyoung Yang, GRA

Subtask 1.1c: UWB antenna design (support of AWINN demonstrations)

Task objective: Develop antennas to support Ultra-wideband (UWB) high data rate links and AWINN demonstrations

Accomplishments during the reporting period: Several antennas were built in support of the AWINN demonstrations, for the robotics, sensing, and container projects. The tentative specifications for the required UWB antennas were reviewed in response to the needs request. This review inspected the feasibility of the given tentative specifications for the actual design. The specifications were then revised to best meet feasible antenna properties, particularly fundamental limits, with the perceived need.

With the review of basic antennas that might be used to meet the needs, an evaluation was conducted of the pros and cons of the antennas for specific needs. Feasibility has been a major concern in the evaluation of the specifications for the actual design. The application of the fundamental limit theory to the design process for new antennas was evaluated on a limited basis. These considerations are directly related to the antenna selection for the AWINN demonstrations.

The considered antenna candidates were as follows:

1. Tapered Slot Antenna
2. TEM Horn
3. Impulse Radiating Antenna (IRA)
4. Helical Antenna
5. Spiral Antennas
6. Log-Periodic Antennas

Several wideband antennas and ultra-wideband antennas were investigated. The tapered-slot antenna, TEM horn and IRA seem to be good candidates for the task of UWB sensing and reflection evaluation. They offer wide bandwidth along with little dispersion, which is critical for pulse transmission and reception.

Some other wideband antennas have also been investigated. The helical antenna, possibly a good candidate, has an omnidirectional beam pattern for the normal mode. The frequency independent antennas, spiral and log-periodic antennas, show the bandwidth needed for pulse transmission. However, both types have severe dispersion associated with them. The dispersion causes a chirp in the transmitted pulse, substantially increasing the ringing period of the response. The dispersion is what causes these two types of antenna to be unsuitable for pulse transmission.

The objective of the sensor work is to develop an antenna for a directional SDR (software-defined radio) receiver. The specifications for the antenna are listed in Table 1.1-1.

Table 1.1-1 Specification of the Antenna Needed

Size	Not a major constraint but an antenna dimension fitting inside a 6" x 6" x 6" is desired
Transmitted Pulse Width	Given a 500 ps pulse input, the transmitted pulse width should be 1000-1500ps, with minimal pulse dispersion or ringing
Gain	Not a major constraint
Weight	Not a concern
Absolute Frequency Range	Any range that is required to achieve the pulse width needed

For this task, a tapered-slot antenna (TSA) was chosen. An impulse-radiating antenna (IRA) and a TEM-horn antenna were also considered. The IRA and TEM horn can be designed to meet the

necessary electrical requirements, but both are large antennas. With the specified dimensions, the TSA was the best candidate for this task. There are two major components that need to be designed in order to build the antenna: a balun and the TSA.
Usually a TSA is excited by a slotline. In order to incorporate the antenna into a system, the antenna has to be integrated with other microwave circuits or common transmission media such as coaxial cable or microstrip line. Since a TSA is a balanced structure, the use of a balun is required in order to make transition between the slot line and any unbalanced transmission media.

Some of the feed schemes considered were a coax-to-slotline transition, a microstrip-to-slotline transition, use of an antipodal TSA, and use of a double-Y balun. The coax-to-slotline transition is very simple to build. The outer conductor is simply electrically connected to one side of the slotline and the center conductor is connected to the other side of the slotline. But, the setup has a high return loss due to self inductance in the feed, making the transition unsuitable. The microstrip-to-slotline transition is a printed transmission structure, making integration easy. However, the length of the stubs are $\lambda/4$, limiting the bandwidth of the transition. There are other microstrip-to-slotline transitions, but the physical dimensions and ease of construction typical increase for those structures.

The antipodal TSA (ATSA) was constructed with the two slot sides on opposite sides of the substrate. It has a good VSWR and radiation pattern, but as the frequency increases there is a substantial amount of cross polarization. This cross polarization lowers the upper limit of the antenna bandwidth.

The double-Y balun is used in many different transitions, including the microstrip-to-stripline transition. This balun shows a very wide bandwidth with very little return loss. The performance of the double-Y balun mainly depends on the quality of the short and the open at the end of the stubs. With its overall performance and the ease of construction, the use of double-Y balun was selected.

There were a couple of antennas that were modified from their original design to fit the specifications for mounting at the corner of a container. The two antennas suitable for UWB transmission are the TEM horn and tapered slot antenna (TSA). Both were modified with a corner ground plane to be suitable for the application.

Half TEM Horn Placed Externally Over a Corner Reflector (HTEM): The time domain response shows a lot of ringing, so it was excluded from the possible candidate. Both responses show ringing after the main pulse response that lasts longer than 1.5 ns, so that this antenna is less than desirable for the requirements.

Half Tapered Slot Antenna Over a Corner Reflector (HTSA): The time domain response results are very promising. The far-field pulse response produced pulses having a width less than 1.5 ns with very little ringing. The antennas were adjusted in separation from a ground plane and showed a distinct pulse present around 4.7 ns as expected. The reflection from bore-sight is indeed distinguishable.

A major change was required when it was realized that there is transient reflection from the cables supporting the containers which provide feedback to the control system to enable better performance in the container motion. A tapered-slot structure was selected for mounting over a ground plane to be suspended below the operator cab. Reasonable impedance reflection was obtained and tests indicated the ability to monitor a cable section to about 6 feet. These results

confirm the application of the Vivaldi style antenna in detecting the range to two crane wires. This range can be increased with increased transmit power. The antenna can be scaled and modified, as necessary, to match the final frequency range and input impedance. Gain can be maximized by extending the taper length, but this results in a narrower bandwidth over which there is consistent gain. The maximum gain possible is approximately 18 dBi when using an infinite ground plane. This can be accomplished based on the range of results obtained during this study.

Links to other tasks: This task supports the Tasks 1.2, 1.3, and 4
Personnel: John Kim (GRA), Terry Vogler (GRA) Randall Nealy (Engineer), and W. Davis (PI)

Subtask 1.1d: Antennas providing polarization, spatial, and pattern diversity

Task objective: Base station/access point antennas providing polarization, spatial and pattern diversity useful in supporting MIMO and space-time coding processing. Evaluation of antennas in a MIMO environment.

Accomplishments during the reporting period: Related dissertation work has been performed by a group graduate student. This work uses UWB modeling to predict the interaction of radiated energy with canonical objects. At present, measurements have been made for a sphere; the complex resonances determined with the associated amplitudes and the results were compared to the theoretical poles (resonances). The agreement was excellent, though several poles were not found. Evaluation of the theoretical amplitudes explains the absence of some poles in the measured data. The purpose of this work was to predict the interaction of radiation with canonical objects in a statistical manner and then apply the principles to the prediction of propagation in a multipath environment, particularly an indoor environment. Such information would be applicable to propagation within a ship cavity or on the cluttered deck of a ship in time or frequency based systems.

As part of the ongoing emphasis on the characterization of wideband propagation environments on the topside/upper-deck and even interior of a warship or destroyer, the efforts focused on ultra-wideband (UWB) pulse measurements in a building hallway. The topside of a navy warship or destroyer is rich in metallic scatterers, which can be approximately characterized by a similar large number of arbitrarily shaped scatterers in an indoor environment. Three scenarios were evaluated for ultra-wideband communication over short distances and include all of the information needed for single frequency applications of choice:

(a) Line-of-Sight (LOS) hallway environment for variable range
(b) Single scatterer controlled hallway environment
(c) UWB propagation around a hallway corner

Ultra-wideband pulse measurements were conducted in a controlled hallway environment with scatterers introduced into the scenario one-by-one. The UWB pulse is a Gaussian pulse corresponding to a frequency range of 50 MHz – 13 GHz. The measurements were conducted using the vector network analyzer (HP 8510) inside one of the rooms and the cables extending to the two planar TEM horn antennas in the hallway.

The frequency response of the link consisting of two planar TEM horn antennas mounted on pedestals at a height of 0.83 m and at a reference distance of 1.96 m. The distance is determined as the separation of between the two feed-points. The TEM horns provide directional properties with typically better than 6 dBi of gain over frequency.

At the reference distance of 1.96 m, the corresponding time-domain received signal consisted only of the direct response from the transmitting antenna. The reflections from the floor, walls or the ceiling were not observed due to the close proximity of the antennas. However, when the distance was increased to 2.90 m, reflections from the floor and the ceiling were observed, but not from the walls due to the directivity of the antennas. Similar observations were made when the distance was further increased to 5.7 m.

The results are indicative of the presence of a specular response from the basic indoor structures such as the floor, walls and the ceiling. Note that for a 2.90 m distance between the antennas, the furthest multipath component arrives 2.93 ns after the first direct LOS component. As the distance between the antennas increases to 5.70 m, the relative path difference between the direct and multipath component reflected off the hallway structure reduces. The furthest multipath component arrives 1.62 ns after the first direct LOS component. This has serious implications when the antenna is resonant, in which case the direct LOS component and the multipath components overlap to distort the received signal.

Ultra-wideband multiple-input multiple-output (UWB-MIMO) pulse measurements were conducted in a controlled hallway environment in line-of-sight and obstructed channel conditions. The UWB pulse is a Gaussian pulse corresponding to a frequency range of 1 GHz – 13 GHz. The measurements were conducted using the vector network analyzer (HP 8510) inside one of the rooms and the cables extending to the two planar TEM horn antennas in the hallway.

Multiple-input multiple-output (MIMO) is a popular approach to improve data rate capacity using multiple antennas at the transmitter and the receiver. Achievable channel capacities are measured in terms of the number of bits transmitted per second over a unit bandwidth in bits/sec/Hz. Under ideal conditions, a MIMO channel with N number of transmit and receiver antennas increases the channel capacity over conventional single-input single-output (SISO) channels by a factor of N. Such large channel capacities are achieved when signal from each of the individual transmitters is received uncorrelated at each of the receiver. Environments rich with scatterers help achieve the true potential of a MIMO channel.

Channel capacities of flat faded (non-dispersive) narrowband applications have been widely reported in literature. However, no analytical expressions for channel capacity have been reported for dispersive channel conditions. Ultra-wideband communications applications experience channel dispersion due to extremely large bandwidths in excess of 500 MHz and even as much as 7.5 GHz. Hence, channel capacity expressions developed for narrowband applications cannot be applied to UWB communications [S. Ray, M. Medard, and Z. Lizhong, "On MIMO capacity in the ultra-wideband regime," Proceedings of the 38th Asilomar Conference on Signals, Systems and Computers, vol. 2, pp. 1516-1520, Nov. 2004.]

The channel capacity of a 2 x 2 UWB-MIMO channel in a LOS channel condition averaged over the frequency range of 1 GHz to 13 GHz was measured. The trend shows that at low transmit power, the capacity of the 2 x 2 UWB MIMO link is only as good as the best of the four individual links. At higher transmit powers, the rate of improvement in channel capacity (given by the slope of the curve) is twice as that of the individual links.

The channel capacities of a single-input single-output (SISO) and a 2 x 2 Rayleigh faded MIMO channels were also estimated. The Rayleigh fading represents worst-case fading and hence, it presents a lower bound on the achievable channel capacity.

Similar channel capacity results are obtained for a 2 x 2 UWB-MIMO channel in an obstructed NLOS channel conditions. As expected, the estimated channel capacities for individual UWB links in LOS conditions is much higher compared to the NLOS channel condition. At low transmit powers, the capacity of the 2 x 2 UWB MIMO link for both LOS and NLOS channel conditions is only as good as the best of the respective four individual links. At higher transmit powers, the rate of improvement in channel capacity (given by the slope of the curve) is twice as that of the individual links.

Links to other tasks: This topic impacts on the frequency selection and interaction of the measurements used for the Sea-Based cargo systems being considered in Task 3.

Personnel: Garauv Joshi, PhD Student

Subtask 1.1e: Support physics/engineering-based models

Task objective: Base station/access point antennas providing polarization, spatial and pattern diversity useful in supporting MIMO and space-time coding processing. Evaluation of antennas in a MIMO environment.

Accomplishments during the reporting period: Some simple modeling of antennas was undertaken as a small task. The orientation is a model of an antenna based on a pole-residue description presented in the dissertation of Stani Licul, Virginia Tech, 2004. Since Wheeler [*Proc. IEEE*, vol. 69, pp. 1479-1484, 1947] introduced the concept of fundamental limits on small antennas, there have been many efforts to find an exact formulation for minimum radiation Q. Chu [*J. Appl. Phys.* vol 19, pp. 1163-1175, 1948] derived a minimum radiation Q expression using circuit models corresponding to spherical-mode wave impedances. The work since Chu has often included conceptual errors in the definition of radiated energy which resulted in higher estimates of the Q than is proper. However, the results of Chu are still found to provide reliable estimates, though a new development has identified a slightly lower bound.

Fundamental-limit theory shows that the designer must trade off factors of antenna size, gain, and bandwidth, and that significant improvement of all quantities in the same design is impossible. Efforts over the past half century have focused on the accuracy of the theory. Only the TM_{01} spherical mode has been emphasized because the TM_{01} mode provides the minimum radiation Q, although such a mode also provides an omni-directional radiation pattern.

Through the on-going study, we explored some new variations on the fundamental-limit theory of antenna performance. These included an equivalent pole-residue model of Chu's circuit model, some implicit assumptions of bandwidth and pattern related to the specific mode of consideration, and the radiated power of electrically-small antennas as a function of antenna size and source conditions (voltage, current, and power sources). These new variations in the fundamental-limit theory of antenna performance provide a new approach to design a optimize antenna which is close to the theoretical limit of antenna performance.

We designed the impulse radiating antenna (IRA) which we expect is close to the response of the ideal antenna that the Chu's model suggested. Using a commercial method of moment code (FEKO), the return loss and the impulse response were found to be as expected, offering a good match and a near perfect impulse response with a differentiation. The designed IRA matches 50 Ohms from 500 MHz to 10 GHz with some mismatch below 500 MHz. The minor mismatch in the band can be improved with a different value of termination resistor or surface resistance, providing a smooth resistance change. The impulse response has a couple of glitches around 3.4

ns and 6.3 ns as expected. These were caused from the direct radiation of feed arms and reflections of mismatched termination resistors.
The radiation gain pattern was also calculated. Basically, the IRA has a maximum gain in the boresight direction and a few side lobes caused from the feed.

Personnel: Taeyoung Yang, GRA

Subtask 1.1f: Wideband balanced antenna/array feed networks

Task objective: Development of array feed networks for wideband balanced antenna systems such as the Fourpoint antenna investigated in the NAVCIITI program

Accomplishments during the reporting period: Problems can arise if a balanced antenna is driven or situated in such a way as to cause an imbalance. The effect of an imbalance can cause the radiation pattern of an antenna to change, in the worst case causing a drastic and undesirable change in the pattern. A general indication of a balanced condition for a system is its symmetry, both electrical and spatial.

Coaxial cables are inherently unbalanced. Feeding a balanced antenna with an unbalanced line can have an undesirable effect on the antenna pattern due to radiation of currents on the exterior of the coax. A balun is used to convert the unbalanced signal from the coaxial cable into a balanced signal that does not adversely affect a balanced antenna pattern.

There are many ways that an otherwise balanced antenna can become unbalanced. The type of antenna feed as well as the orientation of system components can have an effect on the balance of an antenna system. Driving a balanced antenna with an unbalanced feed will produce an unbalanced system. Positioning an otherwise balanced system (feed and antenna balanced) above a ground plane in a certain orientation can cause the antenna itself to become unbalanced. Orienting a feed line, balanced or otherwise, asymmetrically with respect to a balanced antenna can cause an imbalance.

A review was conducted of available balun structures. The Type 1 balun works by presenting infinite impedance looking from the load back towards the feed line. This arrangement is usually narrow band. The Type 2 balun is comprised of two Type 1 baluns in series. This arrangement can provide a bit more bandwidth than the Type 1 balun. The Type 3 balun is a folded variation of the Type 2 balun. Again, this presents infinite impedance when looking from the load towards the feed line.

Other baluns include the half-wave, bypass balun, the natural balun (which can be considered an antenna with a built in balun), and cutaway baluns that can theoretically provide upwards of 100:1 bandwidth ratios. It is not uncommon to combine several particular balun designs to arrive at a hybrid structure.

A balun classification may also be classed as a current balun, a voltage balun, or a power divider. The current balun attempts to balance currents, while the voltage balun attempts to balance a voltage with respect to some reference. Finally, as the name suggests, the power divider attempts to split the power between two ports such that the current and voltage at each port are equal but opposite in the typical case.

There are many different balun designs available. Many of the antenna designs of interest for AWINN are of the compact planar variety. As a result, we have concentrated on balun designs that have a planar form factor. We also concentrated on investigating baluns that are popular and versatile. By "popular," we mean proven balun designs that are widely cited in the literature. A primary factor of interest was the bandwidth of the various balun designs.

We have identified five well-known baluns that can be used to balance wideband to ultra-wideband antennas. This group can accommodate both planar designs and parallel designs (antennas that have elements on the top and bottom of a dielectric substrate) as shown in Table 1.1-2.

Table 1.1-2 Wideband and Ultra-wideband Baluns

Balun Type	**Bandwidth**
Tapered	50:1 to 100:1
Double-Y	6:1
Marchand	2:1 to 4:1
CPW-to-CPS, CPW-to-slot line	2:1

In addition to the review of baluns, measurement techniques were considered to evaluated the effectiveness of the balun. Several methods are presently in wide use. One method for determining balance is to integrate the balun with the desired antenna system and measure a pattern for the antenna. The symmetry of the pattern confirms proper operation of the balun.

Often, it is desirable to characterize the balun directly without integration into a system. The second method accomplishes this goal by considering the balun as a two or three-port device and taking measurements using a vector network analyzer. The amount of balance can be determined by looking at the magnitudes and phases of S_{21} and S_{31}. Another standard practice has been to directly connect two baluns to be measured as a two-port with the balanced output port of one directly connected to the balanced port of the other. This arrangement is known as a back-to-back measurement.

We investigated the details of the standard back-to-back measurement for extraction of critical balance information. A method was developed for increasing the amount of information acquired to help determine a more accurate measure of balance across some specified bandwidth. This method, called direct-invert, connects the baluns for two back-to-back measurements, orienting the balanced port terminals both directly and in a reverse connection, hence the name.

The essential role of a feed network is to allow an antenna to receive the maximum desired signal at its input port or ports without reflections or other adverse affects to the pattern. For single element antennas, the feed network can have several functions: correcting any balance issues; adjusting impedance mismatchs between the feed line and the antenna; and introduce the desired phase and amplitude changes in the signal for the individual elements. Errors can result in deep nulls being filled in. As the number of array elements increases, the complexity and the length of the feed network increases. Ohmic and dielectric losses might become an issue for complicated, and hence long networks, which can degrade the signals reaching the elements. Mitigating these two issues in concert with any matching and balancing functions that the array feed-network must accomplish make them that much more complicated to design for array antennas. An additional factor that must be considered for arrays is the mutual coupling between elements. Many designers go to extreme lengths to minimize mutual coupling, while proper accounting of the

mutual coupling can actually be used to enhance the array performance and even extend the bandwidth of the array.

The four-square antenna is a versatile, broadband, planar antenna element which can be easily incorporated into an array configuration to facilitate beam steering. For this reason, it was chosen as a good antenna for testing balun and feed network designs. A rat-race hybrid was selected for the design. Slight modifications were made to improve the bandwidth of the device. The balun was then integrated in a 4-element feed network and measurements were made that provided the desired wide-band performance.

It was hoped to be able to incorporate the rat race balun (RRB) into the planar feed structure. Because of the close proximity of the 4-square antenna elements there was very little room to add a balun. The original design was to put a RRB under each array element. The substrate required dimensions that didn't allow room for any of the feed network to be routed around the baluns. It was decided to try to put one RRB in the center of a 2x2 array and to feed each element from this. Again trace routing was very difficult, requiring a routing scheme that produced too much coupling between some of the balanced feed lines which caused a phase shift between outputs. It was decided to construct a standard microstrip power splitting feed network which feeds four RRBs. Each RRB is placed perpendicular to the feed network. This configuration was constructed and measured. Balanced patterns were obtained over the spectrum from 2.5 to 3.5 GHz. The patterns begin to become unbalanced as the frequency becomes lower than 2.5 GHz or higher than 3.5 GHz.

Personnel: Scott Bates, GRA

1.1.3 Importance/Relevance

Several important developments were completed during this task that relate to future antenna or propagation needs in the Navy and other services. There was an emphasis on the evaluation of antenna designs for bandwidth, size, and radiation performance. A major focus was placed on the relationship between fundamental limits of antennas and the ability to address specific design specifications.

The demonstrations required wideband antennas, typically UWB (ultra-wideband) antennas for small and omni needs, as well as some directional requirements. The design principles apply to a variety of needs, but the emphasis was on a basic understanding of the radiation mechanisms and near-field effects.

Antennas were designed and constructioned to support the demonstrations, including UWB sensing antennas, balanced dipoles for the robotics demo, and antenna designs for use in the sea-basing demo. The latter included designs for use on containers as well as for receiving reflections from support cables to provide feedback control of the container crane systems.

Interesting results were obtained for the propagation characterization of indoor channels in a UWB measurement environment. The emphasis was on scatterer contamination of the propagation environment and the effects of both specular and resonant reflection were identified. The results led to models of the scattering mechanisms as well as to an investigation of UWB MIMO (multiple-input, multiple-output) concepts. This UWB view of MIMO is a new consideration in channel propagation.

A wideband balun was developed for use with the Four-Square array and other antenna systems. Consideration of bandwidth and size were major factors in the design of the baluns

1.1.4 Productivity

Conference Publications

1. G. Joshi, W. Davis, and W. Stutzman, "UWB Channel Dispersion, Characterization, and Modeling", Symposium on Wireless Personal Communications (Blacksburg, VA), Poster Paper, June 2005.
2. Kai Dietze and Warren L. Stutzman, "Blind MIMO System Identification", Symposium on Wireless Personal Communications (Blacksburg, VA), Poster Paper, June 2005.
3. T. Yang, W.A. Davis, and W.L. Stutzman, "Folded-Notch Dual Band Ultra-Wideband Antenna", IEEE Antennas and Propagation Society International Symposium, (Washington, DC), Poster Paper 17.8, July 3-8 2005.
4. T. Yang, W.A Davis, and W.L. Stutzman, "Small, Planar, Ultra-Wideband Antennas with Top-Loading", IEEE Antennas and Propagation Society International Symposium, (Washington, DC), Poster Paper 33.3, July 3-8 2005.
5. T. Yang, W.A. Davis, and W.L. Stutzman, "Wearable Ultra-Wideband Half-Disk Antennas", IEEE Antennas and Propagation Society International Symposium, (Washington, DC), Poster Paper 60.1, July 3-8 2005.
6. G.G. Joshi, W.A. Davis, and W.L. Stutzman, "Ultra-Wideband (UWB) Channel Dispersion: Classification and Modeling", IEEE Antennas and Propagation Society International Symposium and URSI National Radio Science Meeting (Washington, DC) Poster Paper 24.8, July 3-8, 2005.
7. William Davis, "Development of New Antennas and Applications: Application of UWB Antenna Modeling," IDGA 2005: Military Antenna Systems, Arlington, VA, September 20-21, 2005.
8. Stanislav Licul and William A. Davis, "Unified Frequency and Time-Domain Antenna Modeling and Characterization", IEEE Transactions on Antennas and Propagation, vol. 53, pp. 2882-2888, September 2005.
9. Taeyoung Yang and William A. Davis, "Pole Residue Structure of the UWB Planar Half-Disk Antenna", Proceedings of XXVIII General Assembly of International Union of Radio Science (URSI) (New Delphi, India), 4pp., October 2005.
10. G.G. Joshi, C.B. Dietrich, and W.L. Stutzman, "Adaptive Beamforming Measurements Using Four-Element Portable and Mobile Arrays", IEEE Transactions on Antennas and Propagation, vol. 53, pp. 4065-4072, December 2005.
11. G.G. Joshi, C.B. Dietrich, and C.R. Anderson, W.G. Newhall, W.A. Davis, J. Isaacs, G. Barnett, "Near-ground channel measurements over line-of-sight and forested paths", IEE Proceedings on Microwaves, Antennas, and Propagation, vol. 152, pp. 588-595, December 2005.
12. W.L. Stutzman, W.A. Davis, and T. Yang, "Fundamental Limits on Antenna Size and Performance", Antenna Systems Conference (Santa Clara, CA), Sept. 22-23, 2005.
13. G.G. Joshi, W.A. Davis, and W.L. Stutzman, "Statistical and Fuzzy Pole Characterization of the Complex Poles of a Conducting Sphere and a Wire", URSI National Radio Science Meeting (Boulder, CO), January 2006.
14. Taeyoung Yang and William A. Davis, "Miniaturization of Planar Two-Arm Spiral Antennas Using Slow-Wave Enhancements," URSI National Radio Science Meeting (Boulder, CO), January 2006.
15. Taeyoung Yang, William A. Davis and Warren L. Stutzman, "Normal-Mode, Logarithmic, Ultra-Wideband Tape Helix", Proceedings of IEEE International Workshop

on Antenna Technology: Small Antennas and Novel Metamaterials (White Plains, NY), pp. 301-304, March 2006.

16. G.G. Joshi, W.A. Davis, and W.L. Stutzman, "Fuzzy Pole Representation for SEM based Complex-Pole Scatterer Signature", URSI National Radio Science Meeting (Albuquerque, NM), pp. 147, July 2006
17. S. Licul, N.P. Cummings, W.A. Davis, and W.L. Stutzman, "On Antenna Geometry Synthesis using Pole-Residue Representation", URSI National Radio Science Meeting (Albuquerque, NM), pp. 432, July 2006
18. Taeyoung Yang, William A. Davis, and Warren L. Stutzman, "Some New Aspects of Fundamental-Limit Theory on Antennas", URSI National Radio Science Meeting (Albuquerque, NM), pp. 549, July 2006

Books and Book Chapters

1. W.A. Davis and W.L. Stutzman, "Antenna Theory," Chapter in Wiley Encyclopedia of RF and Microwave Engineering, TK 5103.2 E63, 2005.
2. W.A. Davis and S. Licul, "Antennas," Chapter in An Introduction to Ultra Wideband Communication Systems, Wiley, New York, 2005.

Students completed

G. Joshi, "Ultra-Wideband Channel Modeling using Singularity Expansion Method," PhD, 2006

K. Dietze, "Blind Identification of MIMO Systems: Signal Modulation and Channel Estimation," PhD, 2005

Students supported:

Kai Dietze, Jan 2005 – Aug 2005
Taeyoung Yang, Jan 2005 - present
John Kim, Aug 2005 - present
Scott Bates, Aug 2005 - present
Gaurav Joshi, Jan 2005 – May 2006
Terry Vogler, Aug 2005 - present

Faculty supported:

William A Davis, Jan 2005 – present
Warren L Stutzman, Jan 2005 - present
Carl Dietrich, Research Faculty, Jan. 15, 2005 – present

Staff and other personnel supported:

Randall Nealy, Jan. 15, 2005 – present

1.2 Task 1.2 Advanced Software Radio

1.2.1 Overview

Task Goal: This task investigates an advanced Software Defined Radio (SDR) for Navy applications that takes advantage of the unique properties of Ultra Wideband communication—such as precision position location, ranging, and low probability of intercept.

Organization: This task is directed by the Deputy Director of the Mobile and Portable Radio Research Group (MPRG) using the following personnel:

Jeffrey H. Reed, director
R. Michael Buehrer, faculty
William H. Tranter, faculty
Chris R. Anderson, GRA
Swaroop Venkatesh, GRA
Jihad Ibrahim, GRA
Ihsan Akbar, GRA

1.1.2 Task Activities

Subtask 1.2a Develop flexible software radio platforms that includes cross-layer optimization with capabilities for UWB and ad hoc networking

Task objective: The overall goal of this subtask is to design an advanced software-defined/reconfigurable radio which is optimized for ultra wideband communication, and then implement the system using off-the-shelf components. The software-defined radio implementation provides tremendous flexibility compared to a single hardware implementation—for example, providing the capability to utilize one of several different popular UWB modulation or multiple access schemes, to operate in one of several modes (communication, ranging, or data capture), as well as to utilize more traditional broadband communication schemes.

Accomplishments:

Overview:
Impulse Ultra Wideband (I-UWB) signals have been an important research area for a number of years. Their extremely short time duration results in a communication link that is Low Probability of Intercept (LPI), capable of robust operation in dense multipath environments, and can potentially support high data rate communications. Additionally, I-UWB signals can provide precision ranging or position location information, making them useful in a variety of applications such as RADAR, position location networks, or human vital signs monitoring. At the current time, nearly all commercially available UWB systems have been developed using custom-designed hardware and are optimized for very specific applications. A software defined ultra wideband transceiver, such as the one developed in this subtask, can be used in nearly all of the above applications; additionally, it provides a platform that researchers can use to evaluate receiver algorithms, architectures, and theoretical models or simulation results.

Ultra Wideband Transceiver Testbed:

The primary focus of this subtask was the design, development, and implementation of the Ultra Wideband Transceiver Testbed. The testbed is composed of four different subsystems: the RF Front End, the Transmitter Board, the Receiver Board, and the DC Power Board. With the exception of the Transmitter Board, the testbed was developed with general-purpose commercially available off-the-shelf components to ensure that users had full control over nearly all aspects of the receiver architecture and communication link. To achieve such an aggressive design goal, the receiver is based around a time-interleaved array of ADCs—providing it with an 8 GHz effective sampling frequency and approximately 40 dB Signal to Noise Ratio (or roughly 6.5 – 7.0 Effective Number of Bits of quantization). In addition to UWB signals, the receiver is capable of supporting nearly any other form of broadband communications, resulting in a system whose combination of performance and flexibility is currently unmatched.

Time Interleaved ADC Array Performance:

The performance of a Time Interleaved Sampling array is highly dependant on matching the individual ADC gains, offsets, and timing delays. Mismatches can result in a significant distortion of the received signal and are caused by minor physical differences between ADC components—a problem which is exacerbated when using off-the-shelf components. Although a number of researchers have investigated the performance degradation of Time Interleaved Sampling arrays for CW inputs, to date, no one has investigated the performance of such an array for a UWB signal. Therefore, detailed theoretical analysis and simulations for the performance of such an array with a UWB monocycle was presented in this subtask for an array of eight 8-bit 1 GS/s ADCs. The results indicated that gain, offset, and timing mismatches of no more than ±10% would be sufficient to achieve a no more than 6 dB reduction in the Effective SNR of the ADC array. Additionally, the use of a pilot-based matched filter to mitigate the impact of these mismatches was investigated. The pilot-based matched filter was shown to be reasonably effective, with the pilot-based template capable of achieving up to a 95% correlation with a received data pulse.

Overall System Performance:

The overall UWB SDR Testbed, operating at an Effective Sampling Frequency of 6.4 GHz, operates with a 45 dB dynamic range, and can digitize UWB pulses with only a 2% RMS error. The efficacy of the DPBMF approach was evaluated, and found to perform with bit error rates only 1-3 dB away from the BPSK in AWGN curve. Additionally, measured bit error rates were compared to the BER rates from the system simulation, as well as theoretical bit error rates, and were found to be in good agreement. The only downside was the performance of the RF Front End, which exhibited a gain flatness and phase linearity that was far out of spec, but could still provide acceptable performance under most circumstance

Personnel:

Chris R. Anderson – Transmitter and Receiver Hardware Development
Matt Blanton – Receiver FPGA Code Development

Subtask 1.2b Software radio research applied to UWB, including design parameter space exploration.

Task objective: The objective of this task is to investigate innovative SDR architectures and algorithms for both traditional broadband and UWB communications. These

algorithms will be implemented on the advanced SDR receiver developed in Subtask 1.2a.

Accomplishments:

UWB Signal Detection:

Signal Detection based on Sequence Optimization: A novel approach to UWB waveform design based on sequence optimization for the multipath transmission channel is proposed. The transmit waveform is made up of a train of delayed and scaled pulses, the amplitudes of which can be represented by a real-valued sequence. The waveform results in substantial improvement in energy capture (and thus performance) over the traditional Rake receiver and the more recently proposed transmitted reference (TR) approaches with a simple receiver structure. The design exploits the rich multipath structure of UWB channels allowing improved energy capture. The algorithm is developed for the single-user communication model as well as the multi-user case.

As shown in Figure 1.2-1, the proposed method outperforms Rake and TR receivers and is relatively robust to channel estimation errors.

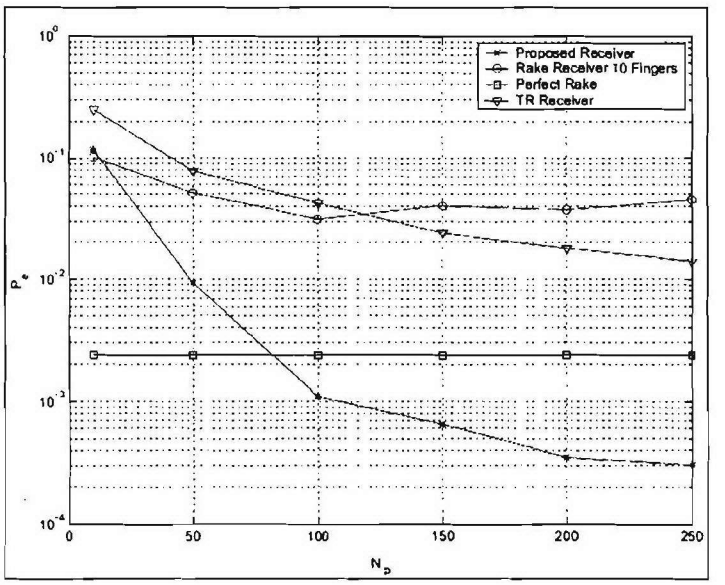

Figure 1.2-1 Performance of sequence optimization method.

Signal Detection based on Data-Aided TR System:

An improved receiver structure based on the TR system is investigated. Specifically, an iterative data-aided pilot-assisted receiver employing low density parity check coding (LDPC) is proposed. This receiver captures the entire received energy, while significantly reducing the required training overhead. The introduction of the LDPC code allows for improved template estimation in the iterative receiver. Moreover, because of impulse-based UWB's low duty cycle, coding can be introduced without severely reducing the system data rate. The proposed approach exploits the synergy between coding, improved channel estimation and large UWB bandwidth to yield large performance gains. It is shown that such a detection strategy potentially outperforms traditional receiver structures (Rake and TR).

The gains observed when incorporating data-aided channel estimation and error correction coding are seen in Figure 1.2-2.

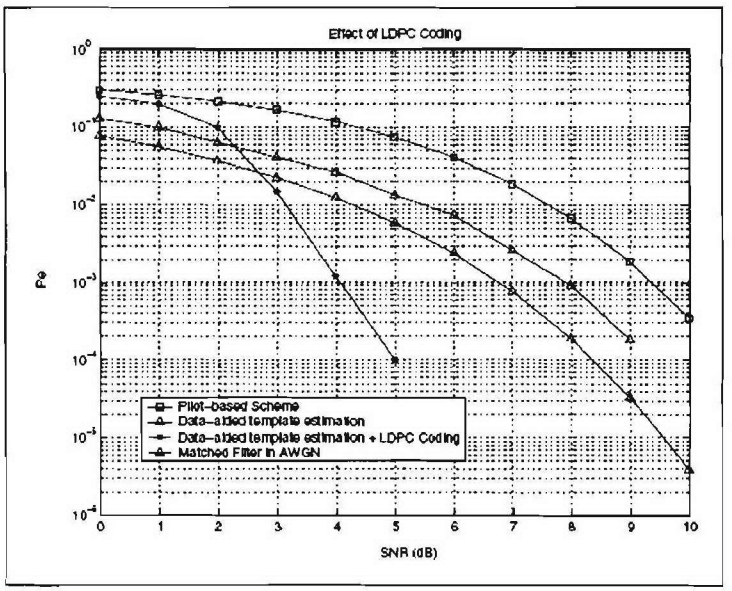

Figure 1.2-2 Performance of data-aided TR receiver.

UWB Acquisition:
Traditional synchronization techniques applied to impulse-radio UWB result in prohibitively long acquisition times, due to the extremely large search space. Additionally, in dense multipath environments, there exist a larger number of cells within the uncertainty region that can lead to acquisition lock. Locking to an arbitrary multipath component may result in unacceptable performance for many applications (range error in positioning systems for example). We present a modified framework for the analysis of UWB acquisition which accommodates multiple lock cells. The framework divides the acquisition process into two distinct phases. The two phases are termed "coarse" and "fine" acquisition. The coarse acquisition phase is a fast implementation of traditional serial search which takes advantage of the large number of cells which can terminate the search process. Fine acquisition exploits statistics derived from the first phase and the clustered nature of multipath arrivals to determine the earliest arriving path, even when it is severely attenuated. It was shown that the first phase provides a substantial improvement in mean acquisition time compared with traditional serial search (see Figure 1.2-3) and that the second phase provides robust estimation of the first arriving path in ranging applications (Figure 1.2-4).

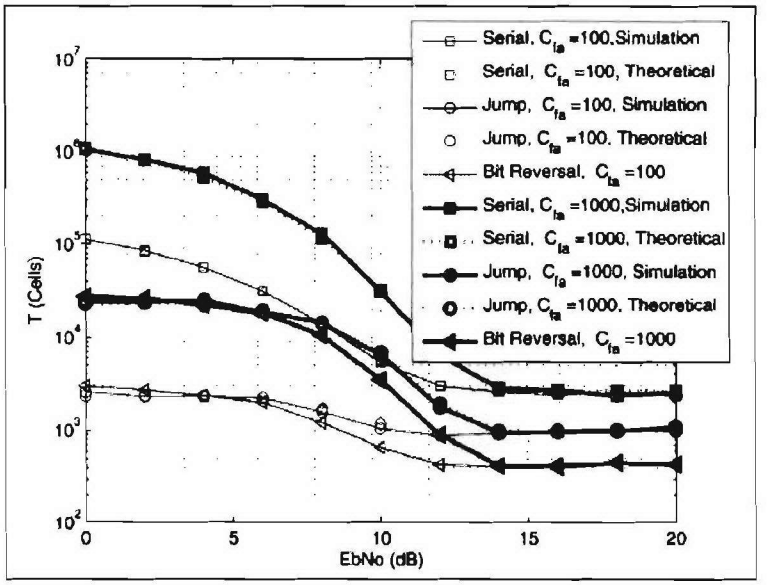

Figure 1.2-3 Mean acquisition for proposed (Jump) search versus serial search.

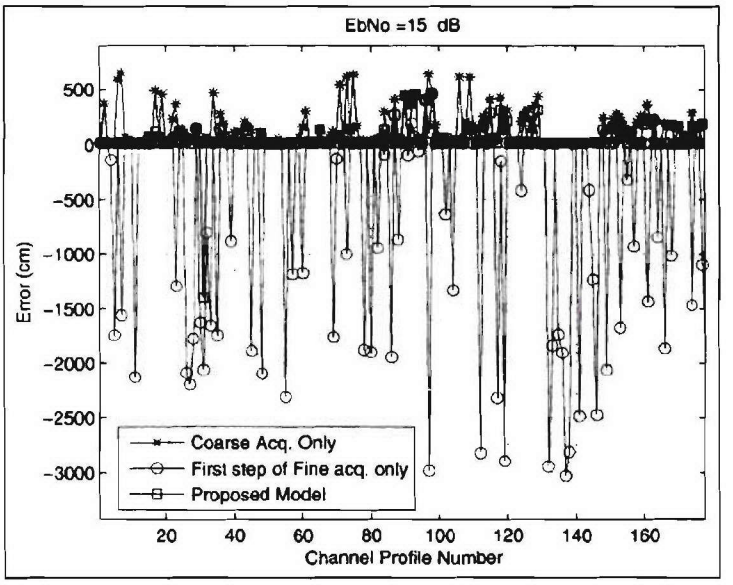

Figure 1.2-4 Performance of fine acquisition in ranging. Spreading code length of 64. SNR = 15 dB. 542 real measured channel profiles are used.

UWB Tracking:

The satisfactory performance of classical tracking circuits presumes that acquisition (coarse synchronization) has provided a good estimate of the correct symbol or frame timing (typically within a fraction of the chip duration). This might not be a reasonable assumption for pilot-assisted UWB receivers in dense multipath, where initial acquisition of the LOS component is highly problematic, and coarse synchronization is more likely to detect an arbitrary multipath component.

We propose a tracking algorithm for pilot-assisted receivers based on a variant of the early-late gate approach, where the circuit's correlation template is matched to the received pulse shape rather than the transmit pulse shape. Data-aided channel estimation is also incorporated into the method. The algorithm is mathematically analyzed then tested by simulation, and it is shown that it can potentially correct timing errors much larger than the transmit pulse duration.

Figure 1.2-5 shows the performance improvement brought by correcting the timing error using the proposed method.

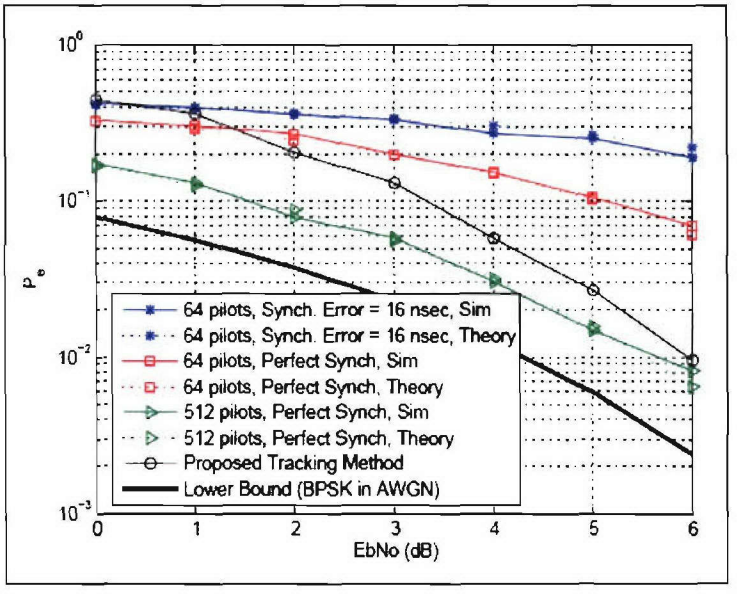

Figure 1.2-5 Performance of the proposed system. Frame holds 512 Symbols.

NBI Mitigation for UWB Systems:
A NBI mitigation scheme for UWB signals using multiple receive antennas is examined. The low spatial fading of UWB signals compared to NBI signals is exploited to provide "interference selection diversity". Whereas classical selection diversity is designed to maximize the desired received signal power, the aim of interference selection diversity is to minimize the effective NBI power. The resulting distribution of the signal-to-interference ratio (SIR) at the receiver is derived for both Rayleigh and Ricean NBI fading scenarios. Expressions for the probability of error of the selection diversity scheme are also derived for a perfect receiver (where the correlator template is matched to the received UWB pulse shape) as well as for a Rake receiver with a limited number of fingers. It is shown that doubling the number of antennas potentially results in a 3-dB performance improvement for the Rayleigh fading case (Figure 1.2-6). Less substantial gains are observed under Ricean fading. The method provides a simple but effective technique to mitigate NBI effects in UWB systems.

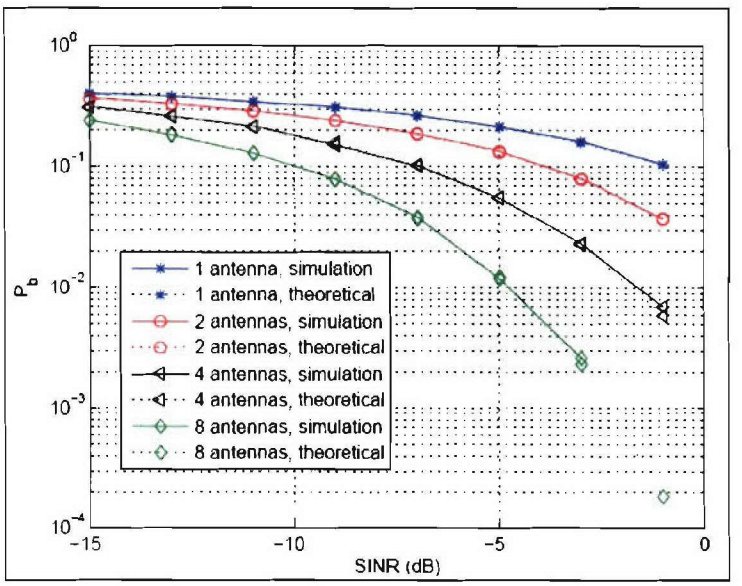

Figure 1.2-6 Performance of multiple antennas system with NBI Rayleigh fading.

Subtask 1.2c Software radio designs for collaborative systems that take advantage of this radio, particularly for interference environments.

Please refer to Task 4, TIP #1.

Subtask 1.2d Vector channel models, including Markov Models, and supporting channel measurements.

Task objective: The objective of this task is to study techniques to find efficient ways to model error traces generated by real world wireless channels. Different discrete channel modeling methods will be implemented and their accuracy, consistency and robustness will be studied.

Accomplishments:

Markov Modeling of Wireless Channel Error Sources:

Accurate modeling of error sources that occur in wireless channels is necessary for a better understanding of network performance and for improving the design of communication protocols. Often these channels contain memory and Markov models are usually used to model these binary error traces. This section deals with the order estimation of HMMs that are developed for modeling the error sources that occur in fading channels. It is found that for a general stationary binary time series that is generated from an arbitrary HMM, a two-state HMM is sufficient. A detailed study on modeling non-stationary error traces is also presented. Two cases of error traces generated by Rayleigh fading channels are discussed here.

First, we study the error trace generated by Rayleigh fading channel with 7 Hz fading rate and the sampling frequency of 1 Kbps, the autocorrelation function (ACF) of the error trace and its corresponding HMMs are shown in Fig. 1.2-7.

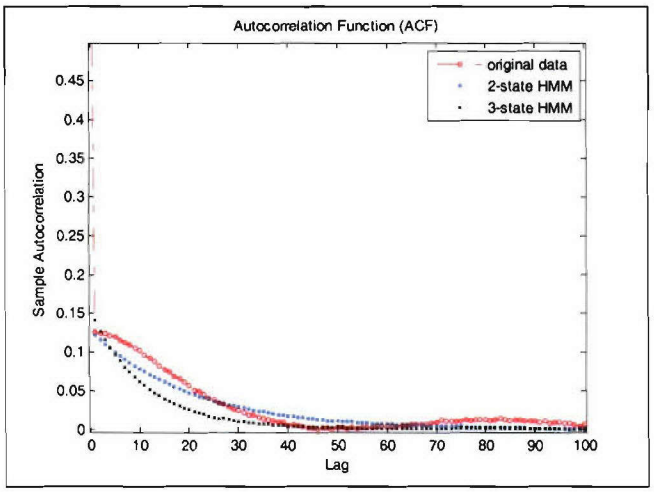

Figure 1.2-7 First 100 lags of ACF of original error trace and its 2-state and 3-state HMMs ACFs. Fading rate = 7 Hz, sampling frequency = 1 Kbps.

We next obtain an error sequence from a Rayleigh fading channel with the same 7 Hz fading rate but with 1 Mbps sampling frequency. The autocorrelation plots are shown in Fig. 1.2-8.

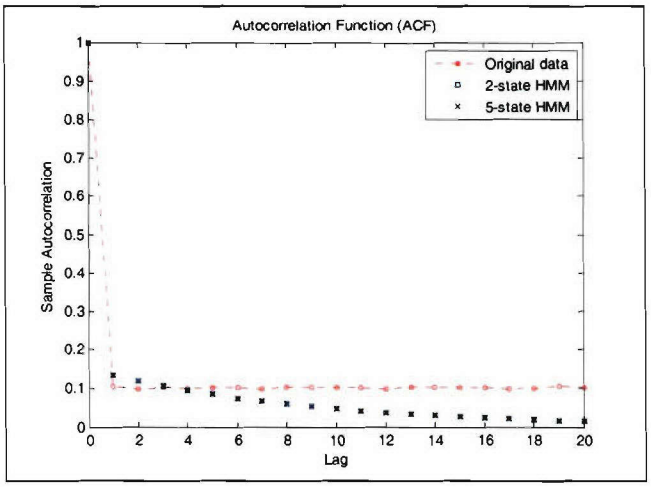

Figure 1.2-8 First 100 lags of autocorrelations of the original error trace and corresponding ACFs of 2-state and 3-state HMMs. Fading rate = 7 Hz fading rate sampling frequency =1 Mbps.

It is found that the no HMM developed for this case could fit the data with reasonable accuracy. We then performed test runs [Bendat (1986)] to check the stationarity and found out that the test rejects the stationary hypothesis for the data generated from 7 Hz sampling frequency and 1 Mbps sampling frequency. The test, however, accepts the stationary hypothesis for 7 Hz sampling frequency and 1 Kbps sampling frequency case. This hypothesis rejection is due to very long stretches of zeros that occur because of high sampling frequency. The summary of these tests is shown in Fig. 1.2-9 and 1.2-10.

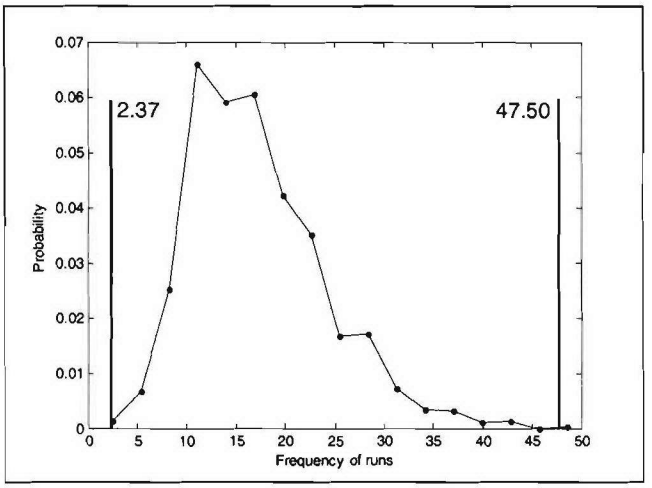

Figure 1.2-9 Runs test of stationarity performed on the 7 Hz and 1 Kbps error trace. The test accepts the null hypothesis that data is stationary.

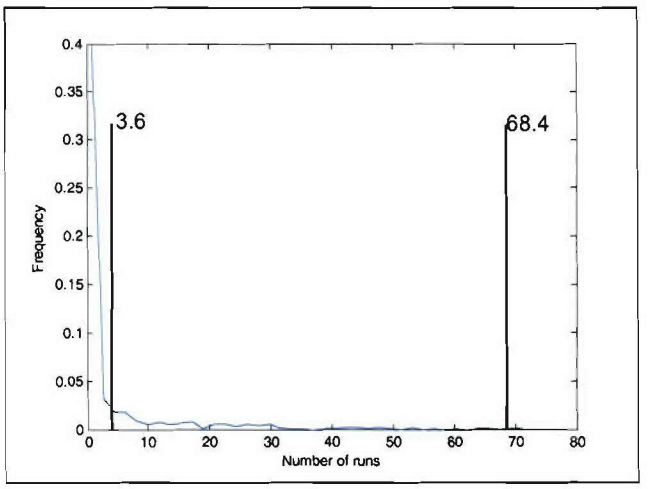

Figure 1.2-10 Runs test of stationarity performed on the 7 Hz and 1 Mbps error trace. The test rejects the null hypothesis that data is stationary.

Non-stationary trace is divided into stationary trace based on the method given in [Konrad (2003)]. The result of runs test performed on the bad trace is shown in Fig. 1.2-11.

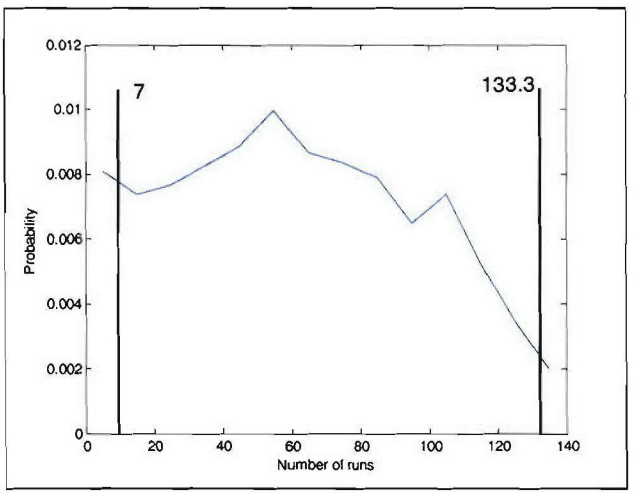

Figure 1.2-11 Runs test of stationarity performed on the bad trace extracted from 7 Hz and 1 Mbps error trace. The test accepts the null hypothesis that data is stationary.

The good trace is then approximated using a standard exponential random variable whereas the bad trace is modeled using HMMs with different states. The results are summarized in Fig.1.2-12. It is interesting to note that the model fitting gets better as we increase the number of hidden states.

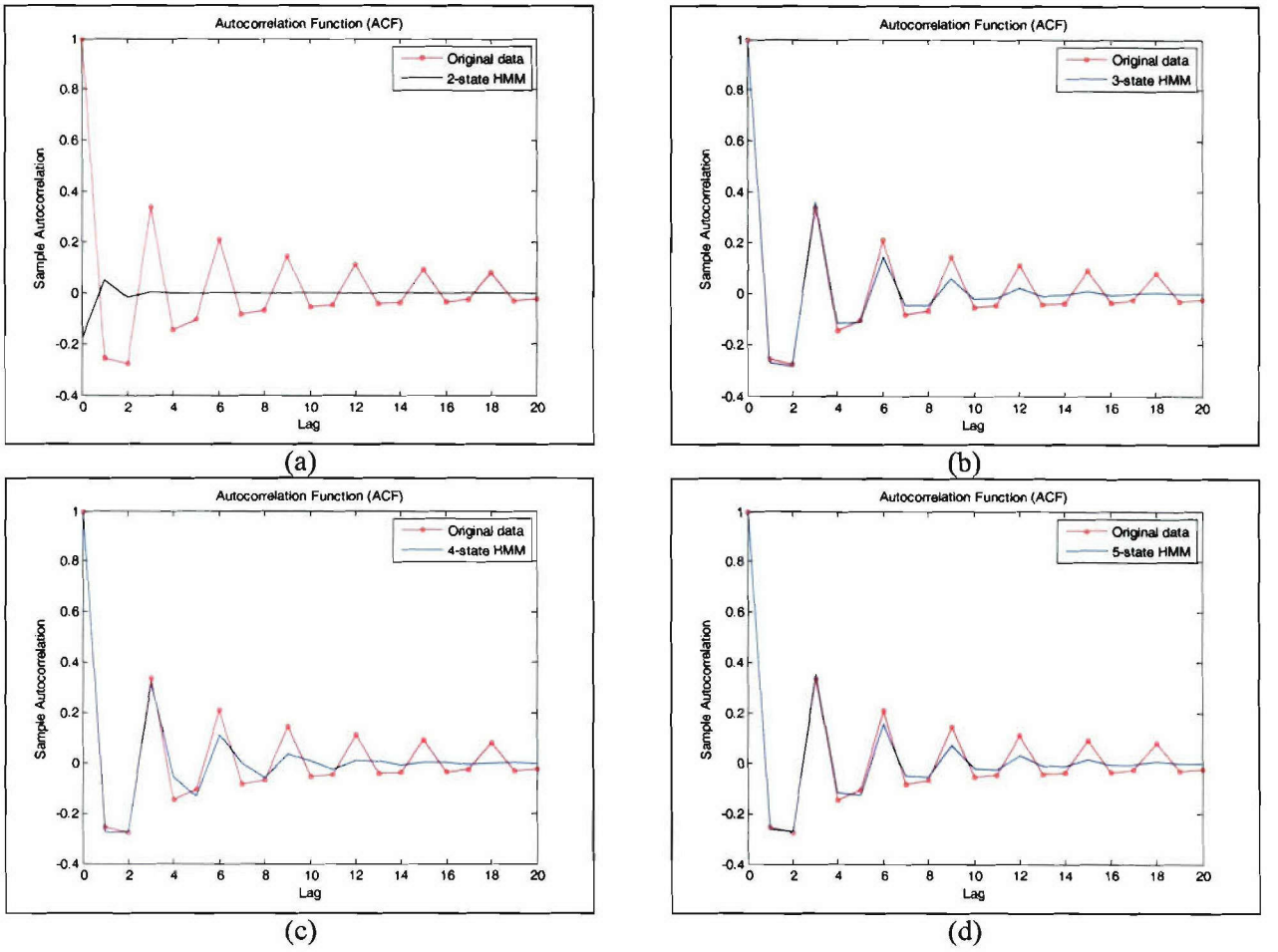

Figure 1.2-12 Comparison of the first 20 lags of autocorrelations of the bad trace and the corresponding HMMs. (a) 2-state HMM, (b) 3-state HMM, (c) 4-state HMM and (d) 5-state HMM.

Signal Classification in Cognitive Radio Using HMMs:

We developed a signal classification system for cognitive radios based on the hidden Markov models. Cognitive radio [Haykin (2005)] is an emerging technology in wireless communications that can improve the utilization of radio spectrum by incorporating some intelligence in their design. It can adapt with the environment and can change its particular transmission or reception parameters to execute its tasks efficiently without interfering with the primary users. One problem that a CR network usually face is the detection and classification of its low power signal that is present in the environment. Because of the low SNRs, these signals cannot be detected using traditional energy detection techniques. We address this problem by using higher order statistics of incoming signals and classifying them using the pattern recognition capabilities of HMMs combined with some cased-based learning techniques. The second order statistics of the signal in frequency domain, which is known as the Spectrum Correlation Function (SCF) and its corresponding peaks for the cycle frequency known as the α-domain profile [Gardner (1988)], are

used. Figure 1.2-13 shows the SCF of a modulated FSK signal and its corresponding α-domain profile.

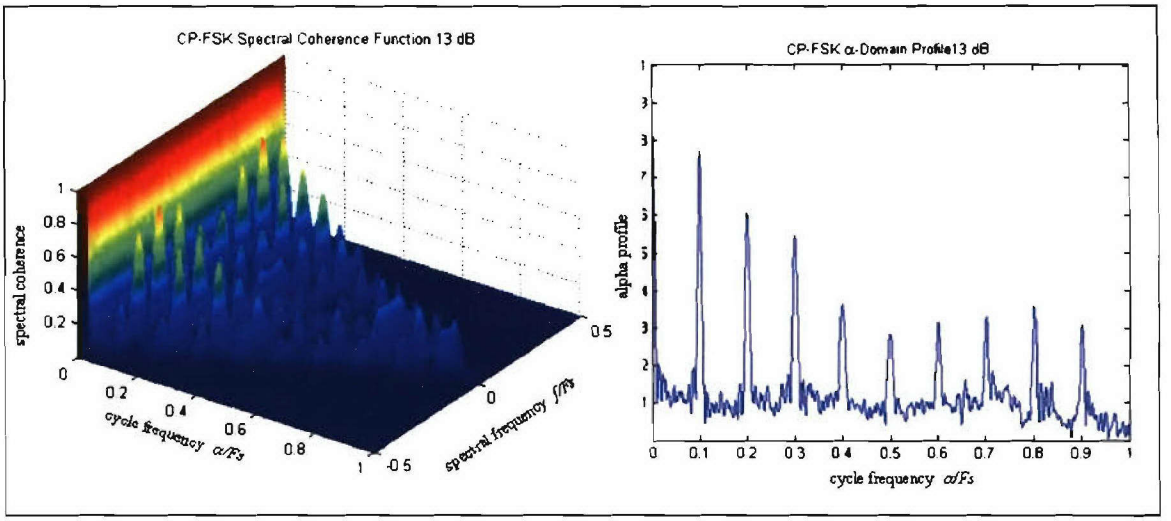

Figure 1.2-13 Continuous-phase binary FSK spectral coherence and α-domain profile with SNR= 9dB. The proposed system is based on the maximum likelihood estimates of the incoming signal using HMMs that are trained for different modulation schemes. We consider five different modulation types, i.e., AM, BPSK, FSK, MSK and QPSK.

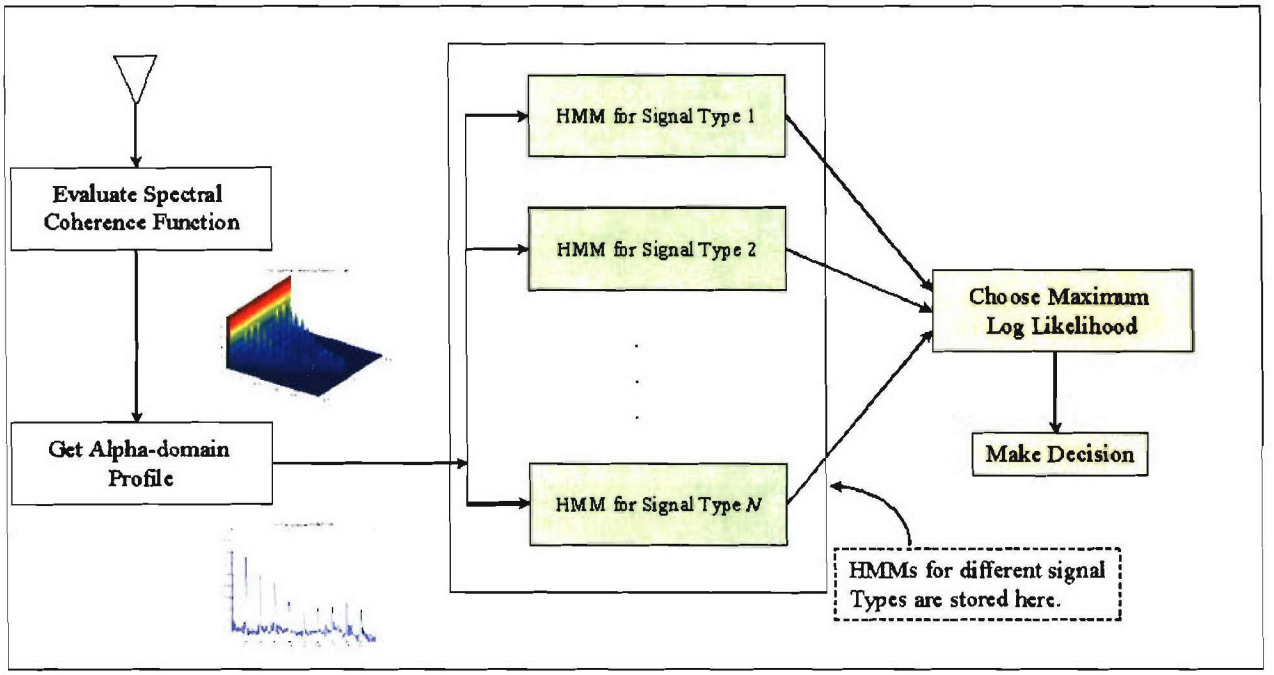

Figure 1.2-14 HMM cognition process block diagram.

Table 1.2-1 shows the confusion matrix with the SNR of training sequences at 13 dB and test signals having unknown SNRs that are randomly chosen from -3, 0, 3 and 13 dB. The block averages in all these cases are 100.

Table 1.2-1 Signal classification simulation result wi unknown SNR.

	AM	BPSK	FSK	MSK	QPSK
AM	494	0	0	0	0
BPSK	6	475	0	0	2
FSK	0	0	500	0	10
MSK	0	25	0	500	0
QPSK	0	0	0	0	488
%	**99.2**	**95**	**100**	**100**	**99.8**

References

J. Bendat and A. Piersol, Random Data: Analysis and Measurement Procedures (Wiley, 1986).

S. Haykin, "Cognitive Radio: Brain Empowered Wireless Communications", IEEE Journal on Selected Areas in Communications, vol 23, pp. 201-220, February 2005.

W. A. Gardner, Statistical Spectral Analysis: A Non-Probabilistic Theory, Prentice Hall, 1988.

A. Konrad, B. Y. Zhao, A. D. Joseph, R. Ludwig, "A Markov-based channel model algorithm for wireless networks," Wireless Networks, vol.9 no.3, pp.189-199, May 2003.

Subtask 1.2e Software radio integration into the AWINN demonstrations.

Task objective: The goal of this subtask is to integrate the software radio developed in Subtask 1.2a into AWINN activities.

Accomplishments: To achieve this objective, the software radio was designed with two distinct modes of operation: a communication mode and a data capture mode.

The communication mode is currently optimized for impulse UWB signals, however, it is capable of operating using any broadband communication technique (such as DSSS or OFDM). The only limitations on the types of signals that the receiver can handle are: (1) the 2.2 GHz analog input bandwidth limitation of the MAX104 ADCs, (2) the 8 GHz effective receiver sampling frequency, and (3) the processing power of the FPGA.

In the data capture mode, the receiver will simply capture ADC samples and store them in the FPGAs RAM memory. The data can then be processed in non-real time using one of the FPGAs PowerPC processors, or the sample values can be transmitted to a host computer via the USB interface. The number of samples that can be captured is limited by the amount of high-speed RAM memory that can be allocated, but is currently estimated to be around 256,000-512,000

samples—corresponding to about 32-64 μsec of captured data. A trigger signal input allows the receiver to estimate the time of arrival of received samples for ranging, and the ability to synchronize multiple receivers to a common clock signal allows for precise position location.

Personnel:

Chris R. Anderson – Transmitter and Receiver Hardware Development
Matt Blanton – Receiver FPGA Code Development

Subtask 1.2f UWB applications to technology development applicable to Sea-Basing: position location, ranging, and imaging.

Please refer to Task 4, TIP #2

1.1.4 Productivity

Journal publications

1. J. Ibrahim, R. Menon, and R.M Buehrer, "UWB signal detection based on sequence optimization for dense multipath channels," IEEE Communications Letters, vol. 10, issue 4, pp. 228-230, Apr 2006.

2. J. Ibrahim and R.M. Buehrer, "NBI Mitigation for UWB Systems Using Multiple Antenna Selection Diversity," to appear, IEEE Transactions on Vehicular Technologies.

3. J. Ibrahim and R.M. Buehrer, "Two-stage acquisition for UWB in dense multipath," IEEE Journal on Selected Areas in Communications, volume 24, issue 4, part 1, pp. 801-807, April 2006.

4. R.C. Palat, A. Annamalai and J.H. Reed, "Efficient Bit Error Rate Analysis of Bandlimited Cooperative STBC Networks under Time Synchronization Errors," submitted to IEEE Journal on Selected Areas of Communications: Cooperative Communications and Networking, February 2006.

Conference Publications

1. J. Ibrahim, R. Menon,, and R.M Buehrer, "UWB sequence optimization for enhanced energy capture and interference mitigation," in Proc. MILCOM 2005, pp. 2086 – 2092, vol. 4, October 2005.

2. J. Ibrahim and R.M. Buehrer, "A data-aided iterative UWB receiver with LDPC," in Proc. 2005 VTC Fall, vol. 1, pp. 33-37, September 2005.

3. J. Ibrahim and R.M. Buehrer, "A Modified Tracking Algorithm for UWB Pilot-Assisted Receivers," to appear, in Proc. 2006 ICUWB, September 2006.

4. C. R. Anderson and J. H. Reed, "Performance analysis of a time-interleaved sampling architecture for a software defined ultra wideband receiver," Proceedings 2005 Software Defined Radio Technical Conference, Anaheim, CA, November 2005, Digest of Papers.

5. D. Agarwal, C. R. Anderson, and P. M. Athanas, "An 8 GHz ultra wideband transceiver prototyping testbed," IEEE 16th International Workshop on Rapid System Prototyping, Montreal, Canada, June 2005, pp. 121-127.

6. S. Venkatesh, C. R. Anderson, R. M Buehrer, and J. H. Reed, "On the use of pilot-assisted matched filtering in UWB time-interleaved sampling," to appear in IEEE International Conference on Ultra Wideband, September 2006.

7. R.C. Palat, A. Annamalai and J.H. Reed, "Probability of Error Analysis under Arbitrary Fading and Power Allocation for Decode and Forward Cooperative Communication," submitted to IEEE Communication Theory Workshop--CTW 2006, Dorado, Puerto Rico, May 21 - 24, 2006.

8. R.C. Palat, A. Annamalai and J.H. Reed, "Node Density and Range Improvement in Cooperative Networks Using Randomized Space-Time Block Coding with Time Synchronization Errors," submitted to IEEE Workshop on Sensor Array and Multi-Channel Processing--SAM 2006, Waltham, Massachusetts, July 12 - 14, 2006.

9. R.C. Palat, A. Annamalai and J.H. Reed, "Efficient ABER Analysis of Bandlimited Cooperative Communication under Time Synchronization Errors," submitted to IEEE Global Communications Conference--GLOBECOM 2006, San Francisco, California, November 27 - December 1, 2006.

10. R.C. Palat, A. Annamalai and J.H. Reed, "On Decode and Forward Cooperative Communication in Wireless Networks," submitted to IEEE Global Communications Conference--GLOBECOM 2006, San Francisco, California, November 27 - December 1, 2006.

11. R.C. Palat, A. Annamalai and J.H. Reed, "Cooperative Relaying for Ad-Hoc Ground Networks Using Swarm UAVS," presented at IEEE Military Communications Conference--MILCOM 05, Atlantic City, New Jersey, October 17 - 21, 2005, page numbers not available.

12. S. Venkatesh and R.M. Buehrer, "A Linear Programming Approach to NLOS Error Mitigation in Sensor Networks," submitted to International Conference on Information Processing in Sensor Networks--IPSN 06, Nashville, Tennessee, April 19 - 21, 2006.

13. S. Venkatesh and R.M. Buehrer, "Some Insights from Bounds on Sensor Localization," submitted to IEEE International Symposium on a World of Wireless, Mobile and Multimedia Networks--WOWMOM 06, Niagara Falls, Buffalo, New York, June 26 - 29, 2006.

14. Ihsan Akbar, Kyouwoong Kim and Jeffrey H. Reed, "Signal Detection and Classification in Cognitive Radio Using HMMs," to be submitted in the *Dynamic Spectrum Access Network 2007 (DySPAN 2007)*, April 2007.

15. Ihsan Akbar and William H. Tranter, "A New Approach to Dynamic Spectrum Allocation in Cognitive Radio Using HMMs," to be submitted in the *Dynamic Spectrum Access Network 2007 (DySPAN 2007)*, April 2007.

Students completed

1. C. R. Anderson, "A Software Defined Ultra Wideband Communication System Testbed for Communications, Ranging, or Imaging", PhD, 2006

2. H. I. Volos, "Ultra Wideband Ranging and Link Budget Design for Naval Crane Applications," MS, 2006.

1.3 Task 1.3 Collaborative and Secure Wireless Communications

1.3.1 Overview

Both sensor networks and swarms of autonomous mobile robots have the potential to perform useful tasks, such as measuring temperature and soil moisture levels for crop management, monitoring seismic activity for earthquake prediction, or monitoring troop movements in a battlefield. Robot swarms can work cooperatively to find missing people or sweep an area for mines. In addition to peer-to-peer message passing, all of these activities require communications with the network outside of the immediate range of the nodes.

This project focused on a hybrid approach to propagate information to and from a distributed, possibly mobile, sensor network. The proposed approach presents a conceptual change to how we interact to sensor networks. When humans interact with a sensor network, it is often more intuitive to treat the network as a single entity instead of addressing individual nodes. Queries such as "What is the wind velocity in Sector 2?" and alerts or responses such as "There is seismic activity near the river." allow us to abstract away the lower-level topology issues. The solution persued here is to essentially give the network a single voice, where it responds to queries as a single entity. The project explores an unconventional method in the physical transport of information, along with collaborative methods of propagating information in response to a query, and is distinguished from the conventional store-forward packet approach. This method has numerous advantages: it forms a fully homogenous network, nodes have reduced transmitter power requirements, it is highly fault tolerant, and it is fair in its ability to share the energy burden with all nodes in the network. In addition, the modulation strategy and propagation protocol are simple, requiring little in terms of computation.

Organization: This task is managed by Directors of Virginia Tech Configurable Computing Lab using the following personnel:

Peter Athanas, Co-Director
Mark Jones, Co-Director
Deepak Agarwal, MSEE (graduated)
Brian Marshall, MSEE (graduated)
Todd Flemming, PhD student
Tingting Meng, PhD student
Yousef Islander, PhD student
James Webb, MSEE student
Matthew Blanton, MSEE student
Marc Somers, MSEE student
Lael Matthews, MSEE student

Summary: Sensor fields and autonomous swarms of mobile robots need to communicate with devices outside of their immediate range to fulfill their missions. Traditionally, this has required nodes to either: a) have strong transmitters powered by heavy batteries, b) be near relay stations, or c) be positioned such that a message can be relayed from the source through a chain of nodes to the base station. Option A increases cost and is inappropriate when size and weight matter (ex. fields of inconspicuous sensors or small unmanned aerial vehicles) as well as increasing the probabilities of interception. Option B complicates deployment by requiring relay stations to be distributed near sensor fields and along the path of mobile robots. Option C causes nodes that are near the base station to consume more energy from relaying traffic than nodes that are at the edge of deployment. These limitations have caused researchers to examine alternative approaches.

Other approaches [1-37] have been demonstrated that allow multiple nodes to transmit a message to gain distance, increase data rate, or to combat interference; these approaches are collectively called *cooperative communications* [1]. Two approaches that are under frequent investigation include distributed beam forming and distributed space-time coding; these are both instances of distributed diversity.

Diversity schemes transmit messages over multiple channels to minimize chance of loss. Common diversity schemes include space diversity, time diversity, frequency diversity, and code diversity. Distributed diversity schemes [1-37] use antennas from multiple independent nodes, and thus are at least space diversity schemes.

Beamforming uses precise positioning, timing, and carrier phase alignment to direct a signal to the receiver; this results in an n^2 power gain, where n is the number of nodes. Distributed beamforming [23-29] uses independent transmitters to direct the beam. Barriac et al. [26] demonstrate that this requires nodes to know their relative positions to within a small fraction of the carrier wavelength; this can be problematic, especially if the carrier is at a high frequency and if the transmitters are in motion. Mudumbai et al. [29] propose an alternative approach that relies on random phase perturbations at the transmitters and feedback from the base station to align the beam; this does not require positional information, but has other drawbacks. After the base station initiates communication, the combined signal coming from the transmitters is likely to be weak because the transmitters' carriers are not yet aligned. The base station must be able to detect small improvements in this very weak signal in order to provide proper feedback to the nodes. Also, it requires a large number of iterations to establish coherence and each iteration requires one round-trip-time between the transmitters and base station.

Transmitters that implement space-time coding split data across multiple antennas and use orthogonal channels; this produces a diversity gain but not a power gain [29]. Distributed space-time coding systems [30-37] use independent transmitters. Mitran et. al. describe one of these systems in [35]. A transmitter sends a symbol. Repeaters decode the symbol in a fraction of the symbol's period then repeat it for the remainder of the period using a different code than the transmitter used. The receiver must know the number of repeaters, the codes they used, and the amount of time that they repeated the message. The receiver uses this information to construct its own codebook, which is used to decode the combined signal. Mitran et. al. [35] prove the existence of codes which will make this scheme work, but do not show how to generate these codes. Mitran et. al. assume that delays between nodes are restricted to integer multiples of the symbol period to construct the proof; this either restricts the positions of repeaters to precise relative positions or requires repeaters to delay their signals based on precise position information.

1.3.2 Task Activities

Task Objectives: This project created a method to enable independent wireless transmitters to combine power to communicate with devices outside their immediate range. This is not store-and-forward, distributed beamforming, or space-time coding approach. Instead, all nodes will simultaneously broadcast the same symbol on the same channel without using different code books and without aligning carriers. This hybrid effort is divided into two parts. The first part is to analyze modulation schemes that enable signals to combine to produce a stronger signal when multiple nodes transmit the same symbol on the same channel at the same time. The second part concentrates on new synchronization schemes that enable multiple independent nodes to simultaneously transmit identical symbols. The first part focuses on the physical transport level,

while the second part relates to both the transport and network layers of the link. The synchronization schemes need to align symbols but do not need to align carriers; the new modulation schemes make carrier alignment unnecessary. A receiver should not have to adjust coding based on node position or on the number of participating nodes; in fact, it should be able to be totally unaware of the number of participating nodes.

Accomplishments: The investigators were able to demonstrate these concepts in a working laboratory prototype. The results obtained were encouraging, promoting the need to refine the concepts and apply them to broader domains. In this project, a variety of modulation schemes were examined along with one synchronization scheme that satisfied the project objectives. The investigators have demonstrated a system with one of the modulation schemes over-the-air with wired synchronization. The investigators demonstrated another system with a different modulation scheme over-the-air, this time with wireless synchronization; this second system had two independent transmitting nodes. The investigators intend to consider additional modulation schemes, synchronization schemes, and node selection schemes. The investigators also plan to consider multiple-access schemes and test this approach with a larger number of nodes.

Concept Viability

This section is organized in two parts. The first section briefly describes each of the modulation schemes considered so far. The second section describes *Ensemble Synchronization* in detail, including the effect of node position on power gain.

Modulation Schemes

The first modulation scheme the investigators found is Random On-Off Keying (ROOK). This uses the presence of a band-limited pseudo-random signal to indicate a one and its absence to indicate a zero. This type of signal is inherently power-additive; if n nodes simultaneously transmit a pseudo-random signal, then the signals will combine to produce n times the power of a single transmitter. Pseudo-random signals must be uncorrelated over the short term; this occurs automatically when the pseudo-random sequence is long, the pseudo-random generators are free-running, and the generators are powered up at slightly different times. The investigators tested this scheme over-the-air using two transmitters synchronized by cable.

The second modulation scheme is a combination of ROOK and Frequency Shift Keying (FSK). The frequency band is split into two halves; nodes transmit a pseudo-random signal in the lower half of the band to represent a *0* and transmit a pseudo-random signal in the top half to represent *1*. Like the first scheme, if n nodes simultaneously transmit the same symbol then the signals will combine to produce n times the power of a single transmitter. This scheme was simulated but not tested over the air.

The third modulation scheme is Random-Phase Frequency Shift Keying (RPFSK) (Figure 1). Like FSK, each symbol is associated with a frequency. Transmitters split each symbol period into several chips and give each chip a different pseudo-random phase. When the transmissions from several nodes combine over the air, some parts of each symbol reinforce each other and some parts weaken each other (Figure). On average, if n nodes transmit the same symbol simultaneously, then the combined signal power will be n times as large as the power from a single transmitter. The power gain variance decreases as the number of chips increase. The investigators tested RPFSK over-the-air using two independent transceivers and one receiver. The two transceivers successfully produced a combined signal that was stronger than the individual signals; this combined signal produced a lower bit error rate and a lower packet loss

rate than the individual signals as measured by the receiver. This test used the over-the-air synchronization scheme described below.

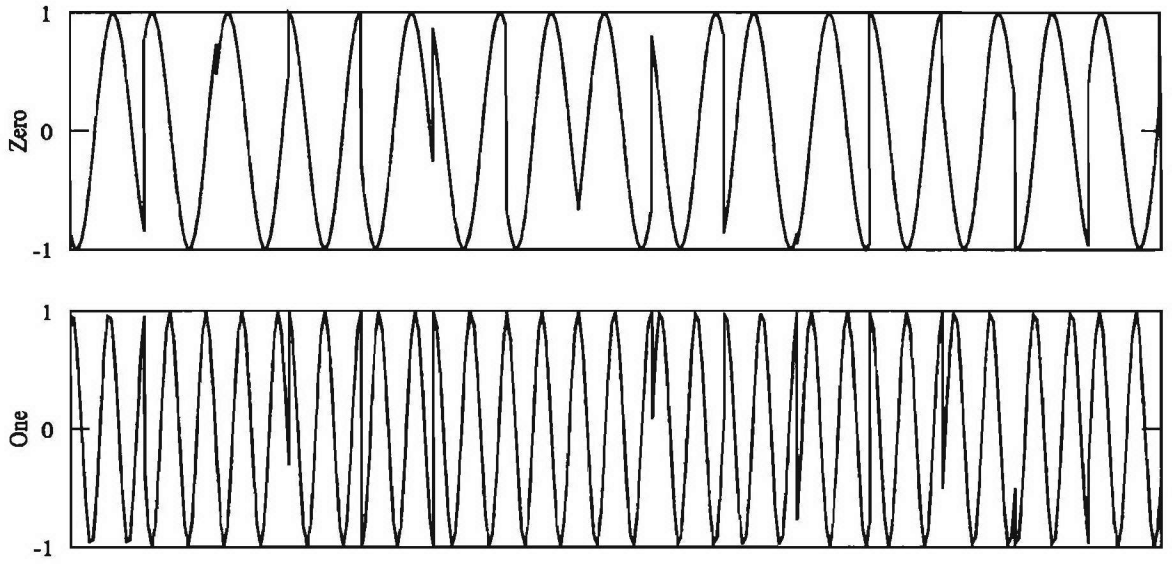

Figure 1.3-1 Random-Phase Binary Shift Keying for two symbols (zero and one).

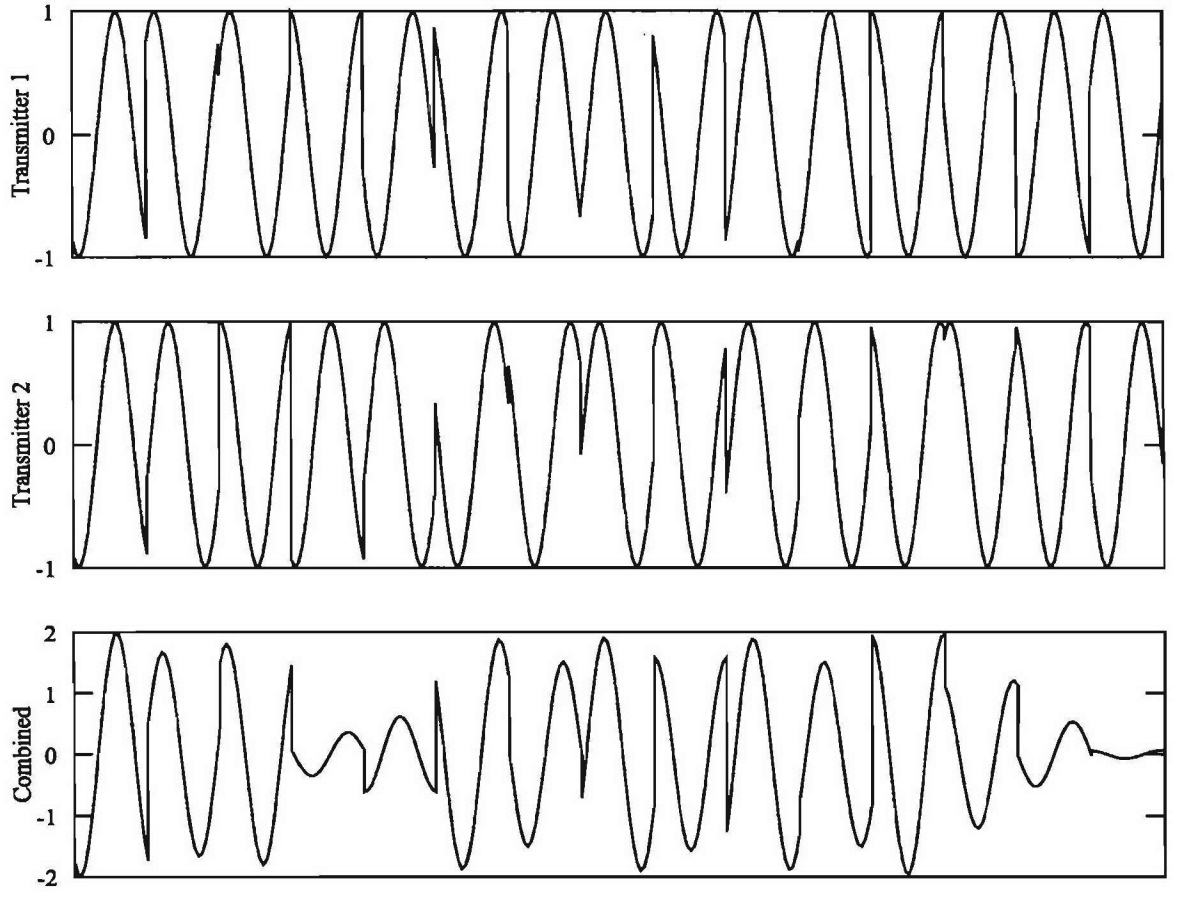

Figure 1.3-2 Combination of two RPFSK signals.

Ensemble Synchronization

The synchronization scheme used is tentatively named *Ensemble Synchronization.* When a node needs to transmit a message a long distance, it first enlists the aid of its nearby neighbors. The source node then switches to transmit mode and the neighbors switch to repeater mode (Figure 1.3-). The source node transmits symbols sequentially (Figure 1.3-4). The repeaters listen for activity on the channel. When they detect a symbol on the channel, they immediately start transmitting that same symbol for a fraction of the symbol period (Figure 1.3-5). They remain silent for the rest of the symbol period then start monitoring the channel for further activity.

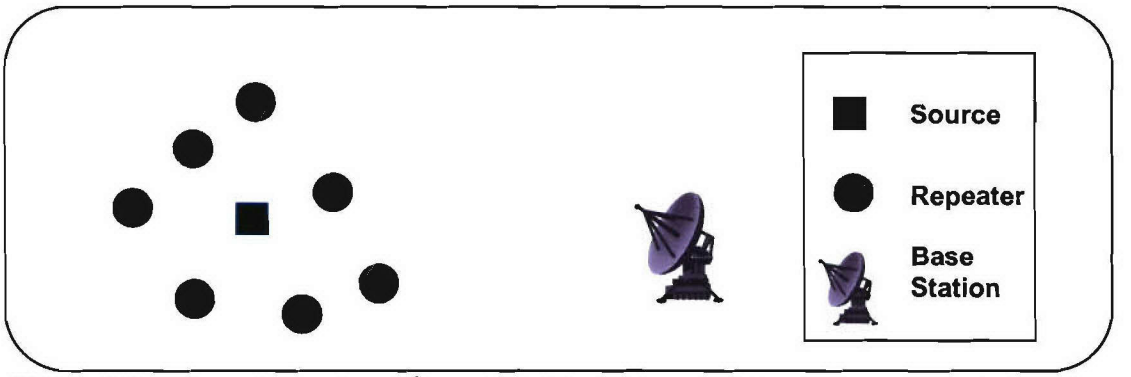

Figure 1.3-3 Ensemble node configuration. The source needs to send a message to the base station.

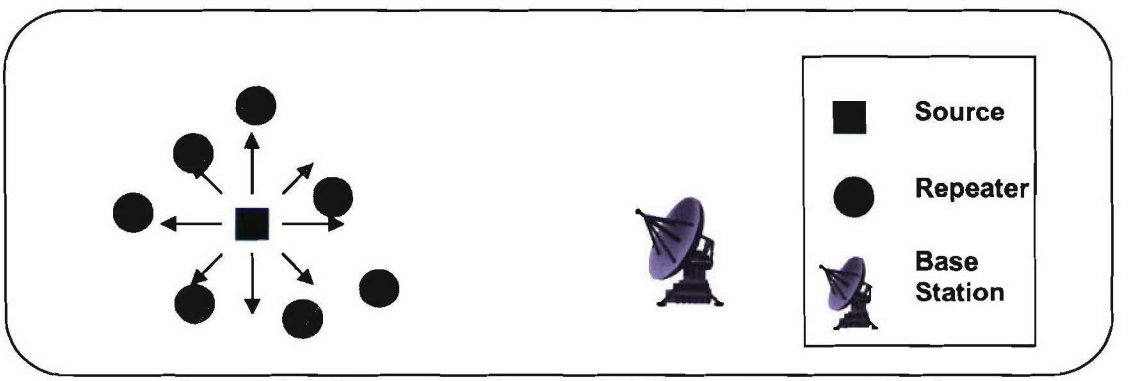

Figure 1.3-4 Source transmits a symbol X; repeaters detect signal.

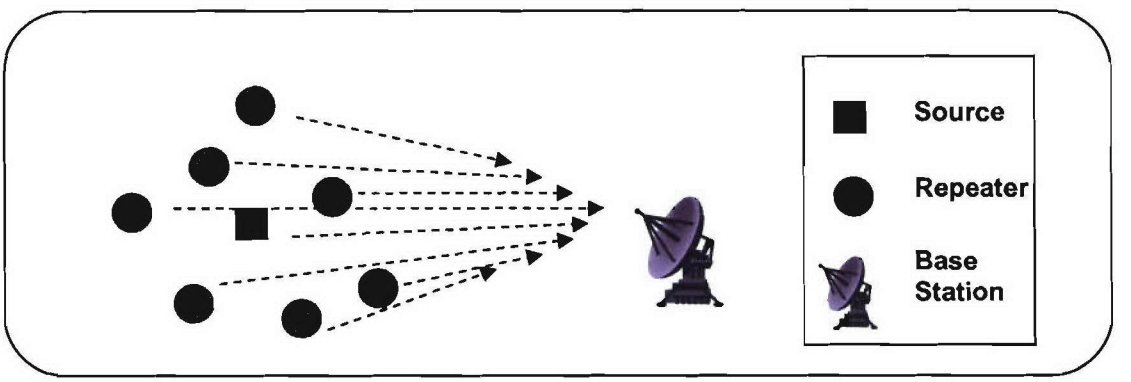

Figure 1.3-5 Repeaters transmit X while source continues transmitting X.

The duration that the repeaters send a symbol is based on their positions relative to the source node. The farther the repeaters are from the source node, the shorter the duration must be to prevent inter-symbol interference. When the repeaters are close to the source, the repeat duration is longer and the combined signal is stronger.

Ensemble synchronization is similar to the synchronization scheme described by Mitran et al. [35] for space-time-coded systems. Unlike [35], Ensemble synchronization does not rely on orthogonal channels; instead the repeaters all transmit on the same channel as the source without using different codes. Ensemble receivers do not need to know about the presence of Ensemble repeaters in order to decode messages; the combined signal has the same modulation and coding as the original signal. Ensemble synchronization does not require precise channel estimation or node placement; only the distance between the source and farthest repeater must be known. Finally, Ensemble synchronization works on modulation schemes to provide power gain, not just diversity gain.

Repeat Duration

Consider the case where there is only one repeater (Figure 1.3-6). Let d_{SR} be the distance between the source and repeater antennas, d_{SD} be the distance between the source and destination antennas, and d_{RD} be the distance between the repeater and destination antennas (Figure 1.3-). Let t_S be the symbol duration. Let t_D be the time it takes a repeater to detect a symbol and begin repeating it after the symbol's initial edge reaches the repeater. Let t_R (repeat duration) be the amount of time the repeater transmits a symbol. Also let c be the speed of light. To prevent inter-symbol interference, the tail edge from the repeater must arrive at the receiver no later than the tail edge from the source. It can be shown that this condition is met when Condition 1 is met. Condition 2 describes a simplified but looser bound. If the positions of all repeaters are within r_{max} of the source and all repeaters have the same t_R, then Condition 3 may be used. t_R must be positive; therefore Condition 3 places an upper bound on r_{max}. It also can be shown that repeaters will not enter into a feedback loop if these conditions are met.

$$\textit{Condition 1} \qquad t_R \le (d_{SD} - d_{SR} - d_{RD})/c + t_S - t_D \qquad (1.3\text{-}1)$$

$$\textit{Condition 2} \qquad t_R \le t_S - t_D - 2d_{SR}/c \qquad (1.3\text{-}2)$$

$$\textit{Condition 3} \qquad t_R \le t_S - t_D - 2r_{\max}/c \qquad (1.3\text{-}3)$$

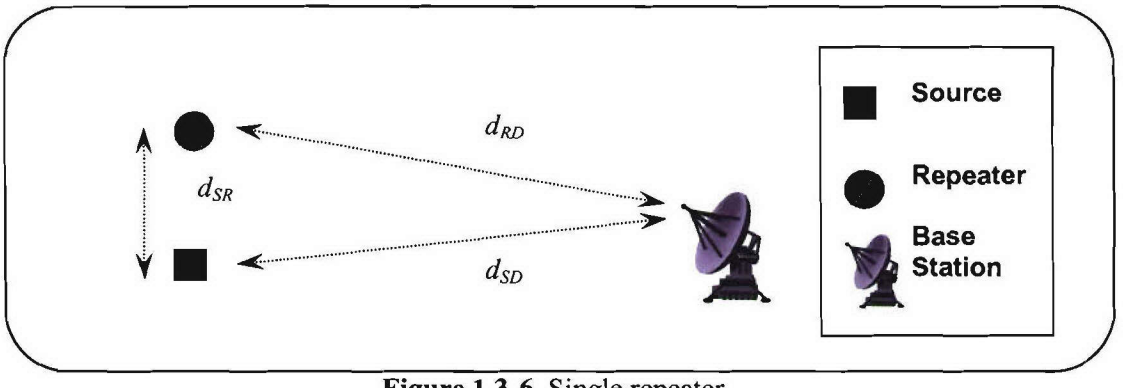

Figure 1.3-6 Single repeater.

Power Gain

The investigators used the channel model in 1.3-4 to predict the power gain from multiple transmitters. $E_{r,i}$ is the energy received for a single bit at the base station from transceiver i, where a and m are constants, $E_{t,i}$ is the transmitted energy, and d_i is the distance between the transceiver and the base station. Let n be the number of repeaters and g be the power gain from using multiple nodes; it can be shown that g has a lower bound given by Equation 1.3-5. This assumes that the energy received from multiple transceivers is additive, which is the case for the modulation schemes listed above. If the repeating nodes are all close to the source node (r_{max} is small) and the maximum repeat duration is used (t_R is close to t_S), then the power gain is close to $1+n$.

$$E_{r,i} = aE_{t,i} / d_i^m \qquad (1.3\text{-}4)$$

$$g \geq 1 + \frac{nt_R d_0^m}{t_S (d_0 + r_{\max})^m} \qquad (1.3\text{-}5)$$

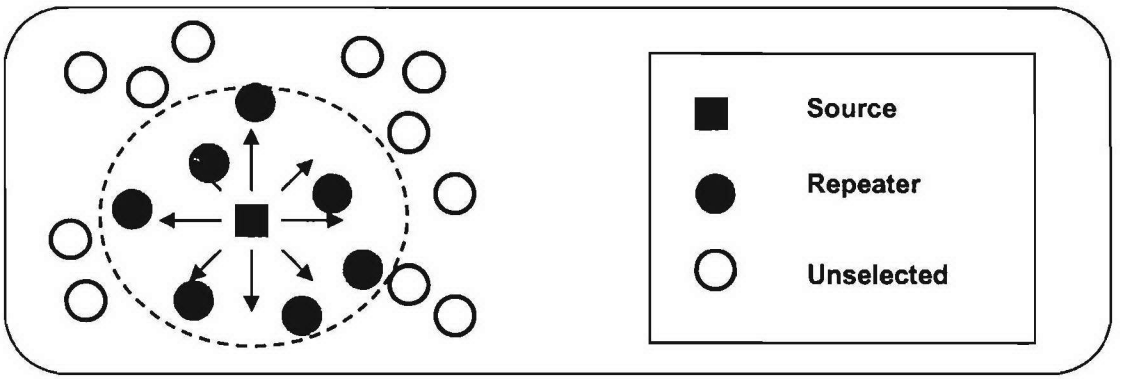

Figure 1.3-7 Repeater selection.

A source node needs to select nearby nodes to be repeaters in order to send a message to the base station (Figure 1.3-). The lower bound for g indicates a tradeoff; see (1.3-5). If the number of repeaters selected (n) is too low, then the energy received by the base station will be too low. However, if r_{max} is too high then the repeat duration (t_R) must be reduced to prevent inter-symbol interference; this will also cause the energy received by the base station to be too low. If the source selects more neighbors than necessary but not so many as to make r_{max} too big, then more nodes will expend energy than necessary. The source needs to select as many nodes as possible to repeat its signal without selecting too many.

The most direct way to select nodes to be repeaters is to select them by their distance to the source. One possible procedure is as follows: Start with an empty set. If the current set of nodes will not produce a signal strong enough to reach the base station, then add the nearest unselected node to the set and repeat. Future work will consider other selection approaches. For example, the source might avoid picking nodes that have low batteries; this may extend the average node lifetime.

References

1.3.3 Importance/Relevance

This work will enable clusters of low-power sensor nodes to be positioned far away from base stations, thus reducing deployment costs. These sensor nodes can monitor various environmental data such as temperature and soil moisture levels for crop management, monitor seismic activity for earthquake prediction, or monitor troop movements in a battlefield. This work will also enable clusters of cooperating mobile robots to travel far from base stations; this could extend the range of these robots when performing search and rescue or other tasks. Software defined radios have the potential of changing the fundamental usage model of wireless communications devices, but the capabilities of these transceivers are often limited by the speed of the underlying processors. Here we make an attempt to solve this problem by using reconfigurable architectures to develop custom datapaths which can handle these high data rates using commercially available FPGAs as an alternative to custom ASICs which lead to the obvious cost and development time benefits. An added advantage of such architecture is the capability to use run-time reconfigurablity to adapt to the effects of pulse shaping, channel coding, error control, and network algorithms on UWB communication. It can also be used to implement advanced cryptosystems or obfuscate communication.

1.3.4 Productivity

Conference Publications

1. Deepak Agarwal, Christopher Anderson, and Peter Athanas, "An 8 GHz Ultra Wideband Transceiver Testbed" at the 16th IEEE International Workshop on Rapid System Prototyping, Montreal, Canada, June 2005.
2. P. Athanas, J. Edmison, M. Jones, T. Mahar, B. Muzal, C. Patterson, J. Stroud J. Graf and B. Polakowski , "Hardware and Software Black Boxes: Preliminary Results for the Secure Software Platform," at the Engineering Reconfigurable Systems and Algorithms Conference, part of the 2005 International MultiConference in Computer Science and Computer Engineering, Las Vegas, NV, June 2005.
3. Anthony J. Mahar, Peter M. Athanas, Stephen D. Craven, Joshua N. Edmison, and Jonathan Graf, "Design and Characterization of a Hardware Encryption Management Unit for Secure Computing Platforms", Proceedings of the 39th Hawaii International Conference on System Sciences, HICSS 2006 / MOCHA 2006, Kauai, HI, Jan 2006.
4. T. Meng and P. Athanas, "Collaborative Signal Reinforcement for Sensor Networks," submitted to the IEEE Symposium on Artificial Life, Feb. 2007.
5. T. Flemming and P. Athanas, "Information Propagation in Sensor Networks," in preparation.
6. Brian Marshall, "A Swarm Intelligence Approach to Distributed Mobile Surveillance," Master's thesis, Virginia Tech, September 2005.
7. Deepak Agarwal, "An 8 GHz Ultra Wideband Transceiver Testbed," Master's thesis, Virginia Tech, December 2005.
8. Matt Blanton, "An FPGA Software-Defined Ultra Wideband Transceiver," Master's thesis, Virginia Tech, September 2006.

Patents, Software, etc.

1. T. Meng and P. Athanas, "Collaborative Method for Wireless Communications"

2. T. Flemming, P. Athanas, and M. Jones, "Signal reinforcement through collaborative reinforcement".

Students completed

1. Brian Marshall, "A Swarm Intelligence Approach to Distributed Mobile Surveillance," Master's thesis, Virginia Tech, September 2005.
2. Deepak Agarwal, "An 8 GHz Ultra Wideband Transceiver Testbed," Master's thesis, Virginia Tech, December 2005.
3. Matt Blanton, "An FPGA Software-Defined Ultra Wideband Transceiver," Master's thesis, Virginia Tech, September 2006.

Students supported:

Deepak Agarwal, Jan. 2005 – Dec. 2005.
Brian Marshall, Jan. 2005 – Dec. 15, 2005.
Todd Flemming, Jan. 2005 – Dec. 15, 2005.
Tingting Meng, Jan. 2005 – December 15, 2005.
Yousef Islander, Jan. 2005 – December 15, 2005.
James Webb, Jan. 2006 – May 2006.
Matthew Blanton, Jan. 2006 – Sep. 2005.
Marc Somers, Jan. 2005 – Jun. 2005.
Lael Matthews, Jan. 2006 – Jun. 2006.

Faculty supported:

Peter Athanas, Jan. 15, 2005 – present
Mark Jones, Jan. 15, 2005 – present

2. TASK 2 Secure and Robust Networks

2.1 Task 2.1 Ad Hoc Networks

2.1.1 Overview

Task goal: This task investigated core network capabilities for quality of service (QoS), security, and routing in ad hoc networks, especially mobile ad hoc networks (MANETs).

Organization: This task was directed by Scott F. Midkiff and involved the following personnel. The period of participation is noted for personnel not involved for the duration of the task.

Scott F. Midkiff, faculty (task director)
Luiz A. DaSilva, faculty
Nathaniel J. Davis, IV, faculty (1/15/05-8/14/05)
Y. Thomas Hou, faculty
Shiwen Mao, post-doctoral researcher (1/15/05-3/31/06)
George C. Hadjichristofi, GRA (1/15/05-5/14/05), post-doctoral researcher (7/25/05-10/31/06)
Waltemar M. de Sousa, GRA (5/15/05-7/31/06)
Unghee Lee, GRA (33% for 4/1/05-5/14/05, 100% for 5/15/05-5/14/06)
Xiaojun Wang, GRA (06/01/05-01/01/06)

Summary: Our research in AWINN Task 2.1 focused on system aspects of ad hoc networks, especially MANETs, with emphasis on improving the capabilities and performance of core network capabilities for quality of service (QoS), security, and routing. We completed and extended work on security mechanisms for ad hoc networks initiated during the NAVCIITI project. We integrated the routing and medium access control (MAC) protocols for ad hoc networks to support multiple channel (MC) operation and implemented support for both Internet Protocol (IP) version 6 (IPv6) and IP version 4 (IPv4), including with IP Security (IPsec) and key management. In addition, we enhanced the utility of the Optimized Link State Routing (OLSR) protocol by developing an application program interface (API) to provide network information to support integration with higher layer protocols and application programs. We designed and implemented a topology control (TC) mechanism that dynamically adjusts the transmission power of nodes to decrease interference and increase the effective network capacity. We also enhanced the capabilities of TopoView, our network monitoring tool, to support both IPv6 and IPv4 operation, as well as to display additional network information. Using the OLSR API, we developed a decentralized network monitoring tool, called OLSR Topology Viewer (OLSR-TV). Furthermore, we investigated how to exploit path diversity in ad hoc networks and demonstrated, through implementation of a cross-layer design using the OLSR API, improved support for video communication based on multiple-description (MD) video. The accomplishments and other details are provided in Section 2.1.2 below.

2.1.2 Task Activities

Subtask 2.1(a): Policy-based Quality of Service

Task objectives: The objectives of this subtask were to investigate and develop quality of service mechanisms that provide differential bandwidth allocation and scheduling based on traffic type, node type, and the current network environment. We increased the adaptability of the QoS

mechanisms to operate more robustly in a variety of environments. We also explored automatic adaptation at the physical and data link layers in response to application and network layer demands, as an initial exploration of cognitive networks as an approach to cross-layer optimization.

Accomplishments: We reevaluated work done and software developed for policy-based network management (PBNM) during the NAVCIITI project and made the decision to not modify the signaling components of PBNM to work with IPv6. The level of effort was too great to justify research benefits, mainly because we relied on an existing implementation of the Common Open Policy Services (COPS) protocol, which needed to be written by us "from scratch" to work with IPv6. Instead, we concurrently support both IPv4 and IPv6 in our test bed, thus allowing PBNM signaling to be carried in IPv4 datagrams. Policy enforcement points (PEPs) in this configuration need to be IPv6 aware to apply policies to both IPv4 and IPv6 traffic.

A more significant contribution in the AWINN project was the development of a topology control mechanism. The TC mechanism coordinates nodes' decisions regarding their transmission ranges (as determined by transmission power), with the objective of reducing interference and generating a physical network topology with higher effective network capacity than if TC were not used. Substantial theoretical development and simulation studies have been performed in the area of TC by the research community, but, prior to our work in this project, there had been a lack of experimental demonstration of the utility of TC techniques in reducing node energy consumption and radio interference.

Figure 2.1-1 shows the implementation structure of our TC mechanism in the Linux operating system. The TC mechanism is composed of four main modules: (i) the TC Engine; (ii) the MSG (Message) Controller; (iii) the Tx (Transmit) Controller; and (iv) the Rx (Receive) Controller. The TC Engine consists of the topology database manager and the topology controller. The topology database manager maintains information about the local neighborhood. This local neighborhood information is node-related information for nodes in the neighborhood, including a node's capabilities and link information, such as directionality and weight. The topology controller implements the distributed TC algorithm based on data collected from the topology database manager. It calculates a localized topology graph and controls a node's transmit power level by issuing commands directly to the wireless device driver. The MSG Controller temporarily stores node information exchanged between the TC Engine and the MSG Controller and generates and analyzes TC messages. The TC messages hold information regarding a node's visible neighborhood and its TC capabilities. The Tx Controller periodically broadcasts TC messages based on the operating system alarm handler. The Rx Controller processes TC messages and communicates the power level statistics of incoming packets to the TC Engine. The statistics are extracted from the wireless device driver.

The development of this mechanism required a number of adjustments to interact dynamically with the wireless device driver. The TC algorithm in the "Topology Controller" module was programmed using the BOOST Graph Library, or BGL.

A related publication is conference paper 5, listed in Section 2.1.4.

Links to other tasks: This subtask had natural synergies with Task 2.4 (Cross-Layer Optimization), as the mechanisms that support QoS in mobile ad hoc networks span the physical, data link, network, and application layers. It also integrated with Task 2.2 (Real-Time Resource Management, Communication, and Middleware) as some of the mechanisms developed here support real-time middleware developed in Task 2.2.

Personnel: The following personnel were assigned to this subtask.

Luiz A. DaSilva, faculty (subtask leader)
Scott F. Midkiff, faculty
Waltemar de Sousa, GRA

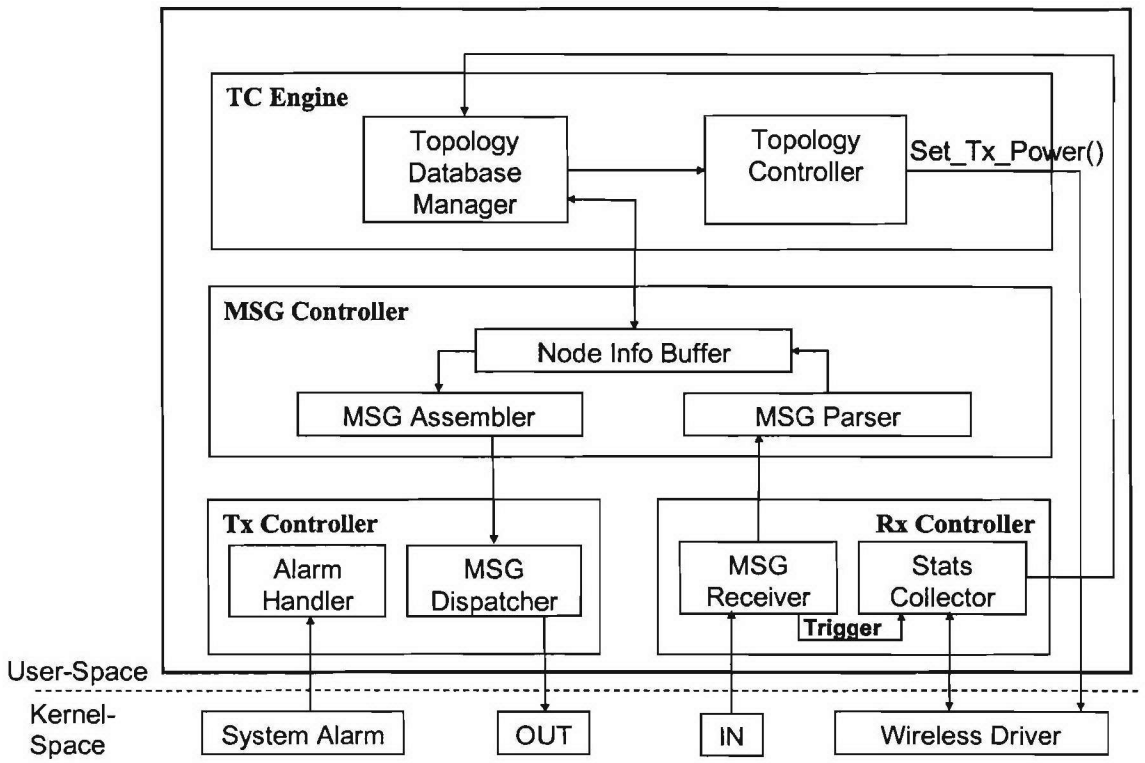

Figure 2.1-1 Implementation structure of the topology control mechanism.

Subtask 2.1(b): Security Mechanisms for Ad Hoc Environments

Task objectives: The objectives of this subtask were to investigate and, where feasible and deemed appropriate, develop security mechanisms that are efficient for ad hoc network environments. Our emphasis was on a distributed key management system (KMS) and associated shared trust schemes.

Accomplishments: Activities focused on the development of a distributed delegated certificate authority (DCA) and trust management scheme. The scheme utilizes a control plane of certificate authorities (CAs) and trusted peers, acting as repositories. It increases security service availability for mobile nodes and is at the top of the tier of services, as depicted in the pyramid of Figure 2.1-2, because it directly offers capabilities to network nodes. Distributed DCAs can be loaded offline from a root CA. If a DCA is not available to provide service to the nodes, then a temporary security association (SA) can be established using a node that has previously obtained a certificate of interest from a DCA. Finally, peer-to-peer trust can be established. Different levels of security should be associated with these three levels of authentication and trust. Trust with peers implies the use of a behavior grading scheme for key management, which is at the center of the pyramid in Figure 2.1-2. At the bottom of the pyramid, there is an intrusion detection system (IDS) that grades overall trust in the network. The concept of behavior grading

– at the local peer and network levels – is particularly important as it is integrated with the key management system to control functions such as revocation of a certificate. Overall, this KMS decreases the need of relying on strict identity authentication and provides a network picture of the trustworthiness of nodes that is independent of the type of IDS utilized in the network.

Performance results of the distributed DCAs and trust management scheme were obtained using a simulator. We evaluated the probability of a node being able to complete authentication using "out-of-band" mechanisms under different assumptions in a mobile ad hoc environment. In particular, our evaluation assessed the need and effectiveness of a control plane for DCAs and trusted peers. The analysis was carried out to investigate the time that it would take for a node to come within close proximity of a DCA or trusted peer and, thus, obtain a certificate.

In addition to simulation analysis, we identified the most suitable solution that would provide network -level security in our test bed and investigated deployment issues of IPsec over IPv6. An upgrade of the Linux kernel was necessary to improve support for IPv6 and IPsec and enable testing and integration of the network functionality in an IPv6-based network. The upgraded test bed utilized a recent Linux kernel with Fedora Core 3. Openswan, a user space IPsec implementation, was integrated with IPsec built into the Linux kernel, thus overcoming the functionality and interoperability limitations that existed when utilizing the FreeS/WAN implementation of IPsec. More specifically, with FreeS/WAN IPsec, a virtual interface was created for a tunnel with keys negotiated using the Internet Key Exchange (IKE) protocol. This allowed packets to be routed through that interface. The functionality of FreeS/WAN IPsec was limited because routing was used to determine the IPsec policy to be applied to every packet since packets destined for a particular subnet and requiring encryption had to be routed through the corresponding IPsec virtual interface. Furthermore, the MANET routing protocol operation conflicted with the FreeS/WAN IPsec operation. The routing protocol modified the subnet routing entries created by IPsec. Both of these limitations have been removed by deploying the Openswan IPsec mechanism since IPsec built into the kernel does not utilize IPsec virtual interfaces.

The KMS development started in the NAVCIITI project was further developed and, then, integrated and tested with Openswan in the AWINN project. The KMS enables certificates to be dynamically distributed in the network to aid in the establishment of security associations in a MANET by utilizing DCAs and trusted peers. We successfully extended the KMS implementation to accommodate SAs between nodes utilizing either IPv6 or IPv4. Any node can establish SAs by utilizing both its IPv4 and IPv6 addresses. The integrated KMS, Openswan, and Linux kernel IPsec mechanisms on our test bed were tested to ensure interoperability with other network functions, including OLSR with Multiple Channels, as investigated in Subtask 2.1(c). This routing and security systems integration was demonstrated during the final project demonstration on August 25, 2006.

Related publications are journal paper 9 and conference papers 16 and 17, listed in Section 2.1.4.

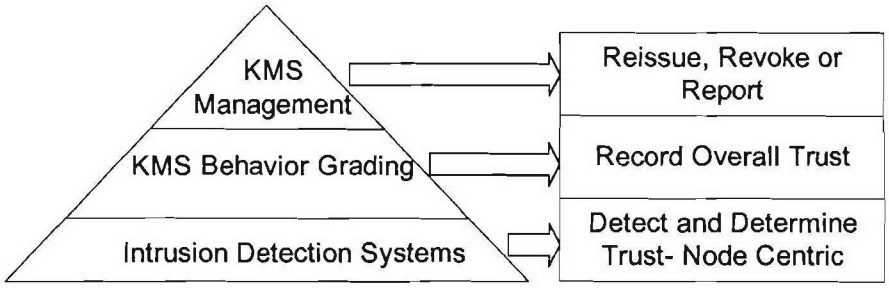

Figure 2.1-2 Illustration of tiers of a robust, secure scheme for key management and behavior grading.

Links to other tasks: This subtask has synergies with Subtask 2.1(c) and Task 2.4 (Cross-Layer Optimization) as link layer and, especially, network layer information can be employed to improve key management and other security functions. We deployed a prototype for evaluation in the test bed developed in Subtask 2.1(e) and used tools of Subtask 2.1(f).

Personnel: The following personnel were assigned to this subtask.

Scott F. Midkiff, faculty (subtask leader)
Nathaniel J. Davis, IV, faculty
George C. Hadjichristofi, GRA and post-doctoral research associate

Subtask 2.1(c): Ad Hoc Routing Optimization

Task objectives: The objectives of this subtask were to investigate schemes to improve routing and to use network layer functionality to improve other network services.

Accomplishments: Our focus was on employing a cross-layer design of the medium access control and routing layers to enable multi-channel operation for capacity improvement, in jointly supporting simultaneous use of both IPv4 and IPv6, and in extending the routing protocols to provide cross-layer optimization by providing network information to higher layer protocols and applications.

As a first step, we extended the design of the Destination-Sequenced Distance-Vector (DSDV) proactive MANET routing protocol to enable use of multiple channels at the MAC layer. The new protocol, DSDV for Multiple Channels (DSDV-MC) was designed and simulated using the ns2 simulation environment. Some illustrative results for a mobile, multi-hop ad hoc network are shown in Figures 2.1-3 and 2.1-4. Figure 2.1-3 compares the goodput (useful throughput) of a baseline case of using DSDV over a single channel with using DSDV-MC with 3 to 11 different channels. The results show that using multiple channels can substantially increase network goodput. Figure 2.1-4 compares the routing overhead for DSDV versus DSDV-MC with 3 to 11 channels. While there is some increase in overhead for DSDV-MC compared to single-channel DSDV, the increase is relatively modest. We also developed specific design principles to guide this and related research.

Through this work, we also designed a Channel Distribution Index (CDI) as a way to improve performance for channel assignment and implemented a mechanism using virtual interfaces that allows control of the channel used for packet forwarding. The CDI is a metric that indicates the fairness of channel distribution in a multi-channel network. Depending on the network topology and traffic pattern, the channel allocation can become unfair and this unfair distribution can

degrade network throughput. We identified the properties and proposed the definition of the CDI based on simulation studies using the Network Simulator 2 (ns2) package.

In addition, we implemented a Virtual Interface Module (VIM). The VIM driver is a logical network interface that implements special-purpose processing on data packets without actual physical packet transmission, while avoiding the complexity of changes to the kernel's network subsystem. This module plays a pivotal role in our prototype implementation, including channel decision, channel switching, and packet lookup functions. The VIM was integrated with existing routing protocols to provide multi-channel versions of the Open Shortest Path First with Minimum Connected Dominating Sets for Multiple Channels (OSPF-MCDS-MC or, simply, OMM) and the Optimized Link State Routing for Multiple Channels (OLSR-MC) MANET routing protocols. Note that OSPF-MCDS was developed as part of the NAVCIITI program and supported only IPv4. With regards to OLSR-MC, we have extended the Naval Research Laboratory (NRL) version of OLSR to operate with multiple channels in an integrated IPv4 and IPv6 environment, as well as concurrently support operation in both modes in the network. This concurrent operation in IPv4 and IPv6 was executed only in the NRL OLSR protocol and not OMM because the NRL version of OLSR supports both IPv4 and IPv6. As mentioned in Subtask 2.1(b), this version of OLSR-MC was successfully demonstrated on August 25, 2006.

Further work in this subtask focused on augmenting the NRL implementation of OLSR by adding network-wide information dissemination capabilities and developing a network information (NI) API that can access local routing information as well as the information disseminated by the routing protocol. The API extracts topology and other link and node state information, and provide the information to protocols and applications, typically at or above the networking layer. It can be accessed both locally and remotely via a client-server application that we developed. Information that was of special immediate interest for the purpose of the AWINN integration task (Task 2.4) was connectivity to a particular node (i.e., reachability information) in a Boolean form and the path length (hop count) to a particular destination. Other information included one-hop neighbor information for topology control calculations in Subtask 2.1(b), network-wide information for network monitoring in Subtask 2.1(f), and network-wide topology and packet drop rate information for video applications in Subtask 2.1(d).

Related publications are journal papers 1 and 2, conference papers 1, 3, 4, 6, 12, 18, and 19, and book chapter 1 as listed in Section 2.1.4.

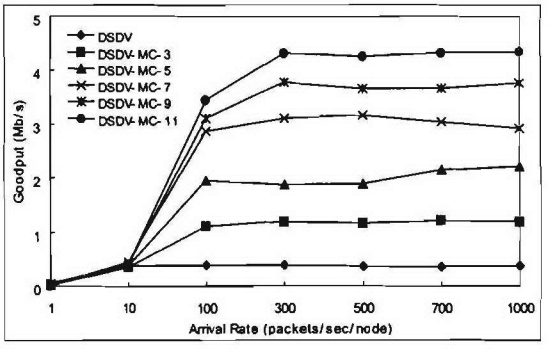

Figure 2.1-3 Goodput for a multi-hop mobile network for a varying packet arrival rate.

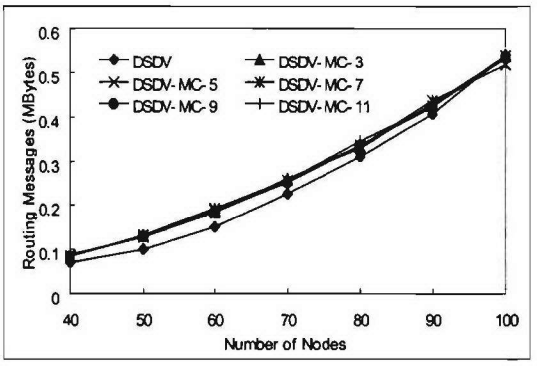

Figure 2.1-4 Routing overhead for a multi-hop mobile network for a varying number of nodes.

Links to other tasks: This subtask has direct ties to Task 2.4 (Cross-Layer Optimization) as our focus made the network layer a key part of our cross-layer optimization schemes. As a more tangible and direct link, our development of the NI API was guided in part by Task 2.2 (Real-Time Resource Management, Communication, and Middleware) and we integrated an application from Task 2.2 into our test bed which used the NI API. We also deployed a prototype of our key concepts in this task, including security, topology control, multi-channel routing, and the NI API for evaluation in the test bed developed in Subtask 2.1(e) and used tools of Subtask 2.1(f).

Personnel: The following personnel were assigned to this subtask.

Scott F. Midkiff, faculty (subtask leader)
Unghee Lee, GRA
George C. Hadjichristofi, post-doctoral research associate

Subtask 2.1(d): Cross-Layer Approach for Routing of Multiple Description Video over Ad Hoc Networks

Task objectives: The objectives of this subtask were to investigate a theoretical foundation for cross-layer approaches for carrying multiple description video over ad hoc networks and to build on this foundation to demonstrate key concepts via a prototype implementation.

Accomplishments: As developments in wireless ad hoc networks continue, there is an increasing expectation with regard to supporting content-rich multimedia communications (e.g., video) in military ad hoc networks. The recent advances in MD video coding have made multimedia applications feasible in such networks. In our approach, we exploit path diversity in ad hoc networks to better support video communications. Instead of just finding multiple paths in the network, we follow an application-centric, cross-layer routing approach with the objective of minimizing the overall video distortion. Furthermore, each video description is coded into multiple layers to cope with diversity in wireless link bandwidths. We found that a meta-heuristic approach, such as use of genetic algorithms (GAs), is effective in addressing this type of complex cross-layer optimization problem. We developed a detailed solution procedure for the GA-based approach, as well as a tight lower bound for video distortion. We developed numerical results to demonstrate the superior performance of the GA-based approach and compared it to several other approaches. This effort provided an important methodology for addressing complex cross-layer optimization problems, particularly those involving application and network layers.

Based on this research, we developed a prototype implementation to demonstrate better support for video communication in ad hoc networks. We implemented the MD algorithm for video over multi-path routing, including video codec, transport control, mobile ad hoc network emulation, and live display of video and video quality based on the peak signal to noise ratios (PSNR) curves. We deployed this implementation on two test bed networks (see Quarter 4 report) and proved that our MD algorithm provides acceptable video quality at the receiver. Furthermore, we demonstrated that cross-layer based multi-path routing improves video quality more than the two-disjoint path routing for MD-coded video, affirming the need for cross-layer optimization for video communications over ad hoc networks. Figure 2.1-5 shows the PSNR of the reconstructed frames delivered by the proposed algorithm and the traditional two-disjoint path routing algorithm. The video frames delivered by the proposed algorithm had much higher PSNR values than those delivered by the traditional algorithm. The successful operations of these components were demonstrated on December 8, 2005 to the AWINN principal investigators.

This prototype implementation was also integrated with the test bed developed in Subtask 2.1(e). The video application obtained network information from the NI API developed as part of Subtask 2.1(c) and utilized accessed topology information to improve video quality through an innovative form of multi-path routing. Figure 2.1-6 shows an example scenario of how the video application was deployed in the test bed. The video server and client were notebook computers, each connected to Gateway (GW) 1 and GW 12, respectively. The topology and link parameters, controlled by the Dynamic Switch, were extracted by the routing protocols developed in Subtask 2.1(c) and were distributed to the video server. The video server utilized a routing algorithm based on the aforementioned GA to take advantage of mesh connectivity and find a pair of paths from GW 1 to GW 12 for the video sessions.

Related publications are journal papers 3-5, 7, and 8, conference papers 2, 8, 11, 13, 14, and 21, and book chapter 1 as listed in Section 2.1.4.

Links to other tasks: This subtask had direct ties to Task 2.4 (Cross-Layer Optimization) as it considered cross-layer optimization schemes that involved applications, in this case, video. The prototype deployed for evaluation was integrated into the test bed developed in Subtask 2.1(e).

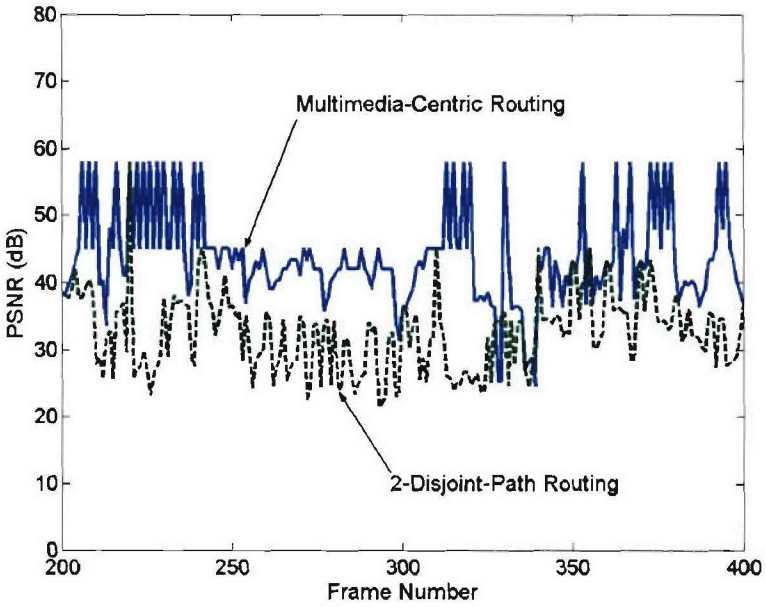

Figure 2.1-5 PSNR values of reconstructed videos.

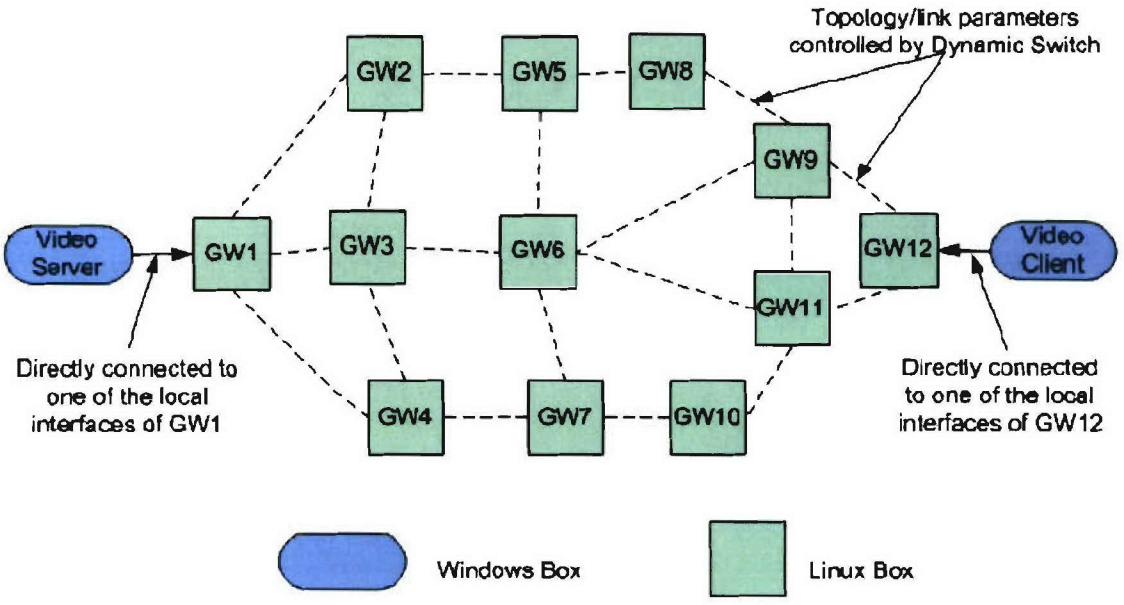

Figure 2.1-6 Integration of the prototype video application integration in the test bed.

Personnel: The following personnel were assigned to this subtask.

Y. Thomas Hou, faculty (subtask leader)
Shiwen Mao, post-doctoral research associate
Xiaojun Wang, GRA

Subtask 2.1(e): Test Bed Evaluation and Demonstration

Task objective: The objective of this subtask was to integrate and demonstrate through research prototype implementations key ideas from Subtasks 2.1(a), 2.1(b), 2.1(c), and 2.1(d) and, as feasible and appropriate, from Task 2.2 (Real-Time Resource Management, Communication, and Middleware), Task 2.3 (Network Interoperability and Quality of Service), and Task 2.4 (Cross-Layer Optimization). The objective involved exploring interactions between different components and functions and evaluating and demonstrating both functionality and performance.

Accomplishments: As noted in descriptions of Subtasks 2.1(a) through 2.1(d), we deployed and tested components to support the evolution of the test bed from supporting only IPv4 to supporting both IPv4 and IPv6. Some minor issues were uncovered and addressed. The majority of the task consisted of: (i) upgrading the operating system in test bed nodes to a recent version of Red Hat Fedora Core Linux; and (ii) testing test bed software and making fixes, as needed. Note that it was not efficient to support all "legacy" test bed capabilities from the NAVCIITI task because some third-party software packages, such as COPS, did not support IPv6 and it was well beyond the scope of this project to make such modifications. We also modified and tested the OLSR-MC configuration to support routing across logical subnets to support our test bed configuration. We extended the OLSR-MC protocol to disseminate network information over the entire network and we have developed an API to extract this information dynamically and provide it to software components in Subtask 2.1(a), 2.1(d), 2.1(f) and Task 2.2. We demonstrated the integration of IPsec, KMS, and OLSR-MC, with combined support of both IPv4 and IPv6 in OLSR-MC on August 25, 2006.

Links to other tasks: The test bed evaluation and demonstrations rely on results from Subtasks 2.1(a), 2.1(b), 2.1(c), 2.1(d), and 2.1(f) as well as Tasks 2.2, 2.3, and 2.4.

Personnel: The following personnel were assigned to this subtask.

Scott F. Midkiff, faculty (subtask leader)
Unghee Lee, GRA
George C. Hadjichristofi, post-doctoral research associate

Subtask 2.1(f): Configuration and Monitoring Tools

Task objectives: The objectives of this subtask were to investigate and develop software configuration and monitoring tools to facilitate network testing and demonstration.

Accomplishments: We enhanced our topology and node state monitor, TopoView, to run in a combined IPv4 and IPv6 environment by translating the IPv4 information acquired by SNMP using the reverse algorithm of OLSR-MC of Subtask 2.1(c). We elected to translate the IPv4-based information rather than to acquire the IPv6 information with SNMP, because the SNMP functionality that handled the routing table information of the IPv6 Management Information Base (MIB) had not yet been implemented in Linux, indicating the lack of maturity of this technology. The code to provide this functionality had to be, instead, written by us from "scratch" and did not provide any research benefits. In addition to providing IPv6 information, we augmented the functionality of TopoView to display the channel index information of the nodes that utilize OLSR-MC and to display the type of SAs established (IPv6 versus IPv4). Figure 2.1-7 depicts a screen capture of latest version of TopoView.

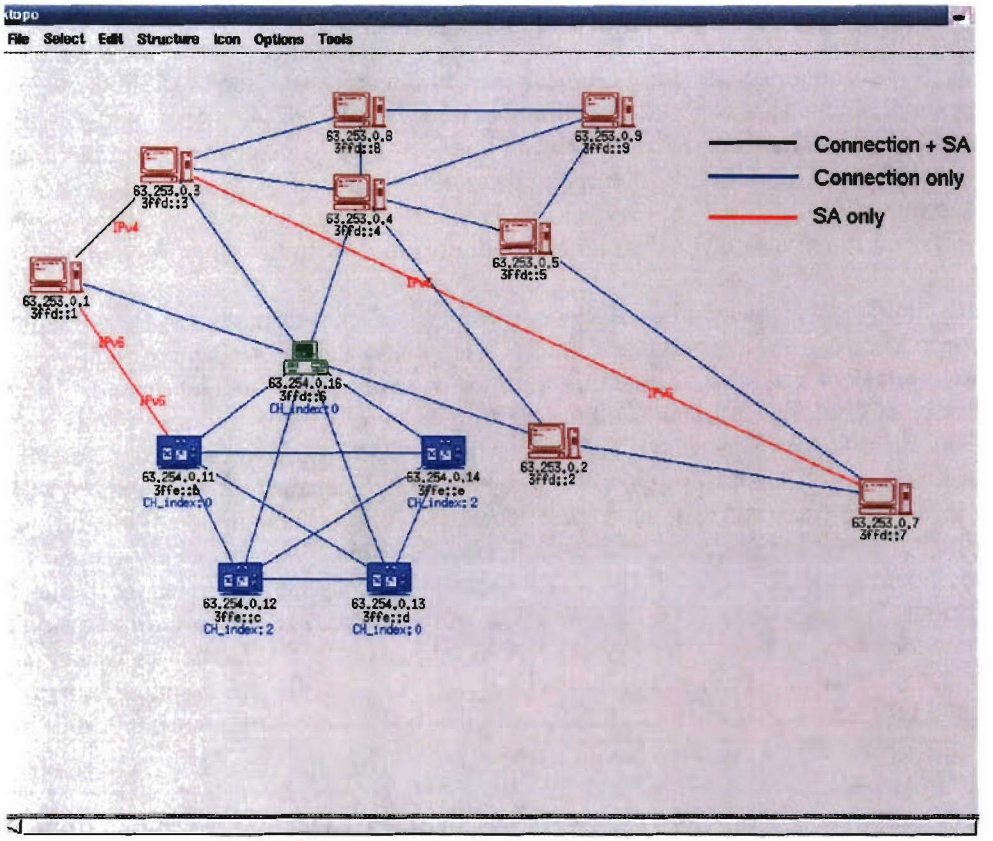

Figure 2.1-7 TopoView with IPv6 address, channel index, and IPv4/IPv6 SAs.

In addition to enhancing TopoView, we have developed a new network monitoring tool that utilizes the network information API of the NRL OLSR developed in Subtask 2.1(c). We call it OLSR Topology Viewer (OLSR-TV) as it provides a dynamic display of the network topology information together with packet drop information per link in the network collected by the routing protocol. Since OLSR-TV utilizes the existing communication transactions of OLSR, it has minimal impact on network overhead. OLSR-TV can be deployed on any computer in the network that uses OLSR. Figure 2.1-8 displays the connectivity of the test bed as extracted from OLSR on the dual-homed node with IPv6 address 3ffd::6/3ff3::10. The red, green, and blue lines indicate the quality of the wireless and emulated links in the network as determined by OLSR based on the drop rate of HELLO messages.

Links to other tasks: The tools support the test bed described above for Subtask 2.1(e).

Personnel: The following personnel were assigned to this subtask during the quarter.

Scott F. Midkiff, faculty (subtask leader)
George C. Hadjichristofi, post-doctoral associate (7/25/05-10/31/06)

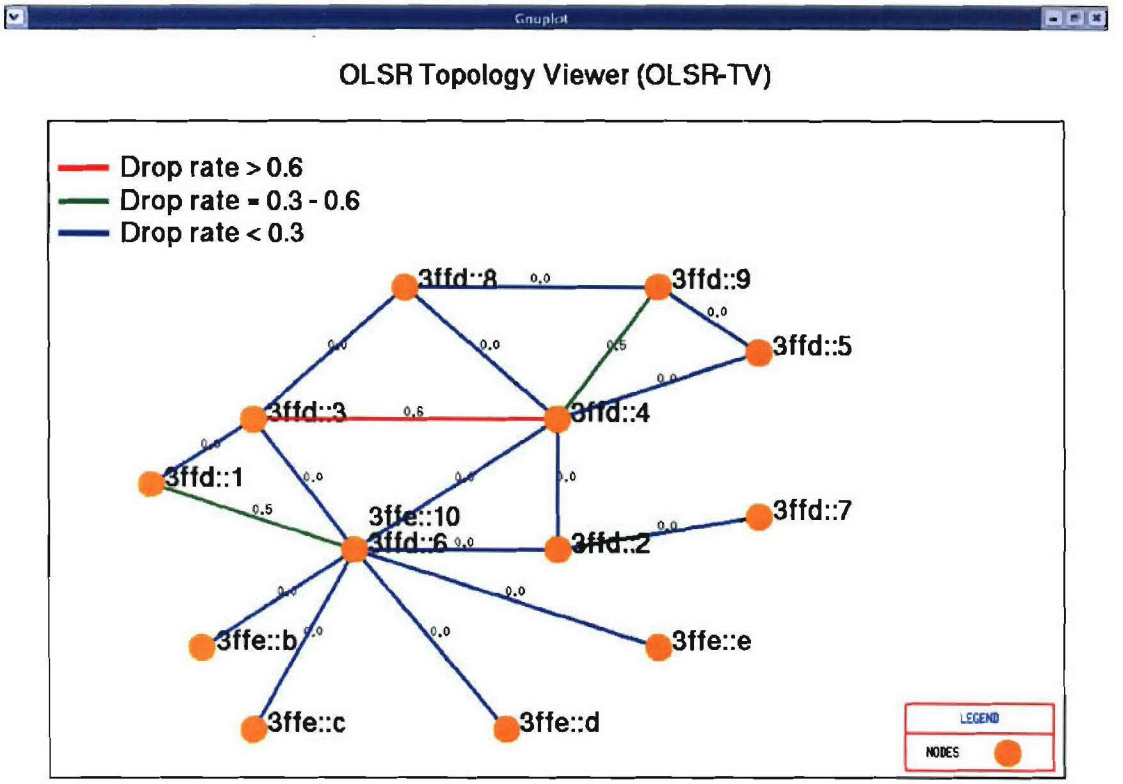

Figure 2.1-8 Backbone connectivity and packet drop rate visualized with OLSR-TV.

2.1.3 Importance/Relevance

Ad hoc networks are of particular importance to the Navy and other Department of Defense (DoD) units because of their ability to be quickly configured and operate without infrastructure. Research in ad hoc networks to date has been dominated by solutions to particular, specific problems and not to general system and network infrastructure issues. This task focused on making ad hoc network operate successfully as a system with efficient routing, the ability to offer quality of service, and the robustness and security required of military networks. We also examined the challenging problem of delivering video, specifically multiple description video, and investigated the effectiveness of topology control in an ad hoc network.

2.1.4 Productivity

This task led to 12 refereed journal papers that have been published or accepted to appear, 22 refereed conference papers, and one book chapter. In addition, two Ph.D. students and one M.S. student completed their degrees with research based on this project. One additional Ph.D. student was supported and he is expected to complete his degree after the award period. Two post-doctoral research associates were supported. Details are provided below.

Journal publications:

1. U. Lee, S. F. Midkiff, and T. Lin, "Routing in multi-channel wireless ad-hoc networks: OSPF-MCDS-MC," *Journal of Communications*, to appear.

2. M. X. Gong, S. F. Midkiff, and S. Mao, "A cross-layer approach to channel assignment in wireless ad hoc networks," to appear, *ACM/Kluwer Mobile Networks and Applications Journal (MONET)*, to appear.
3. S. Mao, Y. T. Hou, X. Cheng, H. D. Sherali, S. F. Midkiff, and Y.-Q. Zhang, "Multi-path routing for multiple description video over wireless ad hoc networks," *IEEE Transactions on Multimedia,* to appear.
4. Y. T. Hou, Y. Shi, J. Pan, A. Efrat, and S. F. Midkiff, "Maximizing lifetime of wireless sensor networks through optimal single-session flow routing," *IEEE Transactions on Mobile Computing*, vol. 5, no. 9, pp. 1255-1266, Sept. 2006.
5. Y. Shi, Y. T. Hou, H. D. Sherali, S. F. Midkiff, "Cross-layer optimization for routing data traffic in UWB-based sensor networks," *IEEE Journal on Selected Areas in Communications*, vol. 24, no. 1, pp. 857-863, April 2006.
6. S. Mao, S. S. Panwar, and Y. T. Hou, "On minimizing end-to-end delay with optimal traffic partitioning," *IEEE Transactions on Vehicular Technology*, vol. 55, no. 2, pp. 681-690, March 2006.
7. S. Mao, S. Kompella, Y. T. Hou, H. D. Sherali, and S. F. Midkiff, "Routing for concurrent video sessions in ad hoc networks," *IEEE Transactions on Vehicular Technology*, vol. 55, no. 1, pp.317-327, Jan. 2006.
8. S. Mao, X. Cheng, Y. T. Hou, and H. D. Sherali, "Multiple description video multicast in wireless ad hoc networks," *ACM/Kluwer Mobile Networks and Applications Journal (MONET)*, vol. 11, no. 1, pp.63-73, Jan. 2006.
9. G. C. Hadjichristofi, W. J. Adams, and N. J. Davis, "A Framework for Key Management in Mobile Ad Hoc Networks," *International Journal of Information Technology (IJIT)*, vol. 11, no. 2, pp. 31-61, 2005.
10. Y. T. Hou, Y. Shi, H. D. Sherali, and S. F. Midkiff, "On energy provisioning and relay node placement for wireless sensor networks," *IEEE Transactions on Wireless Communications*, vol. 4, no. 5, pp. 2579-2590, Sept. 2005.
11. C. Wang, B. Li, Y. T. Hou, K. Sohraby, and K. Long, "A stable rate-based algorithm for active queue management,'" *Computer Communications Journal*, vol. 28, no. 15, pp. 1731-1740, Sept. 2005.
12. J. Pan, L. Cai, Y. T. Hou, Y. Shi, and S. X. Shen, "Optimal base-station locations in two-tiered wireless sensor networks," *IEEE Transactions on Mobile Computing*, vol. 4, no. 5, pp. 458-473, Sept./Oct. 2005.

Conference publications (* indicates presenter):

1. U. Lee* and S. F. Midkiff, "Channel distribution fairness in multi-channel wireless ad-hoc networks using a channel distribution index," *IEEE International Performance Computing and Communications Conference (IPCCC)*, Phoenix, AZ, April 10-12, 2006, pp. 111-118.
2. S. Kompella*, S. Mao, and Y. T. Hou, "Optimal rate control for video transport over multi-hop wireless networks," *IEEE Wireless Communication and Networking Conference (WCNC)*, Las Vegas, NV, April 3-6, 2006, pp. 199-204.
3. U. Lee and S. F. Midkiff*, "OLSR-MC: A Routing Protocol for Multi-Channel Wireless Ad-Hoc Networks," *IEEE Wireless Communication and Networking Conference (WCNC)*, Las Vegas, NV, April 3-6, 2006, pp.331-336.

4. U. Lee*, S. F. Midkiff, and T. Lin, "OSPF-MCDS-MC: A routing protocol for multi-channel wireless ad-hoc networks," *IEEE Communications and Networking Conference (CCNC)*, Las Vegas, NV, Jan. 8-10, 2006, pp. 426-430.

5. R. W. Thomas*, L. A. DaSilva, and A. B. MacKenzie, "Cognitive networks," *IEEE International Symposium on New Frontiers in Dynamic Spectrum Access Networks (DySPAN)*, Baltimore, MD, Nov. 8-11, 2005, pp. 352-360.

6. M. X. Gong, S. F. Midkiff*, and S. Mao, "A combined proactive routing and multi-channel MAC protocol for wireless ad hoc networks" (invited paper), *International Conference on Broadband Networks (BROADNETS)*, Boston, MA, Oct. 3-7, 2005, pp. 479-488.

7. Y. T. Hou*, Y. Shi, H. D. Sherali, and S. F. Midkiff, "Prolonging sensor network lifetime with energy rovisioning and relay node placement," *IEEE Communications Society Conference on Sensor and Ad Hoc Communications and Networks (SECON)*, Santa Clara, CA, Sept. 26-29, 2005, pp. 295-304.

8. Y. Shi, Y. T. Hou*, H. D. Sherali, and S. F. Midkiff, "Cross-layer optimization for routing data traffic in UWB-based sensor networks," *ACM International Conference on Mobile Computing and Networking (MobiCom)*, Cologne, Germany, Aug. 28-Sept. 2, 2005, pp. 299-312.

9. Y. T. Hou*, Y. Shi, and H. D. Sherali, "On base station selection for anycast flow routing in energy-constrained wireless sensor networks," *International Conference on Quality of Service in Heterogeneous Wired/Wireless Networks (QShine)*, Orlando, FL, Aug. 22-24, 2005, 9 pages.

10. K. Channakeshava, K. S. Phanse, L. A. DaSilva, B. Ravindran*, S. F. Midkiff, and E. D. Jensen, "IP quality of service support for soft real-time applications," *Workshop on Real-Time Networks (RTN), EuroMicro Conference on Real-Time Systems (ECRTS)*, Palma de Mallorca, Spain, July 5, 2005, 4 pages.

11. S. Mao, S. Kompella*, Y. T. Hou, and S. F. Midkiff, "A fast greedy algorithm for routing concurrent video flows," *IEEE International Symposium on Circuits and Systems (ISCAS)*, Kobe, Japan, May 23-26, 2005, pp. 3535-3538.

12. M. X. Gong, S. F. Midkiff*, and S. Mao, "Design principles for distributed channel assignment in wireless ad hoc networks," *IEEE International Conference on Communications (ICC)*, Seoul, Korea, May 16-20, 2005, pp. 3401-3406.

13. S. Mao, X. Cheng, and Y. T. Hou*, H. D. Sherali, and J. H. Reed, "Joint routing and server selection for multiple description video in wireless ad hoc networks," *IEEE International Conference on Communications (ICC)*, Seoul, Korea, May 16-20, 2005, pp. 2993-2999.

14. S. Mao, S. Kompella*, Y. T. Hou, H. D. Sherali, and S. F. Midkiff, "Routing for multiple concurrent video sessions in wireless ad hoc networks," *IEEE International Conference on Communications (ICC)*, Seoul, Korea, May 16–20, 2005, pp. 1229-1235.

15. L. A. DaSilva, S. F. Midkiff*, N. J. Davis, J. S. Park, G. C. Hadjichristofi, K. Phanse, and T. Lin, "Interoperable security, routing and quality of service for ad hoc network mobility," *Information Systems Technology Panel Symposium on Military Communications*, NATO Research and Technology Agency, Rome, Italy, April 18-19, 2005, 12 pages.

16. W. J. Adams*, G. C Hadjichristofi, and N. J. Davis, "Calculating a node's reputation in a mobile ad hoc network," *IEEE Performance, Computing, and Communications Conference (IPCCC)*, Phoenix, AZ, April 2005, pp. 303-307.

17. G. C. Hadjichristofi*, W. J. Adams, and N. J. Davis, "A framework for key management in mobile ad hoc networks," *International Conference on Information Technology: Coding and Computing (ITCC)*, vol. 2, Las Vegas, NV, April 4-6, 2005, pp. 568-573.
18. U. Lee*, S. F. Midkiff, and J. S. Park, "A proactive routing protocol for multi-channel wireless ad-hoc networks (DSDV-MC)," *International Conference on Information Technology: Coding and Computing (ITCC)*, vol. 2, Las Vegas, NV, April 4-6, 2005, pp. 710-715.
19. M. X. Gong and S. F. Midkiff*, "Distributed channel assignment protocols: A cross-layer approach," *IEEE Wireless Communications and Networking Conference (WCNC)*, New Orleans, LA, March 13-17, 2005, pp. 2195-2200.
20. Y. T. Hou*, Y. Shi, H. D. Sherali, J. E. Wieselthier, "Online lifetime-centric multicast routing for wireless ad hoc networks with directional antennas," *IEEE INFOCOM*, March 13-17, 2005, pp. 761-772.
21. S. Mao*, Y. T. Hou, X. Cheng, H. D. Sherali, S. F. Midkiff, "Multipath routing for multiple description video in wireless ad hoc networks," *IEEE INFOCOM*, March 13-17, 2005, pp. 740-750.
22. S. Mao*, S. S. Panwar, and Y. T. Hou, "On optimal partitioning for realtime traffic over multiple paths," *IEEE INFOCOM*, March 13-17, 2005, pp. 2325-2336.

Book chapters

1. M.X. Gong, S. Mao, S.F. Midkiff, and B. Hart, "Medium access control in wireless mesh networks," in *Wireless Mesh Networking: Architectures, Protocols and Standards*, Y. Zhang, J. Luo, and H. Hu, eds., Auerbach Publications, CRC Press, Taylor and Francis Group, LLC, New York, NY, 2006, 36 pages (ISBN 0-849-37399-9).

Presentations (in addition to conference presentations listed above)

1. S. F. Midkiff, "Ad-Hoc and Sensor technology: The Defense Industry's Perspective," panel member and presenter, IEEE Conference on Sensor, Mesh, and Ad Hoc Communications and Networks (SECON), Reston, VA, September 28, 2006.
2. S. F. Midkiff, "Information Infrastructure Assurance in an 'Infrastructure-less' Environment," Euro-Atlantic Symposium on Critical Information Infrastructure Assurance, Riva San Vitale, Switzerland, March 23-24, 2006.
3. G. C. Hadjichristofi, W. A. deSousa, S. F. Midkiff, and L. A. DaSilva, AWINN poster presentation, Virginia Tech Advanced Research Institute's Open House (a research showcase event), Arlington, VA, December 7, 2005.
4. S. F. Midkiff, "ICT Everywhere: Ubiquitous & Pervasive Mobile (ad hoc) Communications and Networking," Workshop on Using Information Technology to Enhance Disaster Management, National Research Council (NRC) Computer Science and Telecommunications Board (CSTB), Washington, DC, June 22-23, 2005.

Meetings attended (in addition to conference and other presentations listed above):

1. Dr. Midkiff attended the National Science Foundation Global Environment for Networking Innovations (GENI) "Town Hall" Meeting, Arlington, VA, March 10, 2006.
2. Dr. Mao attended the NSF NOSS Informational Meeting held on Oct. 18, 2005 at Harvard University, Boston, MA.

Students completed:

1. George Hadjichristofi, "A Framework for Providing Redundancy and Robustness in Key Management for IPsec Security Associations in a Mobile Ad-Hoc Environment," Ph.D., 2005.
2. Xiaojun Wang, "Design and Implementation of An Emulation Testbed for Video Communications in Ad Hoc Networks," M.S., 2005.
3. Unghee Lee, "A Proactive Routing Protocol for Multi-Channel Wireless Ad-hoc Networks," Ph.D., 2006.

Students supported:

1. Waltemar de Sousa 7/1/05-07/31/06
2. Unghee Lee, 1/15/05-5/14/05 (33%), 5/15/05-05/15/06
3. Xiaojun Wang, 1/15/05-12/31/05
4. George Hadjichristofi, 1/15/05-5/14/05

Faculty supported:

1. Nathaniel J. Davis, 1/15/05-8/14/05
2. Scott F. Midkiff, 1/15/05-10/31/06
3. Luiz A. DaSilva, 1/15/05-10/31/06
4. Y. Thomas Hou, 1/15/05-10/31/06

Staff and other personnel supported (both post-doctoral research associates):

1. George C. Hadjichristofi, 7/25/05-10/31/06
2. Shiwen Mao, 1/15/05 -03/31/06 (post-doctoral associate)

2.2 Task 2.2 Real-Time Resource Management, Communications, and Middleware

This report discusses the activities of Task 2.2 during the entire project period January 2005 – October 2006.The report has four sections: (1) task overview, (2) task activities for the period, (3) importance to the Navy and technology transitions, and (4) productivity. These are discussed in the subsections that follow:

2.2.1 Task Overview

The objectives of Task 2.2 include:

(1) Develop time/utility function (TUF)/utility accrual (UA) scheduling algorithms for scheduling Real-Time CORBA 1.2's distributable threads [OMG01] with *assured timeliness properties* under failures. Develop distributable thread maintenance and recovery (TMAR) protocols [ggcj95] that are integrated with such scheduling algorithms;

(2) Develop TUF/UA *non-blocking synchronization mechanisms* for synchronizing distributable threads and single-processor threads for concurrently and mutually exclusively accessing shared objects;

(3) Investigate how TUF/UA scheduling algorithms, synchronization mechanisms, and TMAR protocols can co-reside with policy-based network QoS management schemes, and jointly optimize (with network QoS schemes) UA timeliness optimality criteria, as envisaged in Task 2.3; and

(4) Develop the *Distributed Real-Time Specification for Java* (DRTSJ) standard under the auspices of Sun's Java Community Process (JCP)[1], incorporating scheduling algorithms, synchronization mechanisms, and TMAR protocols developed in (1) and (2).

Embedded real-time systems that are emerging such as control systems in the defense domain (e.g., Navy's DDG1000, Air Force's AWACS) are fundamentally distinguished by the fact that they operate in environments with dynamically uncertain properties. These uncertainties include transient and sustained resource overloads due to context-dependent activity execution times and arbitrary activity arrival patterns. For example, many DoD combat systems include radar-based tracking subsystems that associate sensor reports to airborne object tracks. When a significantly large number of sensor reports arrive, it exceeds the system processing capacity, causing overloads, resulting in important tracks to go undetected.

When resource overloads occur, meeting deadlines of all application activities is impossible because the demand exceeds the supply. The urgency of an activity is typically orthogonal to the relative importance of the activity—e.g., the most urgent activity can be the least important, and vice versa; the most urgent can be the most important, and vice versa. Hence when overloads occur, completing the most important activities irrespective of activity urgency is often desirable. Thus, a clear distinction has to be made between the urgency and the importance of activities, during overloads. (During under-loads, such a distinction need not be made, because deadline-based scheduling algorithms such as EDF are optimal for those situations [hor74]—i.e., they can satisfy all deadlines.)

Deadlines by themselves cannot express both urgency and importance. Thus, we consider the abstraction of time/utility functions (or TUFs) [jlt85] that express the utility of completing an application activity as a function of that activity's completion time. Utility is typically mapped to

[1] The DRTSJ effort is currently ongoing under a JCP called JSR-50. The core members of the DRTSJ team include those from The MITRE Corporation and Virginia Tech.

application-level quality of service (QoS) metrics such as track quality and track importance in a command and control application. We specify deadline as a binary-valued, downward "step" shaped TUF; Figure 2.2-1(a) shows examples. Note that a TUF decouples importance and urgency—i.e., urgency is measured as a deadline on the X-axis, and importance is denoted by utility on the Y-axis.

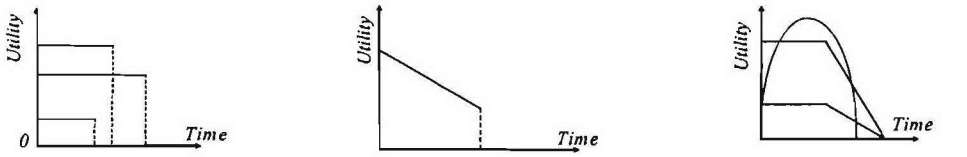

(a) Step TUFs **(b) AWACS TUF** **(c) Air Defense TUFs**

Figure 2.2-1 Example timing requirements specified using Time/Utility Functions.

Many embedded real-time systems also have activities that are subject to *non-deadline* time constraints, such as those where the utility attained for activity completion *varies* (e.g., decreases, increases) with completion time. This is in contrast to deadlines, where a positive utility is accrued for completing the activity anytime before the deadline, after which zero, or infinitively negative utility is accrued. Figures 2.2-1(b) and 2.2-1(c) show examples of such time constraints from two real applications (see [cjk+99] and the references therein).

When activity time constraints are specified using TUFs, which subsume deadlines, the scheduling criteria is based on accrued utility, such as maximizing sum of the activities' attained utilities. We call such criteria, *utility accrual* (or UA) criteria, and scheduling algorithms that optimize them, as UA scheduling algorithms. UA algorithms that maximize summed utility under downward step TUFs (or deadlines) [loc86, cla90, wrjb04] default to EDF during under-loads, because EDF can satisfy all deadlines during those situations. Consequently, they obtain the maximum total utility during under-loads. When overloads occur, they favor activities that are more important (since more utility can be attained from them), irrespective of their urgency. Thus, UA algorithms' timeliness behavior subsumes the optimal timeliness behavior of deadline scheduling.

Task 2.2 accomplishments of this project (during the entire project period) include:

(1) A class of algorithms that provide probabilistic timing assurances on end-to-end distributable thread behavior, in the presence of application- and MANET-induced run-time uncertainties, including that on workloads, node/link failures, message losses, and node membership;
(2) A class of distributed thread integrity protocols that provide bounded time for detecting thread failures, cleaning up orphan segments of the threads, and identifying and notifying new "heads" of the threads from where thread execution can resume;
(3) A class of advanced TUF/UA real-time scheduling and synchronization algorithms for single and multiprocessors; and
(4) Completion of an Early Draft Release of the DRTSJ standard.

We summarize these accomplishments in Section 2.2.2.

2.2.2 Task Activities for the Period:

Probabilistic Real-Time Scheduling Algorithms for Distributable Threads in Ad Hoc Networks

Task 2.2 research developed the *Real-Time Gossip algorithm* (or *RTG*) and two of its derivatives, *RTG-D* and *RTG-R*. RTG [hrj06] considers an application model that is comprised of distributable threads that may be created and arrive arbitrarily, and are subject to end-to-end step TUFs. The worst-case number of remote invocations made by distributable threads (or thread "hops") is assumed to be bounded and known a-priori. The algorithm's synchrony assumptions include known thread section execution time estimates (for normal code and abort handler code), and probability distribution for message communication delay. RTG considers a failure model where nodes are subject to unbounded crash failures, and links are subject to unbounded failures and message losses. Failures may occur at arbitrary times.

RTG provides probabilistic end-to-end timing assurances on distributable thread behavior. In particular, we prove that RTG's thread time constraint satisfactions are probabilistically bounded – i.e., the probability for a thread to satisfy its termination time is computable. Further, we establish that RTG's failure-exception notification times for partially executed portions of failed threads are bounded – i.e., the time needed to notify partially executed sections of a failed thread (so that exception handlers for aborting the sections can be released) is probabilistically bounded. Our experimental studies confirm our analytical results, and illustrate the algorithm's effectiveness.

We built upon RTG, and developed an algorithm called RTG-D (or *RTG for Dependencies*) that allows dependencies among distributable threads including those that are caused by mutual exclusion and precedence constraints [hrj06b]. We consider a resource model, where threads may concurrently share node-local, non-CPU resources (e.g., I/O, disk, NIC) under mutual exclusion constraints using lock-based synchronizers. We prove that thread blocking times – the length of time during which distributable threads wait for their requested lock – are probabilistically bounded under RTG-D. Consequently, we prove that RTG-D's thread time constraint satisfactions are probabilistically bounded. Further, we prove that RTG-D probabilistically bounds deadlock detection and notification times – i.e., time from distributed deadlock detection until notification of abort exceptions for aborting threads to resolve deadlocks is bounded with a computable (high) probability. Furthermore, we show that RTG-D probabilistically bounds failure-exception notification times for aborting partially executed portions of failed threads. Our experimental studies verify the algorithm's effectiveness.

RTG uses randomness to fight "uncertainties" – an idea that is central to the class of *gossip protocols*, which has been used to solve a variety of problems. RTG counters application/network uncertainties through gossip-based communication, broadly as follows. When a distributable thread arrives at a node, RTG decomposes the thread's end-to-end time constraint into a set of local time constraints, one for each of the remaining remote invocations (or thread hops). Obviously, knowledge of the worst-case number of thread hops is the pre-requisite for the decomposition. Local time constraints are used for thread scheduling on nodes. Further, when threads make invocations, they are used for discovering nodes (through gossiping) that host, and can feasibly execute, the invocations.

We further extend RTG, by considering no a-priori knowledge of the number of thread hops, and present an algorithm, called RTG-R (for *RTG with Random fan-outs*) [fhrj07]. RTG-R avoids time constraint decomposition. Instead, distributable threads are scheduled using their end-to-end time constraints. Further, when a thread makes an invocation, the algorithm randomly decides on the "fan-out" (i.e., the number of nodes to which an infected node propagates gossip messages during node discovery), and thereby counters the uncertainty on the number of hops. The fan-out determines the time available for gossip and the remaining thread slack. We prove that RTG-R's thread time constraint satisfactions and failure-exception notification times for thread abortions

are probabilistically bounded. Our simulation results validate our analytical results. Further, they show that RTG-R's performance degradation against RTG due to the lack of hop knowledge is no larger than 15%. The degradation occurs as threads' global slack causes node schedulers of earlier thread invocations to overestimate the actual slack, schedule them late, thereby jeopardizing the later invocations. We also show how this degradation can be reduced through additional randomization.

Thread Maintenance And Repair (TMAR) Protocols for Ensuring Integrity of Distributable Threads

Task 2.2 investigated the problem of recovering from communication and node failures that interfere with distributable threads while providing timeliness assurances. When a computational node hosting *segments* of a distributable thread fails, downstream segments become *orphans*---i.e., thread segments that are causally disconnected from the thread's root segment. A *termination* style exception processing model has been established for recovering from such failures. In this model, orphans must be detected and cleaned up, and failure-exception notification must be delivered to the farthest, contiguous surviving thread segment for resuming thread execution. Cleanup is a cooperative process, with a middleware/distribution layer and TMAR protocol detecting failures and coordinating cleanup, while applications provide application-specific cleanup and recovery logic. Task 2.2 developed a real-time scheduling algorithm called Abort-Assured Utility-Accrual scheduling algorithm (*AUA)*, and three distributable thread integrity protocols (*TPR*, *D-TPR*, and *W-TPR*.) Our work demonstrated that *AUA* combined with any of the protocols presented bounds the orphan cleanup and recovery time, thereby bounding thread starvation durations and maximizing the total thread accrued utility. The algorithm and the protocols are implemented in DRTSJ real-time middleware which supports distributable threads and provides a pluggable TMAR API. Experimental studies with the implementation validate the algorithm/protocols' time-bounded recovery property and confirm their effectiveness. Additionally, the final AWINN demonstration offered a complex example application which illustrates the use of these TMAR protocols in a naval battle management/command and control (BM/C2) application context.

Advanced TUF/UA Real-Time Scheduling and Synchronization Algorithms for Single and Multiprocessors

Task 2.2 developed a class of utility accrual scheduling and synchronization algorithms for dynamic, single and multiprocessor real-time systems. Efficient TUF/UA scheduling algorithms exist for single processors—e.g., the Resource-constrained Utility Accrual scheduling algorithm (RUA) [wrjb04], and the Dependent Activity Scheduling Algorithm (DASA) [cla90]. However, they all use lock-based synchronization. To overcome shortcomings of lock-based (e.g., serialized object access, increased run-time overhead, deadlocks), we consider non-blocking synchronization including wait-free and lock-free synchronization [arj97, hps02, kr93, cb97]. We developed a buffer-optimal, scheduler-independent wait-free synchronization protocol (the first such) [crj05], and developed wait-free versions of RUA and DASA. We also developed their lock-free versions, and upper bound their retries under the unimodal arbitrary arrival model.

The tradeoff between wait-free, lock-free, and lock-based is fundamentally about their space and time costs. Wait-free sacrifices space efficiency in return for no additional time cost, as opposed to the blocking time of lock-based and the retry time of lock-free. We showed that wait-free RUA/DASA outperform lock-based RUA/DASA when the object access times of both approaches are the same – e.g., when the shared data size is so large that the data copying process dominates the object access time of two approaches. We derived lower bounds on the maximum accrued utility that is possible with wait-free over lock-based. Further, we show that when maximum sojourn times under lock-free RUA/DASA is shorter than under lock-based, it is a necessary condition that the object access time of lock-free is shorter than that of lock-based. We also establish the maximum increase in activity utility that is possible under lock-free and lock-based.

Multiprocessor TUF/UA scheduling has not been studied in the past. For step TUFs, periodic arrivals, and under-loads, we first present a non-quantum-based, optimal scheduling algorithm called *Largest Local Remaining Execution time-tasks First* (or LLREF) that yields the optimum total utility. We then developed another algorithm for non-step TUFs, arbitrary arrivals, and overloads, called the *global Multiprocessor Utility Accrual scheduling algorithm* (or gMUA). We showed that gMUA lower bounds each activity's accrued utility, as well as the system-wide, total accrued utility.

We considered lock-based, lock-free, and wait-free synchronization under LLREF and gMUA. We derived LLREF's and gMUA's minimum-required space cost for wait-free synchronization using our space-optimal wait-free algorithm, which also applies for multiprocessors. Task 2.2 also developed lock-free versions of LLREF and gMUA with bounded retries. While the tradeoff between wait-free LLREF/gMUA versus lock-based LLREF/gMUA is similar to that for the single processor case, that between lock-free LLREF/gMUA and lock-based LLREF/gMUA hinges on the cost of the lock-free retry, blocking time under lock-based, and the operating system overhead.

Details of this work can be found in [cho06].

Completion of an Early Draft Review of the DRTSJ Standard

Task 2.2 efforts contributed substantially to the Distributed Real-Time Specification for Java (DRTSJ) which is under development within Sun's Java Community Process (JCP) as Java Specification Request 50 (JSR-50) and lead by the MITRE Corporation. For the real-time research group at Virginia Tech, DRTSJ represents a two-fold opportunity: first, the DRTSJ reference implementation provides an excellent framework in which to implement and integrate cutting-edge scheduling algorithms and thread integrity capabilities; second, the DRTSJ specification effort is a unique opportunity to transition mature technologies from our research into standards and implementations in industry. Our team explored and documented the practical engineering considerations and design decisions settled by the Expert Group, authored the current and proposed forms of the Reference Implementation, and documented and explored a range of open issues. In particular, we presented an approach to integrating the distributable threads programming model with the Real-Time Specification for Java and explored the ramifications for composing distributed, real-time systems in Java.

The JSR-50 Expert Group plans to release an initial Early Draft Review (EDR), implemented under Task 2.2 funding, to preview the distributable threads abstraction in CY2006. The EDR will contain portions of the proposed specification and a reference implementation (RI) implemented at Virginia Tech. The contents of this EDR are described in detail in Conference Publication (20). Along with that EDR, we will make publicly available a version of the AWINN demonstration application from Virginia Tech and a DRTSJ-compatible RTSJ VM from Apogee Software, Inc.

The following technologies will appear in the final DRTSJ specification and have been implemented for the EDR RI by Virginia's Tech's real-time systems lab:

- *Distributable Real-Time Threads*, a proven programming model for constructing sequential control flow applications with end-to-end timeliness properties in distributed systems. The DRTSJ's distributable threads are a real-time generalization of Java's Remote Method Invocation, as originally proposed in JSR-50 (and are a superset of the abstraction provided in the OMG Real-Time CORBA specification 1.2 [OMG01]

- A *Distributable Thread Integrity Framework*, into which application designers may plug appropriate policies for maintaining the health and integrity of distributable threads in the presence of failures

- A *Scheduling Framework*, into which application designers may plug appropriate user space policies for scheduling distributable and local threads

The real-time systems laboratory at Virginia Tech intends to make continued use of the DRTSJ in their work going forward as well as in the classroom. We expect to continue collaboration with the JSR-50 Expert Group as they shepherd the specification to final acceptance by the Java Community Process (JCP).

In order to demonstrate the progress made on DRTSJ and thread integrity protocols under Task 2.2, we constructed a complex demonstration illustrating the application of these TMAR protocols to a naval battle management/command and control (BM/C2) application context.

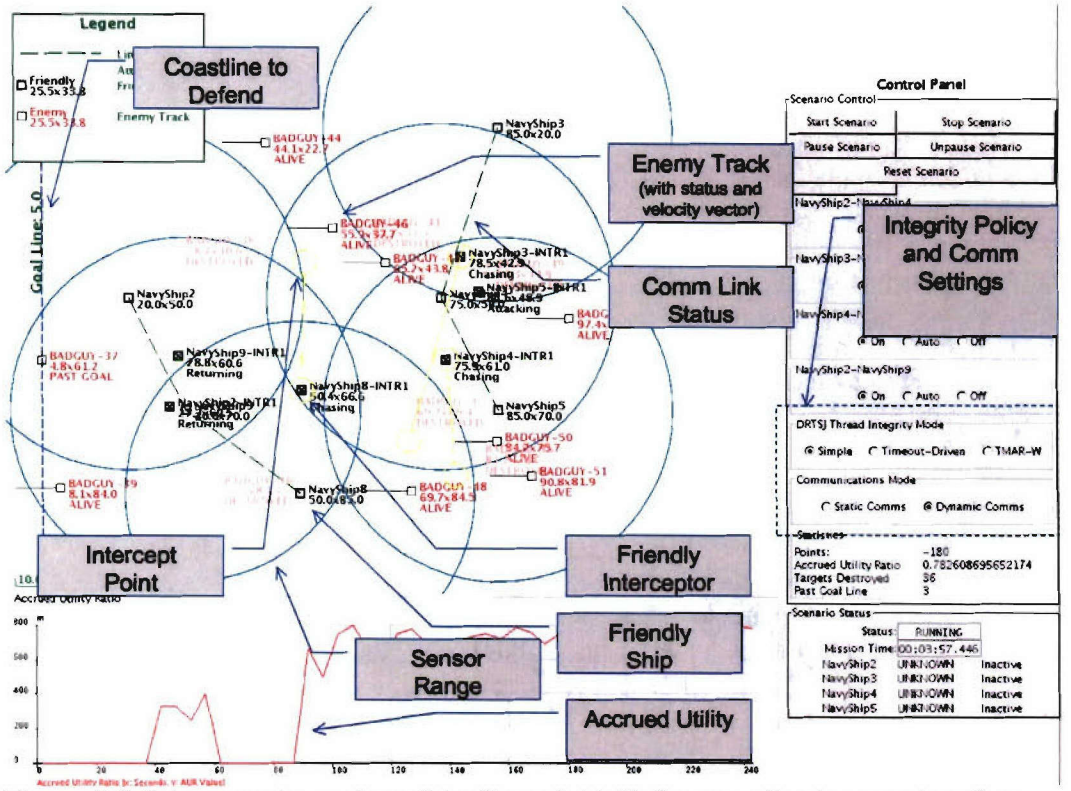

Figure 2.2-2 Annotated snapshot of the Coastal Air Defense application user interface.

The Coastal Air Defense application (user interface example shown in Figure 2.2.-2) focuses on thread integrity protocols that provide timely failure detection and recovery from end-to-end application-level distributed thread failures in dynamic networks. The demonstration uses a notional coastal air defense simulation consisting of a set of distributed components for managing on-board sensors, weapons, tracking systems, and BM/C2 operations in a multi-ship naval warfare context. The simulation testbed platform includes thirteen computer nodes comprising a scenario generator, a MANET/dynamic network simulator, four communications/routing nodes, and seven application nodes running application code atop Linux 2.6 with real-time extensions.

Novel approaches to enforcing distributable thread integrity are demonstrated and evaluated against mission metrics.

The demonstration application is written entirely in Java, compliant with Sun's Real-Time Specification for Java, with extensions -- notably distributed threads -- that are part of the emergent Sun Distributed Real-Time Specification for Java (DRTSJ), executing on a preliminary version of the DRTSJ Reference Implementation.

2.2.3 Importance to the Navy and Technology Transition Plans

The TUF/UA real-time technology developed in this task is directly relevant to DoD's network-centric warfare concept, Navy combatant systems including Aegis and DDG1000, and other DoD systems such as Air Force's next generation command and control aircrafts. In fact, the fundamental aspects of this class of real-time problems include:

(1) Need for transparent programming and scheduling abstractions for distributed computation workflows that are subject to time constraints

(2) Systems that are subject to significant run-time uncertainties that are often manifested in execution and communication times, and event and failure occurrences that are non-deterministically distributed

(3) Systems that are subject to transient and permanent overloads

(4) Need for time-critical and mission-oriented resource management (i.e., timely management of resources in the best interest of the current application mission)

(5) Need for industry/commercial standards- and COTS-based solutions for portability, robustness, and maintainability

All these aspects are directly addressed by Task 2.2 research. In particular, Real-Time CORBA 1.2's and DRTSJ's distributable threads abstraction provides a transparent programming and scheduling abstraction for distributed real-time computation workflows. Further, the class of TUF/UA scheduling algorithms, TMAR protocols, synchronization mechanisms, and policy-based network QoS management schemes target application activities, whose execution/communication latencies and event/failure occurrences are non-deterministically distributed and are subject to overloads. TUF/UA algorithms provide time-critical and mission-oriented resource management by (system-wide) scheduling to maximize system-wide accrued utility, where utility is mapped to application-level QoS. Consequently, utility maximization leads to managing system resources to maximize utility achieved for the users by the system. Furthermore, Task 2.2's work on the DRTSJ industry standard directly promotes industry/commercial standards and COTS-based solutions.

DDG1000 is currently using RTSJ extensively and is building a distributed real-time infrastructure using RTSJ. The DDG1000 team has expressed significant interest in using DRTSJ – in particular, the distributable threads abstraction and end-to-end timing analysis capability. We believe that DDG1000 can directly leverage DRTSJ's advanced adaptive time-critical (TUF/UA) resource management techniques and DRTSJ's synergy with RTSJ.

Task 2.2 research results and contributions to the DRTSJ were presented as the keynote presentation at the US Navy Open Architecture Real-Time Java Workshop, hosted by NAVSEA/Dahlgren, in Crystal City, 1 August 2006. Because the RTSJ is becoming a critical component in Navy distributed, real-time systems, this event represented a significant opportunity to expose DRTSJ to potential users and solicit feedback. Present at the event were a variety of

relevant software vendors (Aicas, Aonix, PrismTech, IBM, etc...), defense contractors (Lockheed-Martin, Raytheon, etc...) and government/military stakeholds (DDG1000, Aegis, etc...) The end-user and vendor input received at this event has and will continue to shape the research and technology transition program in the real-time laboratory to ensure that our work is motivated by our Navy sponsors' end-user and developer needs for cutting edge technology.

Our close collaboration with the MITRE Corporation continues as we seek technology transition opportunities throughout the Navy and broader defense community through tangible contributions in standards processes such as the Java Community Process; through concrete implementation and integration of our research results in the DRTSJ; and by presenting those concrete implementations in Navy-relevant application contexts. Through our demonstration applications we have sought to ensure that the fruits of our research and development program have been motivated by and available to the broadest swath of our sponsors' constituency. This work continues, as we anticipate a late September demonstration at MITRE McLean to program representatives from Army and Navy combat systems personnel and standards organizations.

References

[cla90] R. K. Clark, "Scheduling Dependent Real-Time Activities," PhD thesis, CMU CS Dept., 1990

[cjk+99] R. K. Clark, E. D. Jensen, et al., "An adaptive, distributed airborne tracking system," In *IEEE WPDRTS*, pages 353--362, April 1999

[cho06] H. Cho, "Utility Accrual Real-Time Scheduling and Synchronization on Single and Multiprocessors: Models, Algorithms, and Tradeoffs," *PhD Thesis*, August 2006

[cur06] E. Curley, "Recovering from Distributable Thread Failures with Assured Timeliness in Real-Time Distributed Systems," *Master's Thesis*, anticipated Fall 2006

[fhrj07] S. Fahmy, K. Han, B. Ravindran, and E. D. Jensen, "Randomized Real-Time Gossip: Scheduling Distributable Threads in Ad Hoc Networks Under Unknown Number of Thread Hops," *2007 IEEE Infocom*, Submitted August 2006 (under review), Available: http://www.real-time.ece.vt.edu/infocomm.pdf

[hor74] W. Horn, "Some Simple Scheduling Algorithms," *Naval Research Logistics Quarterly*, 21:177--185, 1974.

[jlt85] E. D. Jensen, C. D. Locke, and H. Tokuda, "A time-driven scheduling model for real-time systems," In *IEEE RTSS*, pages 112--122, December 1985

[loc86] C. D. Locke, "Best-Effort Decision Making for Real-Time Scheduling," PhD thesis, Carnegie Mellon University, 1986

[wrjb04] H. Wu, B. Ravindran, E. D. Jensen, and U. Balli, "Utility Accrual Scheduling Under Arbitrary Time/Utility Functions and Multiunit Resource Constraints," *IEEE Real-Time Computing Systems and Applications*, April 2004

[kr93] H. Kopetz and J. Reisinger, "The non-blocking write protocol NBW", *IEEE RTSS*, 131--137, 1993

[cb97] J. Chen and A. Burns, "A fully asynchronous reader/writer mechanism for multiprocessor real-time systems," *Technical Report YCS-288*, CS Dept., University of York, May 1997.

[hps02] H. Huang, P. Pillai, and K. G. Shin, "Improving wait-free algorithms for interprocess communication in embedded real-time systems," *USENIX Annual Technical Conference*, pages 303--316, 2002

[hrj06] K. Han, B. Ravindran, E. D. Jensen, K. Han, B. Ravindran, and E. D. Jensen, "Real-Time Gossip: Probabilistic, Reliable Real-Time Scheduling of Distributable Threads in Ad Hoc Networks," Available: http://www.real-time.ece.vt.edu/rtss-rtg.pdf

[hrj06b] K. Han, B. Ravindran, and E. D. Jensen, "Probabilistic, Real-Time Scheduling of Distributable Threads Under Dependencies in Ad Hoc Networks," *2006 International Conference On Principles Of Distributed Systems*, Submitted July 2006 (under review), Available: http://www.real-time.ece.vt.edu/hrj_scheduling_opodis2006.pdf

[arj97] J. H. Anderson, S. Ramamurthy, and K. Jeffay, "Real-time computing with lock-free shared objects," *ACM TOCS*, 15(2):134--165, 1997

[crj05] H. Cho, B. Ravindran, and E. D. Jensen, "A space-optimal, wait-free real-time synchronization protocol," *IEEE ECRTS*, 2005.

[ggcj95] J. Goldberg, I. Greenberg, R. K. Clark, E. D. Jensen, K. Kim, and D. M.Wells, "Adaptive fault-resistant systems (chapter 5: Adpative distributed thread integrity)," Tech. Rep. csl-95-02, Computer Science Laboratory, SRI International, Menlo Park, CA., January 1995, http://www.csl.sri.com/papers/sri-csl-95-02/.

[OMG01] OMG, Real-time CORBA 2.0: Dynamic scheduling specification," Tech. Rep., Object Management Group, September 2001, OMG Final Adopted Specification, http://www.omg.org/docs/ptc/01-08-34.pdf.

2.2.4 Productivity

Journal publications

(1) H. Cho, C. Na, B. Ravindran, and E. D. Jensen, "On Scheduling Garbage Collector in Dynamic Real-Time Systems With Statistical Timeliness Assurances," *Journal of Real-Time Systems*, Accepted August 2006, To appear

(2) K. Han, B. Ravindran, and E. D. Jensen, "Real-Time Gossip: Probabilistic, Reliable Real-Time Scheduling of Distributable Threads in Ad Hoc Networks," *IEEE Transactions on Computers*, Submitted September 2006

(3) H. Cho, B. Ravindran, and E. D. Jensen, "Utility Accrual Real-Time Scheduling and Synchronization for Multiprocessor Embedded Systems," *ACM Transactions on Embedded Computing Systems*, Submitted July 2006

(4) P. Li, B. Ravindran, and E. D. Jensen, "Utility Accrual Real-Time Resource Access Protocols with Probabilistically Assured Individual Activity Timeliness Behavior," *IEEE Transactions on Computers*, Submitted March 2006, Communicated May 2006 (second revision in progress)

(5) H. Cho, B. Ravindran, and E. D. Jensen, "On Lock-Free Synchronization for Dynamic Embedded Real-Time Software," *ACM Transactions on Embedded Computing Systems*, Submitted January 2006, Communicated June 2006 (second revision in progress)

(6) H. Wu, U. Balli, B. Ravindran, J. Anderson, and E. D. Jensen, "Utility Accrual Real-Time Scheduling Under Variable Cost Functions," *IEEE Transactions on Computers*,

Submitted November 2005, Communicated March 2006, Resubmitted June 2006 (under second review)

(7) H. Wu, B. Ravindran, E. D. Jensen, "Utility Accrual, Real-Time Scheduling Under the Unimodal Arbitrary Arrival Model with Energy Bounds," *ACM Transactions on Embedded Computing Systems*, Submitted November 2005

(8) P. Li, H. Wu, B. Ravindran, and E. D. Jensen, "On Utility Accrual Resource Management with Assured Timeliness Behavior," *IEEE Transactions on Computers*, Submitted October 2005

(9) H. Cho, B. Ravindran, and E. D. Jensen, "Space-Optimal Wait-Free Real-Time Synchronization," *IEEE Transactions on Computers*, Accepted August 2006, To appear

(10) H. Wu, B. Ravindran, E. D. Jensen, and P. Li, "Energy-Efficient, Utility Accrual Scheduling under Resource Constraints for Mobile Embedded Systems," *ACM Transactions on Embedded Computing Systems*, Accepted September 2005, To appear

(11) P. Li, H. Wu, B. Ravindran, and E. D. Jensen, "A Utility Accrual Scheduling Algorithm for Real-Time Activities With Mutual Exclusion Resource Constraints," *IEEE Transactions on Computers*, Volume 55, Issue 4, pages 454 - 469, April 2006

(12) K. Channakeshava, B. Ravindran, and E. D. Jensen, "Utility Accrual Real-Time Channel Establishment in Multi-hop Networks," *IEEE Transactions on Computers*, Volume 55, Issue 4, pages 428 - 442, April 2006

(13) H. Wu, B. Ravindran, E. D. Jensen, and P. Li, "Time/Utility Function Decomposition Techniques for Utility Accrual Scheduling Algorithms in Real-Time Distributed Systems," *IEEE Transactions on Computers*, Volume 54, Number 9, pages 1138 - 1153, September 2005

Conference publications[2]

(1) K. Han, B. Ravindran, and E. D. Jensen, "Probabilistic, Real-Time Scheduling of Distributable Threads Under Dependencies in Ad Hoc Networks," *2006 International Conference On Principles Of Distributed Systems*, Submitted July 2006

(2) S. Fahmy, K. Han, B. Ravindran, and E. D. Jensen, "Randomized Real-Time Gossip: Scheduling Distributable Threads in Ad Hoc Networks Under Unknown Number of Thread Hops," *2007 IEEE Infocom*, Submitted August 2006

(3) H. Cho, B. Ravindran, and E. D. Jensen, "An Optimal Real-Time Scheduling Algorithm for Multiprocessors," *2006 IEEE Real-Time Systems Symposium (IEEE RTSS)*, To appear

(4) E. Curley, J. Anderson, B. Ravindran, and E. D. Jensen, "Recovering from Distributable Thread Failures with Assured Timeliness in Real-Time Distributed

[2] Author who presented the paper at the conference is underlined.

Systems," *2006 IEEE Symposium on Reliable Distributed Systems (IEEE SRDS)*, To appear

(5) C. Na, H. Cho, B. Ravindran, and E. D. Jensen, "Garbage Collector Scheduling in Dynamic, Real-Time Multiprocessor Systems," *2006 IEEE International Conference on Embedded and Real-Time Computing Systems and Applications (RTCSA)*, Sydney, Australia, August 16-18, 2006

(6) H. Cho, H. Wu, B. Ravindran, and E. D. Jensen, "On Multiprocessor Utility Accrual Real-Time Scheduling With Statistical Timing Assurances," *2006 IFIP International Conference on Embedded And Ubiquitous Computing (EUC)*, August 01-04, 2006, Seoul, Korea

(7) P. Li, B. Ravindran, and E. D. Jensen, "Utility Accrual Real-Time Resource Access Protocols with Assured Individual Activity Timeliness Behavior," *International Conference on Real-Time and Network Systems (RTNS)*, pages 77-86, Poitiers, France, May 30-31, 2006

(8) H. Cho, C. Na, B. Ravindran, and E. D. Jensen, "On Scheduling Garbage Collector in Dynamic Real-Time Systems With Statistical Timeliness Assurances," *IEEE International Symposium on Object and component-oriented Real-time distributed Computing (ISORC)*, pages 215 - 223, Gyeongju, Korea, April 24-26, 2006

(9) H. Cho, B. Ravindran, and E. D. Jensen, "Lock-Free Synchronization for Dynamic Embedded Real-Time Systems," *ACM Design, Automation, and Test in Europe (DATE), Real-Time Systems Track*, pages 438-443, Munich, Germany, March 6-10, 2006

(10) H. Wu, B. Ravindran, and E. D. Jensen, "Utility Accrual, Real-Time Scheduling with Energy Bounds," *ACM Symposium On Applied Computing (SAC), Track on Embedded Systems*, pages 933-934, Dijon, France, April 23-27, 2006

(11) H. Cho, B. Ravindran, and E. D. Jensen, "On Utility Accrual Processor Scheduling with Wait-Free Synchronization for Embedded Real-Time Software," *ACM Symposium On Applied Computing (SAC), Track on Embedded Systems*, pages 918-922, Dijon, France, April 23-27, 2006

(12) H. Wu, U. Balli, B. Ravindran, and E. D. Jensen, "Utility Accrual Real-Time Scheduling Under Variable Cost Functions," *IEEE International Conference on Embedded and Real-Time Computing Systems and Applications (RTCSA)*, pages 213-219, Hong Kong, August 17-19, 2005

(13) H. Cho, B. Ravindran, and E. D. Jensen, "A Space-Optimal, Wait-Free Real-Time Synchronization Protocol," *IEEE Euromicro Conference on Real-Time Systems (ECRTS)*, pages 79 - 88, Palma de Mallorca, Balearic Islands, Spain, July 6-8, 2005

(14) B. Ravindran, E. D. Jensen, and P. Li, "On Recent Advances in Time/Utility Function Real-Time Scheduling and Resource Management," *IEEE International Symposium on Object-oriented Real-time distributed Computing (ISORC)*, pages 55 - 60, Seattle, Washington, USA, May 18-20, 2005

(15) P. Li, H. Cho, B. Ravindran, and E. D. Jensen, "Stochastic, Utility Accrual Real-Time Scheduling with Task-Level and System-Level Timeliness Assurances," *IEEE International Symposium on Object-oriented Real-time distributed Computing(ISORC)*, pages 216- 223, Seattle, Washington, USA, May 18-20, 2005

(16) H. Wu, B. Ravindran, and E. D. Jensen, "Energy-Efficient, Utility Accrual Real-Time Scheduling Under the Unimodal Arbitrary Arrival Model," *ACM Design, Automation, and Test in Europe (DATE)*, Real-Time Systems Track, pages 474-479, Vol. 1, Munich, Germany, March 7-11, 2005

(17) S. Feizabadi, B. Ravindran, and E. D. Jensen, "MSA: A Memory-Aware Utility Accrual Scheduling Algorithm," *ACM Symposium On Applied Computing (SAC), Track on Embedded Systems*, pages 857-862, Santa Fe, New Mexico, USA, March 13-17, 2005

(18) K. Channakeshava, K. Phanse, L. A. DaSilva, B. Ravindran, S. F. Midkiff, and E. D. Jensen, "IP Quality of Service Support for Soft Real-Time Applications," *International Workshop on Real-Time Networks (RTN), IEEE Euromicro Conference on Real-Time Systems (ECRTS)*, pages 5-8, Palma de Mallorca, Balearic Islands, Spain, July 6-8, 2005

(19) H. Wu, B. Ravindran, and E. D. Jensen, "The Impact of Scheduler Overhead on the Performance of Mobile, Embedded Real-Time Systems," Work-In-Progress (WIP) Session, *IEEE Euromicro Conference on Real-Time Systems (ECRTS)*, pages 37-40, IRISA Research Report, Number: PI-1723, ISSN 1166-8687, Palma de Mallorca, Balearic Islands, Spain, July 6-8, 2005

(20) J. Anderson and E.D. Jensen, "Distributed Real-Time Specification for Java: A Status Report", Invited Conference Presentation, *4th International Workshop on Java Technologies for Real-time and Embedded Systems (JTRES06)*, to appear, Paris, France, October 11-13, 2006.

Students completed

(1) Hyeonjoong Cho, PhD 2006, PhD Dissertation (in Computer Engineering): "Utility Accrual Real-Time Scheduling and Synchronization on Single and Multiprocessors: Models, Algorithms, and Tradeoffs," Dissertation Defended August 24, 2006

(2) Edward Curley, MS 2006, Master's Thesis: "Recovering from Distributable Thread Failures with Assured Timeliness in Real-Time Distributed Systems"

(3) Umut Balli, MS 2005, Master's Thesis: "Utility Accrual Real-Time Scheduling Under Variable Cost Functions," Defended July 28, 2005

(4) Haisang Wu, PhD 2005, PhD Dissertation (in Computer Engineering): "Energy-Efficient, Utility Accrual Real-Time Scheduling," Dissertation Advisor, Dissertation Defended July 29, 2005

Students supported

(1) Jonathan Anderson, January 2005 – present
(2) Hyeonjoong Cho, January 2005 – present

(3) Edward Curley, May 2005 – present
(4) Chewoo Na, September 2005 – present
(5) Joseph Hickman, August 2005 – May 2006
(6) Michael Nachmias, January 2006 – March 2006

2.3 Task 2.3 Network Interoperability and Quality of Service

2.3.1 Overview

Task goal: The goal of Task 2.3 was to integrate network services (as investigated in Task 2.1) with real-time middleware (as investigated in Task 2.2). Specifically, we investigated and developed methods and mechanisms to integrate capabilities at the network level, and perhaps at the link layer, with real-time services offered by middleware.

Organization: This task is directed by Scott Midkiff using the following personnel:

Scott F. Midkiff, faculty and task director
Luiz A. DaSilva, faculty
Binoy Ravindran, faculty
George C. Hadjichristofi, post-doctoral research associate
Jonathan Anderson, graduate research assistant

Summary: Task 2.3 integrated results from Tasks 2.1 and 2.2. During this integration additional components were developed to support Task 2.2, as described in Subtask 2.1(c). Based on this integration we made adjustments to the test bed being developed in Subtask 2.1(e).

2.3.2 Task Activities

Task objective: The objective of Task 2.3 was to integrate network services (from Task 2.1) with real-time middleware (from Task 2.2).

Accomplishments: Integration required adjustments for the various network functions as well as hardware augmentations to the test bed. A distributed multi-ship version of the Naval Air Defense application has been implemented in Java and installed on the test bed.. The distributed real-time specification for Java (DRTSJ) applications programming interface (API) was modified to support wireless Thread Maintenance and Repair (TMAR) implementations and exploit dynamic network information from Subtask 2.1(c). The test bed was modified to provide a control channel to the backbone nodes and the Dynamic Switch so as to remotely initiate and control the dynamic scenarios generated during the demonstration of this task. We presented this integration on August 25, 2006 in Blacksburg, Virginia.

Links to other tasks: This task integrates results from Task 2.1 and Task 2.2. It is also potentially synergistic with Task 2.4 (Cross-Layer Optimization) as it may be possible to integrate optimizations at the link and network layer with requirements presented by the real-time middleware.

2.3.3 Importance/Relevance

Many military systems rely on real-time operation, but can often be characterized using "soft" real-time constraints. This work paves the way to providing real-time capabilities, based on time-utility functions (TUFs), in an ad hoc network environment.

2.3.4 Productivity

Task 2.3 was tightly integrated with Tasks 2.1 and 2.2. Refer to reports on those tasks for relevant productivity measures.

2.4 Task 2.4 Cross-Layer Optimization

2.4.1 Overview

Task Goal: This task investigates the benefits of cross-layer system design by examining two specific types of networks: (a) UWB-based ad hoc networks and (b) position-location networks. The main goal is to determine the benefits to network performance available from design strategies that span across multiple network functional layers, including the physical layer, the medium access layer, and the network layer.

Organization: This task is managed by the Mobile and Portable Radio Research Group (MPRG) using the following personnel

R. Michael Buehrer, faculty
Qiao Chen, GRA
Jeong-Heon Lee, GRA
Swaroop Venkatesh, GRA

Summary: In this task, we examined cross-layer optimization by specifically examining two types of networks. The first type of network is an ad hoc network using an Ultra Wideband (UWB) physical layer. The investigation of UWB-based ad hoc networks showed that network performance benefits can, indeed, be realized by the joint design of physical (PHY), medium access control (MAC) and networking (NET) layers. Specifically, waveform optimization in the PHY has clear impacts on the MAC as it increases the probability of simultaneous transmissions thus reducing the amount of coordination required for setting up time-slots (i.e., MAC scheduling). Traditional CSMA-based approaches are impractical for UWB systems, but results also show that pure CDMA approaches are not typically viable. However, with proper PHY optimization nearly pure CDMA is viable in small networks thus reducing required network overhead and coordination. This was shown to also impact networking. Specifically, waveform and MAC optimization mitigated the need for minimum energy routing (in favor of longer hops) in order to control interference and thus increase network flow, although in general MER routing is still preferable to DIR routing.

In the second sub-task we investigated position-location networks, focusing on the benefits of integrating the application layer (APP) design into PHY and MAC design. Among the conclusions/results of this sub-task were: (1) Investigating the relationship between MAC protocol performance and localization accuracy showed that throughput can be directly tied to localization accuracy; (2) We proposed a spread-spectrum MAC scheme for UWB position location networks and demonstrated that the scheme outperforms the CSMA protocol in terms of localization accuracy at any time; (3) We investigated the use of power-control algorithms to improve localization accuracy in indoor position-location networks and showed that power control which is driven by the application layer is superior to power control driven by the PHY; and (4) We characterized the NLOS problem in indoor UWB position location networks and proposed a novel linear-programming technique for NLOS mitigation in indoor position-location networks.

2.4.2 Task Activities for the Period

Subtask 2.4a Cross-Layer Design for Ultra-Wideband Position-Location Networks

Primary Accomplishments

- We investigated the relation between MAC protocol performance and localization accuracy and showed that increasing throughput results in better localization accuracies.
- We proposed a spread-spectrum MAC scheme for UWB position location networks and demonstrated that the scheme outperforms the CSMA protocol in terms of localization accuracy at any time.
- Investigated the use of power-control algorithms to improve localization accuracy in indoor position-location networks; Showed that power control which is driven by application layer is superior to power control driven by PHY
- We characterized the NLOS problem in indoor UWB position location networks and proposed a novel linear-programming technique for NLOS mitigation in indoor position-location networks.

In this subtask, we investigated the possibilities in cross-layer design for infrastructure-based UWB Position-Location Networks (PoLoNets). The network architecture assumes the presence of fixed UWB radios or reference nodes in the area of interest whose locations are known *a priori*. These reference nodes aid the estimation of the locations of mobile nodes entering the area of interest via ranging and triangulation. The network of reference nodes provides TOA-based range estimates at the mobile node, which are used to estimate its location (in terms of 2D-coordinates). The mobile nodes periodically update their location estimate by ranging to reference nodes in order to maintain accuracy of location estimates. The deployed reference nodes also serve as a multi-hop communication network to relay position information to and instructions from a data sink (possibly C&C) as shown in Figure 2.4-1.

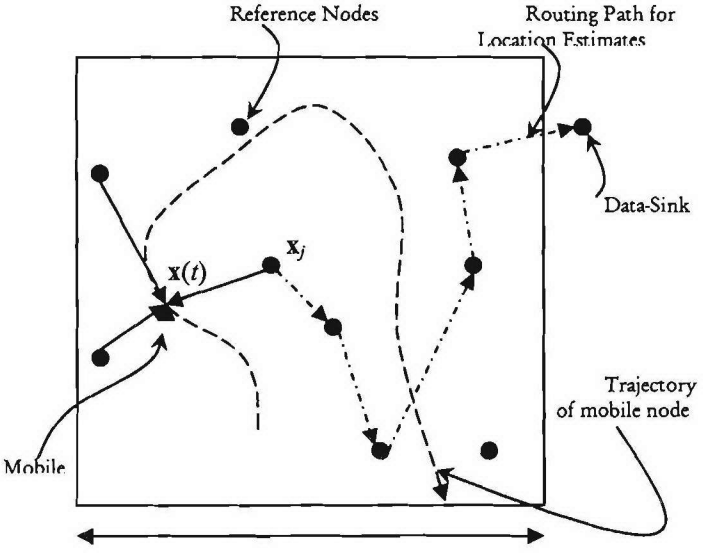

Figure 2.4-1 Position location network architecture.

As suggested above, we see that the described PoLoNet requires the fusion of point-to-point communication, localization and routing capabilities. For emergency-response applications,

localization accuracy is an extremely important characteristic of UWB PoLonets. For instance, in a fire-fighter position-tracking system, the knowledge of whether a firefighter is on one side of a door or the other could be critical. Consequently, our focus is on cross-layer design aspects with regard to localization accuracy.

Range Estimates and Localization Accuracy: The Cramer-Rao lower bound (CRLB) on the accuracy of TOA-based range estimation indicates that the variance of the range estimates is inversely proportional to the signal-to-noise ratio SNR (or signal-to-interference-and-noise, SINR):

$$\sigma_R^2 = \frac{K_R}{\xi} \tag{2.4-1}$$

This indicates that as the distance between nodes, the interference, or the path loss exponent increases, the accuracy of the range estimates degrades. Given $m \geq 3$ such range estimates (for two-dimensional position location), an estimate of a node's location can be obtained via estimators such as least-squares (LS). The study of the CRLB on the accuracy of location estimation given noisy unbiased Gaussian range estimates show that the average localization accuracy always improves as:

- The number of range estimates available increases
- The accuracy of individual range estimates improves

Figure 2.4-2 shows the average localization error as the number of range estimates available is increased. Even in the case of the LS location estimator, we see that as the number of range estimates increases, the average localization error decreases. As expected, localization accuracy degrades as inter-node distance and path loss exponent increase.

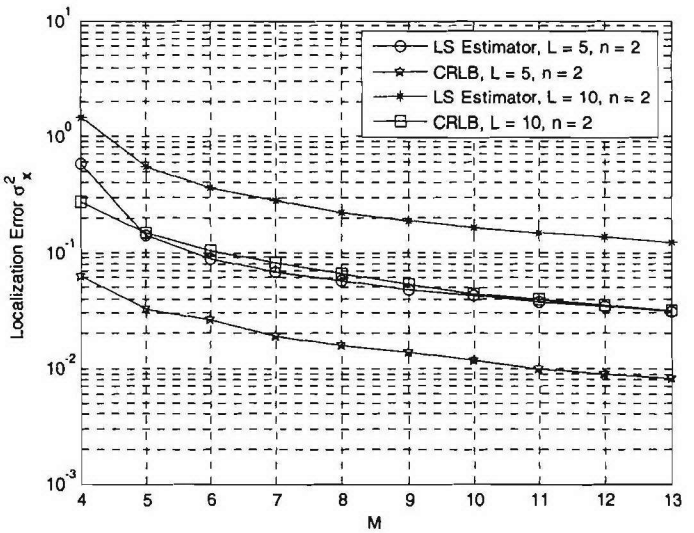

Figure 2.4-2 The effect of the number of range estimates (m) on the localization error. L is the dimension of the area in which reference nodes are randomly distributed and n is the path loss exponent.

MAC Design: Minimizing Localization Error: It is clear from Figure 2.4-2 that the accuracy of a location estimate of an unlocalized node is determined by the number of range estimates it receives from other localized nodes. From the perspective of MAC design, it stands to reason that a protocol that allows each unlocalized node to accumulate a large number of range estimates in a given duration increases the likelihood that an accurate estimate of the sensor's location is

computed at the end of that duration. Based on this reasoning, as time progresses, a MAC protocol which provides a higher effective throughput of range estimates to unlocalized nodes should allow faster convergence of sensor location estimates to the true locations.

In order to verify this conjecture, we investigated the theoretical performance of a synchronous spread-spectrum multiple access (SSMA) scheme for UWB PoLoNets. The scheme is based on the assignment of Time-Hopping (TH) codes that are proposed extensively for UWB communication. We demonstrate the parameters such as the probability of packet transmission p that maximize the packet throughput η, which was shown to be given by:

$$\eta = (1-p)(1-e^{-p})\mathrm{erfc}\left(\frac{p\pi\Lambda R^2}{\sqrt{\frac{4N_s}{K_1\pi}\left(\frac{1}{\xi_T}-\frac{1}{\xi_0}\right)}}\right), \tag{2.4-2}$$

also minimizes the localization error at any instant of time as shown in Figure 2.4-3.

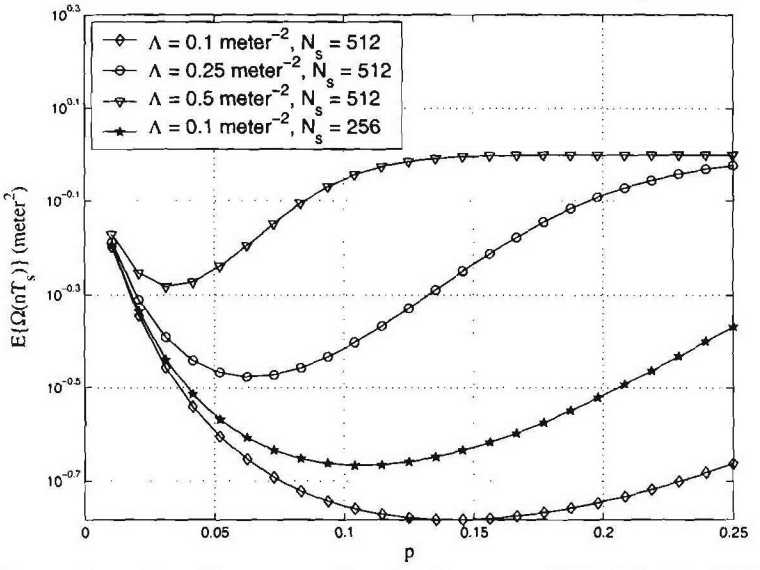

Figure 2.4-3 Lower bound on the average localization error $E\{\Omega(t)\}$ at $t = 100T_s$ versus the transmission probability p. The value of $\sigma_0 = 0.5$ meter.

The selection of MAC protocols for UWB PoLoNets favors spread-spectrum multiple access approaches due to the following reasons: (1) A spread-spectrum multiple access scheme is a "multi-channel" approach that allows simultaneous transmissions at the cost of incurring multi-access interference. This leads to graceful degradation in performance as the number of nodes is increased. (2) Due to significant spreading (transmission-bandwidth to data-rate ratio) inherent in the use of UWB signals for low data-rate applications, "single-channel" collision-avoidance approaches appear wasteful. (3) The covertness of UWB signals makes sensing the channel for collision-avoidance schemes inherently unreliable.

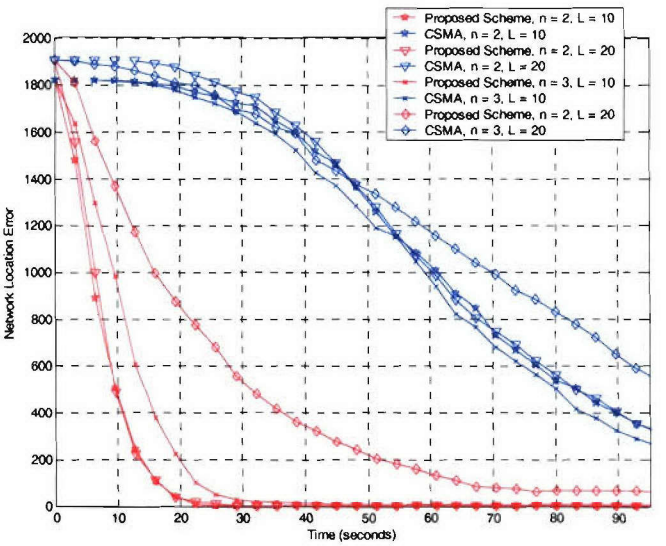

Figure 2.4-4 A comparison of the performance of the proposed protocol and CSMA in terms of the average network localization error versus time for different values of the path loss exponent (n). Note that the network localization error decreases much faster for the proposed approach than for the CSMA scheme. L is the dimension of the area in which nodes are deployed.

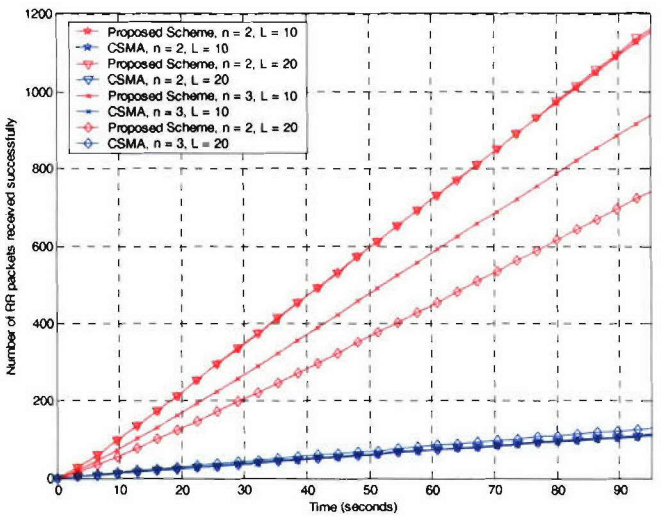

Figure 2.4-5 A comparison of the performance of the proposed protocol and CSMA in terms of the average number of ranging packets received successfully within the network versus time. The proposed approach clearly has a much higher effective throughput of ranging packets.

It was demonstrated via simulations that a proposed SSMA approach outperforms the CSMA MAC protocol in terms of localization accuracy as seen in Figure 2.4-4, which can be attributed to the higher effective throughput achieved by the SSMA approach, as seen in Figure 2.4-5.

Cross-Layer Design from Localization Accuracy Perspectives: From the above observations, we can summarize the cross-layer interactions between different layers. Localization algorithms are assumed to belong in the application layer. We see that there is significant interaction between the

design techniques can be used to considerably enhance the localization accuracy achieved by the network.

Impact of NLOS Measurements: The design of ad hoc position-location networks typically requires the capability of obtaining peer-to-peer range or distance measurement. A node whose location is unknown can estimate its location based on range measurements from location-aware "anchors" whose locations are known or estimated *a priori*. Range estimates from anchor nodes could be obtained using received signal strength (RSS) or time-of-arrival (TOA) estimation techniques. Due to the fine time-resolution afforded by UWB signals, the estimation of distances between nodes in UWB networks typically relies on the estimation of the time-of-arrival (TOA) of earliest multipath component.

However, in dense multipath propagation environments, especially indoors or in urban scenarios, the LOS path between nodes may be obstructed. As a result, in NLOS conditions, TOA-based range estimates are positively biased with high probability, since the first arriving multipath component travels a distance that is in excess of the true LOS distance. A similar effect is seen in the case of RSS-based range estimates, where the received signal power is reduced due to the obstruction of the LOS path. These effects result in range estimates that are often much larger than the true distances and therefore, in NLOS scenarios, the accuracy of node location estimates can be adversely affected.

Direct incorporation of these biased range estimates into practical location estimators such as the Least-Squares (LS) estimator, without the mitigation of these bias errors, can potentially lead to severe degradation in the accuracy of node location estimates. On the other hand, with certain geometries of anchor nodes, NLOS range estimates can be used to improve the accuracy of location estimation. Further, discarding the biased range estimates may not be a viable option, since the number of range estimates available may be limited. We present a novel NLOS bias mitigation scheme, based on linear programming, that (i) allows us to incorporate NLOS range information into location-estimation, but (ii) does not allow NLOS bias errors to degrade node localization accuracy.

The positively-biased NLOS range estimates are used to create a feasible region for the unlocalized node's location, thereby limiting the possibility of large localization error. This allows the "soft-activation" of NLOS range information: the NLOS range estimates are not incorporated directly, but are used in conjunction with LOS range estimates when LOS range estimates alone do not guarantee accurate node location estimates. The main advantages of this computationally-efficient linear programming approach are that

- the statistics of the NLOS bias errors are not assumed to be known *a priori*,
- no range information is discarded,
- it outperforms the LS estimator in terms of average localization accuracy, given a mixture of LOS and NLOS range estimates,
- it can be generalized and extended to handle degenerate cases with insufficient LOS range estimates, as well as to three-dimensional localization scenarios.

Subtask 2.4b Cross-Layer Design of Ad Hoc UWB Networks

In this task, we examine cross-layer design to optimize the performance of an ad hoc wireless network utilizing a UWB physical layer. The cross-layer optimization is done from the physical layer through the network layer which can provide strong benefits for many emerging

physical, MAC and application layers. Further, the selection of routes for the routing of location estimates and other information between the unlocalized nodes and command-and-control can be performed with the help of the estimated locations. This is termed Location-Aided Routing (LAR) and represents the interaction between the network and application layers.

To highlight some of these interactions, we observe the following in Figure 2.4-6:

- PHY-MAC-APP Interaction: A general increase in transmit power or the probability of transmission (PHY parameters) (a) increases interference, degrades SINR, reduces the accuracy and throughput of range estimates ⟶ Higher Localization Error, (b) increases connectivity with anchors, resulting in *potentially* larger number of range estimates ⟶ Lower Localization Error.
- MAC-NET-APP Interaction: Increasing the throughput of the MAC protocol, improves localization accuracy which improves efficiency in route selection.
- MAC-NET-APP Interaction: Applying power control techniques (MAC layer) reduces interference, increases throughput, decreases localization error, resulting in more efficient routing.
- APP-NET Interaction: Degradation of location estimates makes selected routes sub-optimal, increasing latency in the delivery of location estimates at command and control.

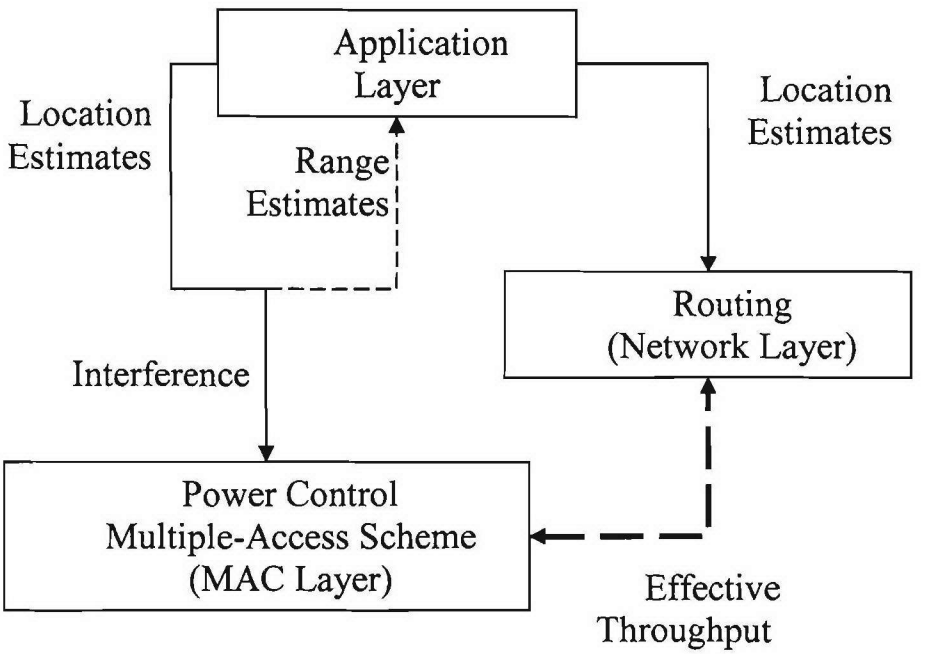

Figure 2.4-6 Block diagram of interaction between different design layers of a UWB Position Location Network.

Additionally, deployment scenarios and propagation conditions can also affect performance considerably. For instance, in NLOS scenarios, range estimates can be severely biased, resulting in poor localization accuracy. New NLOS mitigation techniques allow improvement of localization accuracy in NLOS propagation scenarios. Further, the deployed density of fixed anchors or reference nodes plays a significant factor in overall performance. In conclusion, we see that there is considerable interaction between the layers of the network design, and cross-layer

applications, particularly for energy constrained wireless networks. In this work, we employ an optimal codeword design (PHY), a minimum mean square error (MMSE) receiver (PHY) and a hybrid TDMA/CDMA MAC (based on the concept of the exclusion region) to mitigate multi-access interference in UWB-based wireless networks. In addition, we also consider various UWB routing protocols (NET) in order to maximize the sum of flow rates of the UWB-based network. In this report, we first discuss the MAC, NET and PHY models used for network optimization and then describe the actual optimization process. Once the network functions/optimizations are described, we present simulation-based results for centralized and ad-hoc scenarios

MAC Protocol Model: A MAC protocol is an essential component in a wireless network due to the inherent characteristics of the multiple access broadcast medium. No matter which physical layer technology is employed, the main theme remains the same: to coordinate the shared medium as efficiently as possible. Nevertheless, it is noted that the spread spectrum nature of UWB radio (which is interference-limited unlike collision-limited narrowband radio) demands different multiple access strategies to tackle problems such as secondary multi-access interference, the near-far effect, and the limited capability of carrier sensing. Due to these challenging issues, traditionally, spread spectrum based wireless networks have been developed in a centralized manner such as cellular CDMA networks where a fixed base station coordinates access to the channel and manages resources among contending users. Each node residing in a geographical cell is assigned a spreading code, transmit power, and other necessary information according to channel and network conditions. In a star topology where all data and control traffic are exchanged with the central station, such a centralized multiple access scheme is an effective method for monitoring network dynamics and controlling interference. On the other hand, in ad hoc wireless networks where no infrastructure can be established in advance, many attractive centralized MAC schemes adopted for spread spectrum communications may not perform well. Moreover, the unique UWB PHY attributes such as extremely low transmit power spectral density and the transmission of pulses of very small duration call for different approaches to UWB MAC design.

In this work we have investigated a distributed receiver-initiated UWB MAC protocol to enable independent UWB nodes to cooperate so that various techniques such as sequence optimization and exclusion regions (discussed in the following sections) can be employed. In particular, to actually implement the exclusion region and give a feedback of the optimal sequence information through the MAC protocol, we introduce a novel multiple access scheme that uses control packets, termed tokens, spread with specific PN codes. Also, the receiver-initiated polling scheme inherently makes it possible to avoid primary collisions (i.e., collisions due to concurrent transmissions to the same destination) and hidden/exposed node problems for multihop UWB wireless networks while allowing secondary collisions.

Our comparisons of various methods across the protocol layers in this work are based on a combination of key PHY (i.e., sequence optimization) and MAC (i.e., exclusion region) components. Since various cross-layer effects including routing are examined along with these combinations, we first introduce a UWB MAC protocol that realizes such cross-layer concepts. Our MAC approach is briefly summarized by the following questions and the corresponding answers.

- **How do we establish an exclusion region around each receiver?** – A receiver periodically broadcasts an invitation control packet called the *beacon token* at a certain power level which determines the optimal size of the exclusion region. Neighboring nodes receiving this packet compute an SINR and compare it with the predefined SINR threshold. Nodes with a computed SINR higher than the threshold assume that they are in

the exclusion region, thus refraining from transmission. Those outside of the region are free to transmit. Thus, it can be thought of as a hybrid CDMA/TDMA MAC and the degree of such a mixture dynamically varies according to the size of the adaptive exclusion region.

- **How do we compute and exchange the optimal codeword?** – When a receiver schedules dynamic time slots for each active link, it includes the optimal codeword in the *transmit token* and sends this back to the transmitter. The sequence is computed based on the link state which is estimated from the transmitter's response to the *beacon token*.

Protocol Description

As noted earlier, a spread spectrum based wireless network is inherently interference limited. Thus, we should be careful when applying the concept of the exclusion region since it could cause performance degradation by preventing unnecessarily some simultaneous transmissions. Our MAC protocol called spread spectrum token radio access (STRA) is based on receiver-initiated polling through the use of a novel form of the token as demonstrated in Fig. 2.4-7.

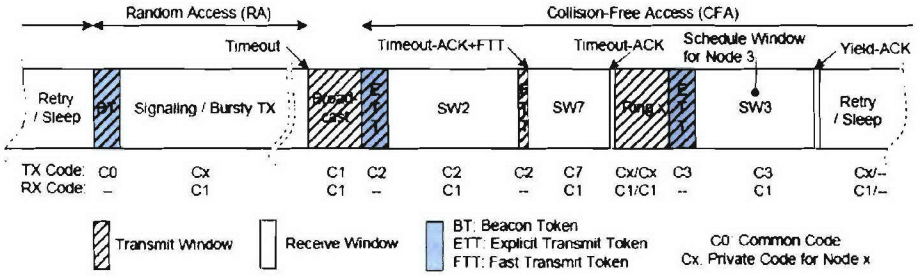

Figure 2.4-7 STRA time frame

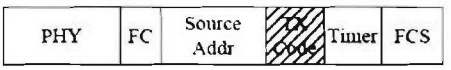

BT- common code. TT- private code

Figure 2.4-8 Token frame structure

A *token* is a special sequence of bits that indicates permission to transmit data. Nodes that acquire the token are allowed to begin transmission. Based on the spreading code used, tokens are classified as either a beacon token (BT), an explicit transmit token (ETT), or a fast transmit token (FTT) as seen in Fig. 2.4-7. Figure 2.4-8 shows the frame structure of BT and ETT where the transmit code field is only used for a BT. Note that the destination address is not needed and whichever node acquires the token is allowed to begin transmission, thereby reducing UWB MAC overhead.

There are three main functional components of STRA: the spreading code protocol, the channel access protocol, and the timeout protocol. The spreading code protocol determines the proper spreading code of a token based on the token type and its intended recipient. The code assignment for transmission and reception is determined based on the corresponding time interval in Fig. 2.4-7. As noted, STRA employs a simple spreading protocol such that it spreads a transmitted packet with the receiver code, regardless of the type of packet it is, with the exception of the fast token. The fast token is a piggybacked token onto ACK used for a receiver to initiate fast transmission of the successor while reducing the packet overhead. In our work, the receiver code corresponds

to the optimal sequence based on the link SINR. This optimal sequence information is easily added in the neighborhood table and updated as needed. Also, the participants only need to listen on their own optimal sequences, unless involved in fast transmission mode.

The second key component is the channel access protocol. As seen in Fig. 2.4-7, this consists of two alternating time periods: random access (RA) and collision-free access (CFA) similar to what is used in the beacon-based IEEE 802.1x MAC. However, we should note that a large difference exists between the proposed protocol and the IEEE 802.1x or any other similar polling MAC protocol. The latter maintains static time slots assigned to every polled node, even when it has no packet to send, thus managing time slots in an inefficient manner. On the other hand, STRA dynamically assigns time slots only to active *and* intended transmit nodes. Also, the latter is designed for a single-hop centralized star topology, while STRA is distributed and can be applied to various multi-hop network topologies and data rates.

Initially, the channel access protocol maintains only an RA period. This is because in the initial phase most packets are signaling control packets to identify neighbors and learn the network topology which is low-rate, bursty traffic. Note that this RA period is essential to initiate packet exchange since nodes do not know when and which neighboring nodes want to send a packet. The start of the RA period of some neighboring node or the identification of whether the node is awake is known by the reception of its periodic BT. Broadcasting the BT ensures neighboring nodes that it is awake and listening. This explicit notification is imperative to multi-hop routing scenarios to minimize transmission delay and packet loss. Upon the reception of the BT, the node transmits a packet after a random back-off window similar to the collision resolution mechanism employed in ALOHA.

The CFA period following the RA period is initiated based on a request during the RA period. As the channel load becomes higher, a node noticing an increase in its queue length requests a schedule to the intended receiver. Once the requested node is polled and receives an admission during the broadcast period from the receiver as illustrated in Fig. 2.4-7, the channel access protocol notifies the spreading protocol to listen on its reception code. In other words, as the node's needed data rate increases and the RA mode cannot accommodate its rate, the CFA scheduling mode clears up its buffer upon request without further signaling overhead. In the case where the "channel load" becomes lower and can be accommodated by the RA mode, a node only maintains the RA period. Notice that as network population changes due to, for example, mobility or battery exhaustion, it can adapt to this change through the use of such adaptive transmission modes.

As depicted in Fig. 2.4-7 and Fig 2.4-8, the timeout mechanism employed in STRA is effective in the sense that it can dynamically control the size of the RA, CFA periods, and the receive window of each active transmit node in a distributed manner. Another advantage of a timeout mechanism in UWB ad hoc wireless networks is to enable broadcasting or multicasting which is a challenging issue. By including a timer in the BT, a node can make the entire or a group of active neighbors listen during the specific broadcast period. On the other hand, a timer in ETT or ITT enables fair channel access or differentiated services to contending transmit nodes as well as efficient sleep scheduling.

Routing Protocol Model: In this project, we use both single and multi-hop routing protocols. A single-hop routing protocol implies that nodes directly send data to their destinations. We call this protocol a direct routing protocol (DIR). On the other hand, every node generally acts as both a source and a router in multi-hop routing scenarios. In many wireless applications such as sensor networks, a multi-hop routing protocol is often desired to minimize the total network energy and

we adopt a minimum energy routing protocol (MER) in this report. The routing path is determined through the Dijkstra algorithm, and the weight of each link is calculated by a cost function. In our simulation model, the link cost function depends on the average transmit power, path loss, and the interference power. Since nodes with optimal sequences adapt to the time-varying channel conditions, the cost function does not necessarily adapt to such time-varying channel statistics. In the case where a node mitigates interference through the use of an exclusion region when it is in receive mode, each link cost changes accordingly, thereby changing the routing path.

PHY Optimization: We showed that by transmitting an optimized code sequence, the SNR at the receiver is greatly enhanced by exploiting the rich mulitpath in the UWB channel. Furthermore, for multi-access scenarios, the sequence can optimized for SINR in order to mitigate MAI and improve the SINR of a target link. It should be noted that the results in are valid for centralized network scenarios, while we are primarily interested in *ad hoc* scenarios. In the succeeding work, we have combined optimal codeword design with receiver design and MAC and NET layer optimization. The three transmission algorithms that were investigated include:

Algorithm 1: All concurrent links transmit optimal SNR sequences with a matched filter at each receiver

Algorithm 2: One link (i^{th}) is randomly chosen to maximize its SINR by transmitting optimal SINR sequence, while other concurrent links retain their original optimal SNR sequences and matched filters used for Algorithm 1.

Algorithm 3: All concurrent links transmit optimal SNR sequences with MMSE receivers instead of matched filters.

The SINR expressions for these three transmission algorithms under both centralized and ad-hoc scenarios are summarized as follows:

Centralized network: For the i^{th} user, we denote p_i as the node's transmit power, s_i as its signature sequence vector, b_i as the data bit transmitted, and H_i as the channel matrix from the i^{th} user to its receiver. Assuming K concurrent transmissions, the received signal within one symbol interval can be written as:

$$r_i = \sum_{i=1}^{K} \sqrt{p_i} H_i s_i b_i + n \tag{2.4-3}$$

where n is a vector of independent, zero-mean Gaussian random variables with variance $\sigma^2 = \frac{N_0}{2}$.

Given its matched filter C_i at the receiver, the signal after correlation is:

$$C_i^T r = C_i^T \sqrt{p_i} H_i s_i b_i + C_i^T \sum_{j \neq i}^{K-1} \sqrt{p_j} H_j s_j b_j + C_i^T n \tag{2.4-4}$$

Denoting $I_i = \sum_{i \neq j}^{K-1} \sqrt{p_j} H_j s_j b_j$, the interference-plus-noise matrix is defined as:

$$Z_i = I_i * I_i^T + \sigma^2 I \tag{2.4-5}$$

Hence, the output SINR of the i^{th} user is

$$SINR_i = \frac{p_i (C_i^T H_i s_i s_i^T H_i^T C_i)}{C_i^T Z_i C_i} \tag{2.4-6}$$

Because the channel matrix $H_i^T H_i$ is a semi-positive-definite matrix, s_i is chosen to be the eigen-vector corresponding to the largest eigen-value of the channel matrix. By applying singular-value decomposition (SVD), the channel matrix can be written as $H_i^T H_i = V\Sigma V^T$. Then $H_i = U\Sigma^{\frac{1}{2}} V^T$, and $H_i s_i = U\Sigma^{\frac{1}{2}} V^T s_i = U\begin{bmatrix} 0 \\ \cdots \\ \sqrt{\lambda_s^i} \end{bmatrix} = \sqrt{\lambda_s^i} U_s^i$ where U_s^i is the s^{th} column of H_i, λ_i is the maximum eigen-value of the i^{th} channel matrix, U is a unitary matrix, and

$$\Sigma = \begin{bmatrix} \lambda_1^i & & & \\ & \lambda_2^i & & \\ & & \cdots & \\ & & & \lambda_s^i \end{bmatrix} \text{ where } \lambda_1^i < \lambda_2^i < \cdots < \lambda_s^i . \tag{2.4-7}$$

Therefore, the cross channel interference matrix Z_i simplifies to:

$$Z_i = \sum_{j \neq i; j=1}^{K} p_j H_j s_j s_j^T H_j^T + \sigma^2 I = \sum_{j \neq i; j=1}^{K} p_j \lambda_s^j U_s^j (U_s^j)^T + \sigma^2 I \tag{2.4-8}$$

Further, $H^T Z^{-1} H s_z = \lambda_z s_z$ and the resulting SINR's of i^{th} channel for the three algorithms are:

- Algorithm I - $C_i = H_i s_i$:

$$SINR_i = \frac{p_i \lambda_s^i}{\left(U_s^i\right)^T \left\{ \sum_{j \neq i; j=1}^{K} \lambda_s^j p_j U_s^j \left(U_s^j\right)^T \right\} U_s^i + \sigma^2 I} \tag{2.4-9}$$

- Algorithm II: For i^{th} channel, the transmit sequence is s_z, the correlation template is $Z^{-1} H_i s_z$, $SINR_i = p_i \lambda_i$. For the other channels, each transmits sequence: s_k, and SINR of k^{th} concurrent channel is

$$\frac{1}{SINR_k^*} = \frac{1}{SINR_k} + \frac{\left(U_s^j\right)^T p_i H_i s_z s_z^T H_i^T U_s^j - \lambda_s^i p_i (U_s^j)^T U_s^i \left(U_s^i\right)^T U_s^j}{P_j \lambda_s^j} \tag{2.4-10}$$

- Algorithm III:

$$SINR_i = p_i s_i^T H_i^T Z_i^{-1} H_i s_i = p_i \lambda_s^i \left(U_i^i\right)^T Z^{-1} (U_s^i) < p_i \lambda_z^i \tag{2.4-11}$$

Ad-hoc network: Analogous to the centralized network, let C_i be the matched filter at i^{th} receiver. Now, rewriting (2.4-4), the received signal after correlation is

$$C_i^T r = C_i^T \sqrt{p_i} H_{ii} s_i b_i + C_i^T \sum_{j \neq i}^{K-1} \sqrt{p_j} H_{ji} s_j b_j + C_i^T n \tag{2.4-12}$$

If we let $I_i = \sum_{j \neq i}^{K-1} \sqrt{p_j} \hat{H}_{ji} s_j b_j$, the interference-plus-noise matrix has the same format as (2.4-5), and following the same development as centralized network, we can derive the appropriate SINRs. However, simple close forms do not exist for the three algorithms as they do in centralized networks, so we do not list results here.

Cross-Layer Optimization Model: With the considered PHY, MAC, and NET algorithms now defined, we can describe the cross-layer optimization portion of the network design. Specifically, we adopt linear programming to jointly design the physical, MAC and network layers of the UWB wireless network. The specific optimization equations are:

$$
\begin{aligned}
&\textbf{max} \quad \sum_{i=1}^{I} \log(f^i) && \text{(a)}\\
&s.t.\ Bf \le \sum_{n=1}^{L+1} w_n r^n && \text{(b)}\\
&r_l^n = K * SINR_l^n && \text{(c)}\\
&\sum_{n=1}^{L+1} w_n = 1 && \text{(d)}\\
&\sum_{l:l.src=0} 1_{\{p_l^n>0\}} + \sum_{l:l.des=0} 1_{\{p_l^n>0\}} \le 1 && \text{(e)}\\
&P_l^n \le P_l^{MAX} && \text{(f)}
\end{aligned}
\qquad (2.4\text{-}13)
$$

where n, l, B, f, and r represent the time slot, link, routing matrix, flow vector, and averaged link rate respectively, w_i is the weight of the ith time slot, P is the transmit power of a node, and K is an arbitrary constant. There are L concurrent links and I total flows.

Equation 2.4-13(a) is our maximization equation which shows that our optimization target is to maximize the utilities of the flow rates in the network, subject to several constraints. The constraints are listed in equations 2.4-13(b) - 2.4-13(f), and their physical meanings are as follows:

2.4-13 (b) The total flow rates cannot exceed the sum of the given link channel capacity for any link

2.4-13 (c) The achievable data rate (i.e., capacity) of each link is proportional to the link SINR

2.4-13 (d) The sum total time slot allocation is normalized to one.

2.4-13 (e) Due to flow conservation, a node cannot transmit and receive data simultaneously

2.4-13 (f) The transmit power of each node cannot exceed maximum power constraints

The impact of PHY, MAC and NET layer adaptation on (2.4-13) can be summarized as follows:

PHY: The adaptation of optimal codewords and the MMSE receiver mitigate the MAI in the wireless network, thus improving each link's $SINR_l^n$

MAC: The setup of the exclusion region (i.e., the TDMA portion of the hybrid TDMA/CDMA) results in two scheduling algorithms: one where all notes are scheduled to transmit simultaneously (pure CDMA); and the other which considers exclusion regions when determining the time slots required as well as the data rate vector r_l^n and $SINR_l^n$. (Note that if the exclusion region is extremely large, we approach pure TDMA.)

NET: The routing table defines the total number of links (L) in the network. Hence, DIR and MER routing protocols change the size of the routing matrix B affecting the data rate vector r_l^n and $SINR_l^n$

Simulation Model: In this task, we investigate the interaction between the UWB physical layer and the higher layers such as MAC and NET layers. Two specific scenarios are simulated: a centralized network where all flows go to a single receiver and an ad hoc network were tx/rx pairs are uniformly distributed throughout the simulated area. To better reflect practical UWB networking scenarios, each link of the network is randomly assigned an indoor non-line of sight (NLOS) channel based on impulse response measurements taken at the Mobile and Portable Radio Research Group (MPRG) at Virginia Tech. The results are compared for different

combinations of optimal codewords, routing protocols with/without setting an exclusion region around a receiver. Results for both centralized and ad-hoc network are examined.
The simulation details are described as follows.

Physical layer: we use three transmission algorithms for PHY layer optimization.
Routing protocol: we compare DIR and MER routing protocols
Scheduling/MAC: two scheduling strategies are proposed, the first allows concurrent transmissions by all transmit nodes relying on the PHY for channel isolation (i.e., pure CDMA). The second reduces the number of concurrent flows by setting an exclusion region around each receiver thus improving the SINR per link (hybrid TDMA/CDMA).

Results: Figure 2.4-9 shows the system throughput under different PHY, MAC and NET protocols. It is seen that the MER is superior to the DIR routing protocols under all conditions. Thus, while the PHY and MAC make the two routing protocols closer in terms of performance, we still must rely on multi-hop transmission to mitigate network wide interference. Hence, all further results presented in this report assume that the routing protocol is MER. Also note that even with PHY layer control of interference, network performance is still improved through MAC layer control.

Focusing on MER routing, simulation results in Figure 2.4-10 show that when the number of nodes in a wireless network is low, the exclusion region is unnecessary and the resulting output utility is less than when allowing concurrent transmissions and controlling interference via the PHY. When the node density in a UWB-based wireless network is small, the interference can be effectively mitigated just by transmitting optimal SNR (or SINR) sequences. However, when we restrict the number of flows that can be assigned during the same time slot through the use of an exclusion region, we reduce the output utility under the same routing protocol and transmission algorithms. As the node density of wireless network grows, more and more interference is introduced, and the output utility achieves best results with the help of an exclusion region.

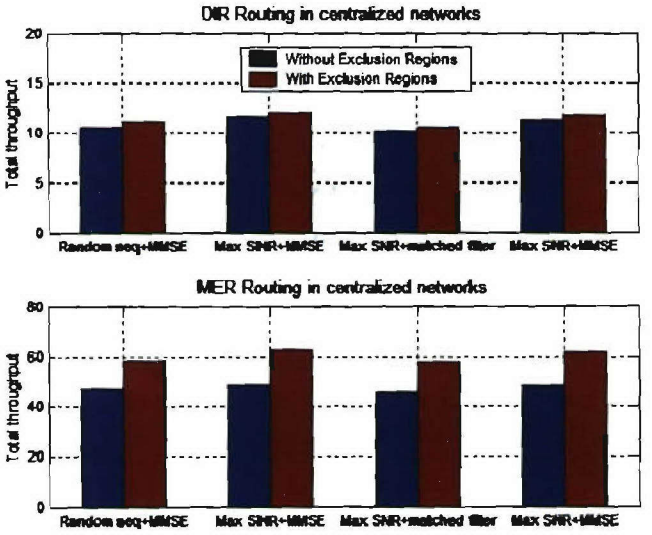

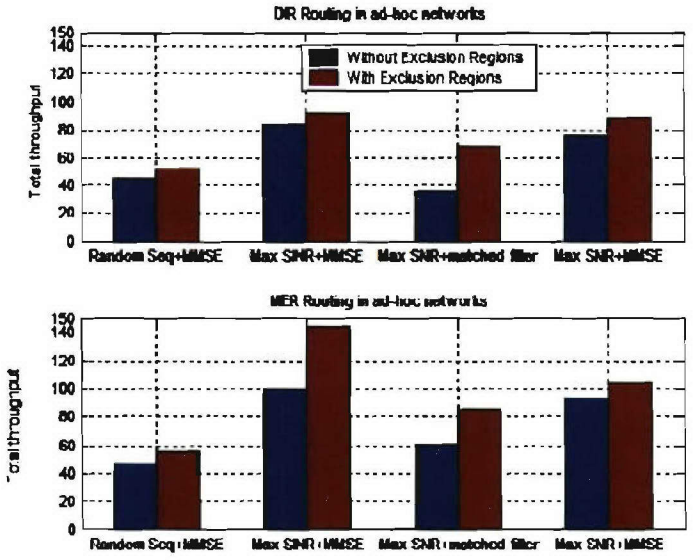

Figure 2.4-9 The Output Utilities for UWB-based centralized and ad-hoc wireless networks.

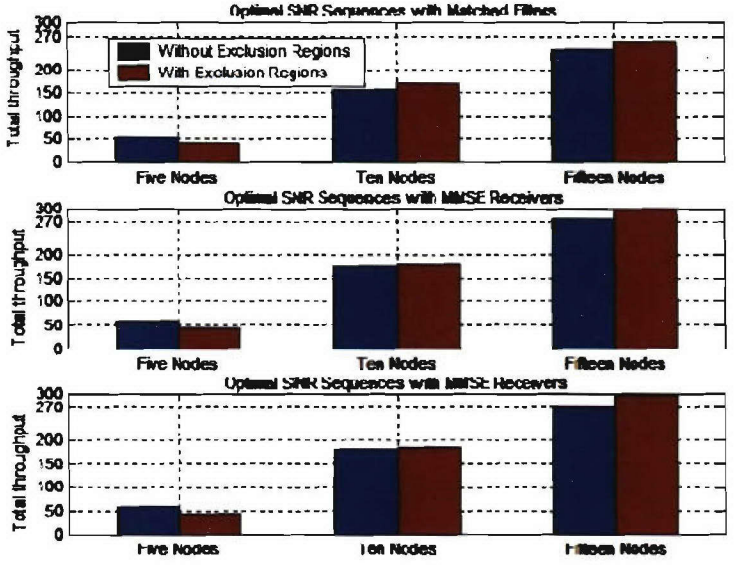

Figure 2.4-10 The Output Utility under MER Routing Protocol-ad-hoc network.

PHY Optimization Algorithm comparison: The above discussion illustrates that the best network performance can achieved by employing the MER (NET) routing protocols, and a combined TDMA/CDMA MAC via exclusion regions and optimized code sequences. Since we have three different PHY optimization algorithms, we focus for a moment on the PHY layer performance. In Figure 2.4-11, an empirical CDF is plotted for both centralized and ad-hoc networks for the three PHY optimization techniques. By choosing Algorithm 1 (max SNR sequences with matched filter

receivers) as the reference, the improvement for the other two algorithms are shown as a percentage. The '*' line in Figure 2.4-11 represents the output SINR of user *i*, who adopts Algorithm 2. Correspondingly, the '♦' curve shows the SINR of the other users who keep the original SNR sequence in Algorithm 2. It is seen with small probability the SINR of the other users falls in the negative range, which indicates that the performance of the other users is degraded when user one chooses Algorithm 2. However, the histogram remains in the positive range more frequently. For ad-hoc networks, the algorithms show more improvement over the baseline than in the centralized case. Additionally, it is notable that the performance degradation of the concurrent channels when one channel is randomly chosen to transmit the optimal SINR sequence is not as severe as in centralized networks. If general we can say that the following relationships hold for the PHY performance:

- Algorithm 2 > Algorithm 3 > Algorithm1 (user one)
- Algorithm 3 > Algorithm 2 > Algorithm1 (other users)

Additionally, we compared the network throughput performance using Algorithms 2 and 3. It is shown in Figure 2.4-12 that Algorithm 2 provides performance nearly equal to Algorithm 3 under the same MAC and routing protocol. Due to the practical considerations, since the SNR+MMSE algorithm (i.e., Algorithm 2) requires less feedback, which results in less overhead, it thus a better candidate than Algorithm 3. As a conclusion, for both centralized and ad-hoc networks, the best performance is achieved by the combination of the MER routing protocol, hybrid TDMA/CDMA through exclusion region and optimal SNR transmission sequence assignment and the employment of an MMSE receiver.

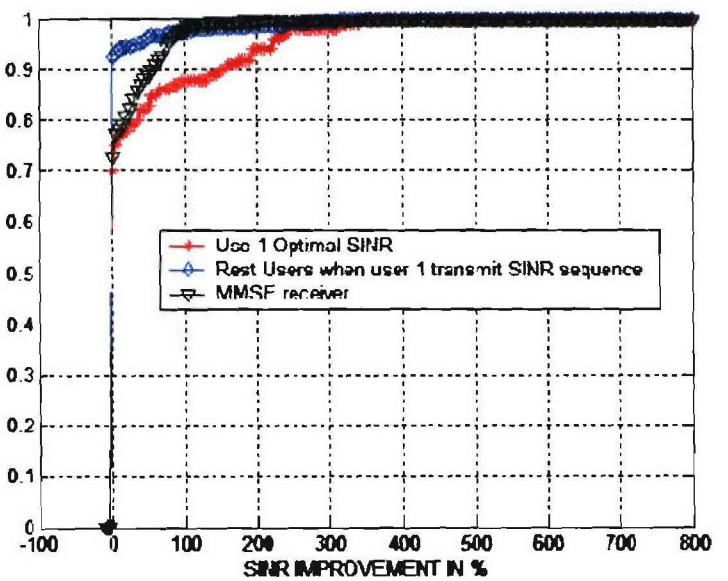

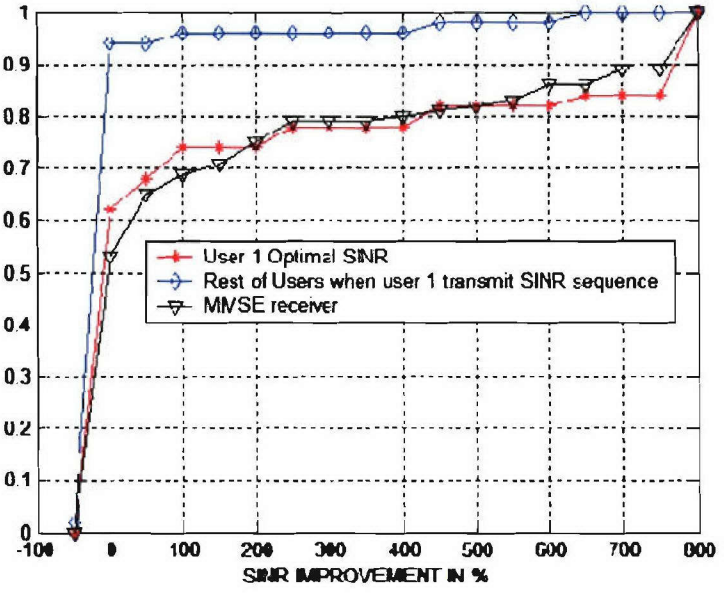

Figure 2.4-11 CDF of SINR Improvement: baseline: algorithm I. *: Performance of user 1 when it transmits optimal SINR sequence. ♦: Performance of other concurrent users corresponding to the *curve. ∇ : All users transmit optimal SNR sequences with MMSE receivers. Upper Plot: Centralized UWB networks. Lower Plot: ad-hoc networks.

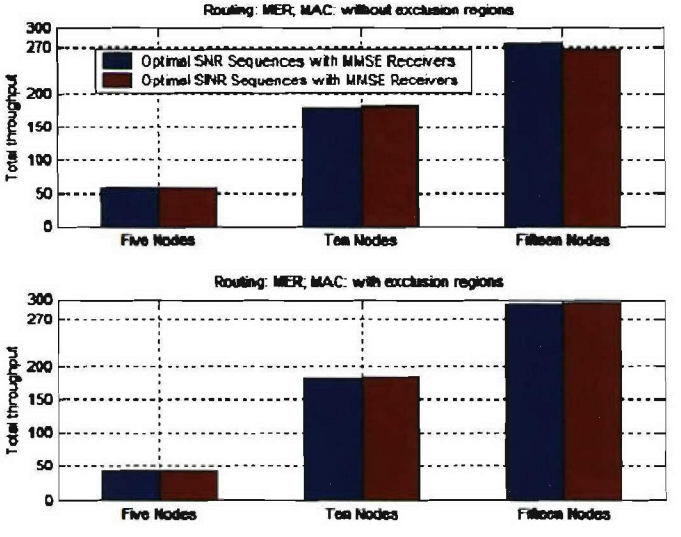

Figure 2.4-12 The Output Utility under different MAC and transmission algorithms for ad-hoc networks.

CDF of Link SINR: When the transmit power of concurrent flows are not equal (the typical case), the near-far problem is introduced into the network. In the above simulation, although we assume that all nodes have uniform transmission power, the near-far problem still exists due to node positions. We would like to further examine the SINR improvement due to the PHY by

comparing the CDF of the link SINR when using the chosen PHY algorithm as compared to a standard random sequence with a (10-finger) Rake receiver.

Figure 2.4-12 plots the empirical CDF of link SINR for random ad-hoc networks. It is seen that the CDF curve which corresponds to the optimal codeword PHY design has two improvements. First, the mean SINR is clearly improved by approximately 10 dB. Additionally, the CDF is somewhat steeper indicating less variation in the link SINR. In another words, the optimized codeword design is superior to traditional DS-UWB spreading codes in dealing with near-far problems.

Furthermore, although we could not derive a closed-form mathematical expression for the link SINR in ad-hoc networks for our codeword design, the plots show that such PHY layer design will greatly improve link SINR. For instance, for a traditional DS-UWB network, there is a 50% chance that a given link's SINR is less than -8 dB. By comparison, when optimizing the codeword, there is less than a 25% chance of being below -8 dB. As shown in optimization equations (2.4-13 c), the channel capacity is proportional to link SINR in UWB-based networks, thus Figure 2.4-12 also indicates that optimal codeword design can provide benefits to UWB-based ad-hoc network capacity.

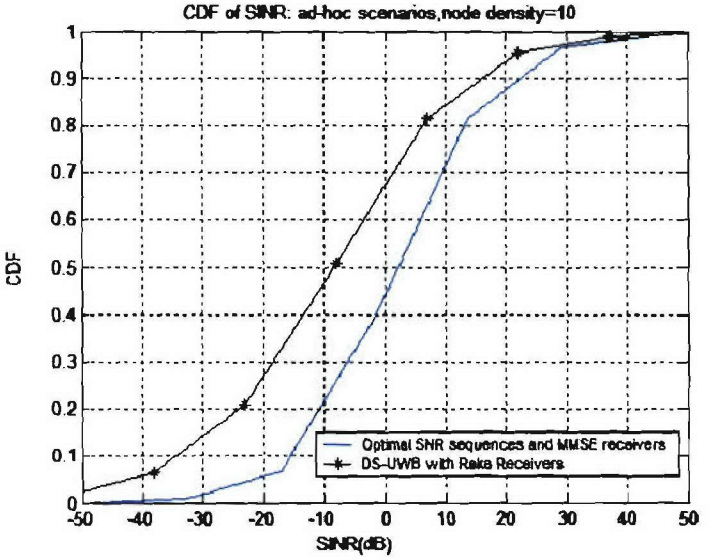

Figure 2.4-13 CDF of link SINR in ad-hoc networks.

Analysis: The purpose of this section is to derive the expectation of the link SINR in the case where we use MMSE receivers. In contrast to the previous analysis above, we tried to avoid applying SVD to each UWB channel for the SINR calculation. Instead, by applying the central limit theorem, we use the mean and variance to characterize MAI, and examine the expected value of the link SINR. First, we apply the system model given previously, and denote matrix P = diag{P_1, P_2, ..., P_K }and D = diag{Ed($U_s^1(U_s^1)^T$), Ed ($U_s^2(U_s^2)^T$), · · ·Ed ($U_s^K(U_s^K)^T$)}. The expectation of yy^T is calculated as

$$E(yy^T) = \sum_{k=1}^{K} E(p_k H_k S_k S_k^T H_k^T) + \sigma^2 I = \lambda \mathbf{PD} + \sigma^2 I \qquad (2.4\text{-}14)$$

The MMSE receiver for the first user is

$$c = E(b_1^* y)E(yy^T) = (\lambda \mathbf{PD} + \sigma^2 I)^{-1} \lambda_1 U_s^1 \sqrt{P_1} \tag{2.4-15}$$

and its SIR for MMSE receiver is

$$SIR_m = p_m S_m^T H_m^T (\sum_{j \neq m} p_j H_j S_j S_j^T H_j^T + \sigma^2 I)^{-1} H_m S_m = \frac{S_m^T H_m^T Z^{-1} H_m S_m p_m}{1 - S_m^T H_m^T Z^{-1} H_m S_m p_n} \tag{2.4-16}$$

where $\mathbf{Z} = \mathbf{HSPS^T H^T} + \sigma^2 \mathbf{I}$. Using the matrix inversion formula,

$$\mathbf{Z}^{-1} = \frac{\mathbf{I}}{\sigma^2} - \frac{\mathbf{HS}}{\sigma^4}(\mathbf{P}^{-1} + \frac{\mathbf{S^T H^T HS}}{\sigma^2})^{-1} \mathbf{S^T H^T} \tag{2.4-17}$$

Given the optimal SNR sequence, (2.4-15) is simplified into

$$\mathbf{Z}^{-1} = \frac{\mathbf{I}}{\sigma^2} - \frac{\mathbf{HS\Xi S^T H^T}}{\sigma^4} \tag{2.4-18}$$

where $\Xi = diag(\frac{p_1\sigma^2}{p_1\lambda_1+\sigma^2}, \frac{p_2\sigma^2}{p_2\lambda_2+\sigma^2}, , \frac{p_K\sigma^2}{p_K\lambda_K+\sigma^2})$. Combining the last three equations, the SINR of i^{th} user is given by

$$SINR_i = \frac{\beta_i}{1-\beta_i} \tag{2.4-19}$$

where

$$\beta_m = \lambda_m U_m^T \frac{1}{\sigma^2}(I - \sum_{i=1}^{K} \frac{\lambda_i p_i U_i U_i^T}{p_i \lambda_i + \sigma^2}) U_m p_m = \frac{p_m \lambda_m}{\sigma^2}(I - \sum_{i=1}^{K} \frac{\lambda_i p_i U_m^T U_i U_i^T U_m}{p_i \lambda_i + \sigma^2}) \tag{2.4-20}$$

and U_i is the column vector corresponding to the maximal eigen value of its channel matrix. By applying central limit theorem:

$$\sum_{i=1, i \neq m}^{K} \frac{\lambda_i p_i U_m^T U_i U_i^T U_m}{p_i \lambda_i + \sigma^2} \Rightarrow N(\mu, \sigma^2) \tag{2.4-21}$$

Hence, (2.4-18) can be rewritten as:

$$\beta_m = \frac{p_m \lambda_m}{p_m \lambda_m + \sigma^2} - \frac{p_m \lambda_m}{\sigma} \chi = a - b\chi \tag{2.4-22}$$

where $\chi \sim N(\mu, \sigma^2)$.

Denoting $y = 1 - a + b\chi$, where $y \sim N(1 - a + \mu, b^2\sigma^2)$, $SINR_i = \frac{1-y}{y}$, the pdf of SINR is:

$$f_{SINR_i}(z) = \frac{(1+z)^{-2}}{\sqrt{2\pi b^2 \sigma^2}} exp^{-\frac{(1-(1-a+\mu)(1+z))^2}{2b^2\sigma^2(1+z)^2}} \tag{2.4-23}$$

Then the expectation of SINR is:

$$E(SINR_i) = E(\frac{1}{y}) - 1E(\frac{1}{y}) = \int_{-\infty}^{\infty} \frac{-exp^{\frac{(y-(1-a+\mu))^2}{2b^2\sigma^2}}}{y\sqrt{2\pi b^2\sigma^2}} dy = \int_{-\infty}^{\infty} \frac{-exp^{\frac{(Y)^2}{2b^2\sigma^2}}}{(Y+1-a+\mu)\sqrt{2\pi b^2\sigma^2}} dY \tag{2.4-24}$$

Applying the Taylor Expansion for the term $\frac{1}{Y+1-a+\mu}$ at $Y = 0$, and denoting $s = 1 - a + \mu$, then integrating (2.4-24), the expected value of SIR can be written as:

$$E(SINR_i) = -1 + \frac{1}{s} + \frac{E(y^2)}{2!s^3} + \frac{E(y^4)}{4!s^5} + \frac{E(y^6)}{6!s^7} + \cdots \quad (2.4\text{-}25)$$

Conclusions: The work in this sub-task examined four techniques to combat multi-access interference in both centralized and *ad hoc* UWB networks: sequence optimization (PHY), the MMSE receiver (PHY), exclusion region (MAC), and multi-hop routing (NET). Further, we presented a new UWB MAC protocol called STRA and how it tackles scalability issues by exploiting unique UWB PHY features. STRA shows one realization of the exclusion region concept and provides a guideline of cross-layer UWB MAC design.

Several conclusions are drawn based on our simulation results as follows.

- Physical layer waveform design may replace the requirement of the exclusion region in small scale UWB wireless networks, which will greatly simplify UWB MAC design. The PHY cannot replace the MAC without penalty in medium to large scale networks, although they reduce the required exclusion region and thus the MAC signaling overhead.

- We compared the performance of two routing protocols: DIR and MER. In both centralized and ad hoc UWB systems, both protocols perform similarly when the exclusion region is assigned to control the mutual interference. Without the exclusion region, MER routing is always superior to DIR routing.

- The exclusion region used for UWB MAC design generally increases the total throughput of UWB ad hoc networks. However, the implementation of the MMSE receiver can replace the requirement of the exclusion region and, actually, in some cases achieve higher throughput.

- The numerical results show that the MMSE receiver provides substantially higher capacity than the Rake receiver in the case of UWB ad hoc networks, with some penalty in implementation complexity.

- Although using optimum SINR sequences at each transmitter and MMSE receivers at each node provides the best results among all PHY optimization algorithms, because of computational complexity and the similar performance, using only the optimum SNR sequence along with the MMSE receiver should be chosen for a more practical receiver design in UWB ad hoc networks.

2.4.3 Importance/Relevance

The work presented in this task is useful for the design of ad hoc communication and position location networks. Such networks are of immense use in the modernization of military communications.

2.4.4 Productivity

Journal publications

1. S. Venkatesh and R. M. Buehrer, "NLOS Mitigation in UWB Location-aware Networks Using Linear Programming", *accepted for publication in IEEE Transactions on Vehicular Technology*
2. S. Venkatesh and R. M. Buehrer, "NLOS/LOS Identification and its Impact on Position Location," *invited paper in IEE Proceedings on Microwaves, Antennas & Propagation: Special Issue on Antennas Systems and Propagation for Future Wireless Communications.*
3. J.Ibrahim and R.M. Buehrer, " Two-Stage Acquisition for UWB in Dense Multipath," *IEEE Journal on Selected Areas in Communications*, vol. 24, no. 4, pp. 801-807, April 2006.
4. J. Ibrahim, R. Menon, and R.M. Buehrer, "UWB Signal Detection Based on Sequence Optimization for Dense Multipath Channels," *IEEE Communications Letters*, vol. 10, no. 4, pp. 228-230, April 2006.
5. J. Ibrahim and R.M. Buehrer, "NBI Mitigation for UWB Systems Using Multiple Antenna Selection Diversity," accepted for publication in *IEEE Transactions on Vehicular Technology.*

Conference Publications

1. S. Venkatesh, N. Kumar and R. M. Buehrer, "A Spread-Spectrum MAC Protocol for Impulse-Radio Networks", 2005 IEEE Vehicular Technology Conference (VTC Fall 2005), Vol. 1, pp. 665–669, September 25th-28th 2005, Dallas, Texas.
2. S. Venkatesh, C. R. Anderson, R. M. Buehrer and J. H. Reed, "On the use of Pilot-Assisted Matched Filtering in UWB Time-Interleaved Sampling", to appear in the Proceedings of the 2006 IEEE International Conference on Ultra-Wideband (ICUWB 2006), 2427 September 2006, Waltham, Massachusetts, USA.
3. S. Venkatesh and R. M. Buehrer "Multiple-Access Design for UWB Position-Location Networks", *Proceedings of the 2006 IEEE Wireless Communications and Networking Conference (WCNC 2006)*, 3-6 April 2006, Las Vegas, USA.
4. S. Venkatesh and R. M. Buehrer, "Power-Control for UWB Position-Location Networks", *Proceedings of the 2006 IEEE International Conference on Communications (ICC 2006)*, 11-15 June 2006, Istanbul, Turkey.
5. S. Venkatesh and R. M. Buehrer, "A Linear Programming approach to NLOS error mitigation in Sensor Networks", *Proceedings of the Fifth International Conference on Information Processing in Sensor Networks (IPSN '06)*, pp. 301-308, 19th-21st April 2006, Nashville, USA.
6. S. Venkatesh and R. M. Buehrer, NLOS Mitigation in UWB Position Location Networks Using Linear Programming", Invited Paper, *Proceedings of the IEE Seminar on Ultra Wideband Systems, Technologies and Applications*, 20th April 2006, London.
7. S. Venkatesh and R. M. Buehrer, "Multiple-Access Insights from Bounds on Sensor Localization", *Proceedings of the IEEE International Symposium on a World of Wireless, Mobile and Multimedia Networks,* Niagara-Falls, Buffalo-NY, 26th-29th June 2006.
8. J. Ibrahim and R.M. Buehrer, "A UWB Multiple Antenna System for NBI Mitigation under Rayleigh and Ricean Fading," *IEEE International Conference on Communication*, ICC 2006, June 2006.
9. J. Ibrahim and R.M. Buehrer, "A Novel NBI Suppression Scheme for UWB Communications Using Multiple Receive Antennas," *IEEE Radio and Wireless Symposium*, RWS 2006, January 2006.

10. R. Menon, J. Ibrahim, and R.M. Buehrer, "UWB Signal Detection Based on Sequence Optimization", *Proceedings of WIRELESSCOM 2005*, June 2005.

Students completed

1. S. Venkatesh, "Position Location Networks", Ph.D., December 2006.
2. J. Ibrahim, "UWB Receiver Design", Ph.D., Spring 2007.

3. TASK 3 Visualization of Wireless Technology and Ad Hoc Networks

3.1 Overview

Task Objective: The objective of this task is to identify and investigate AWINN enabling technologies for the Close-in Sea Basing.

Organization: The task is directed by Ali Nayfeh and Rick Habayeb. The personnel list follows.

Rick Habayeb, faculty
Ali Nayfeh, faculty

Summary: This task supported the integrated crane demonstration described in Sections 4.2 and 4.4. In addition, a crane controller was installed on a Shanghai Zenhua Port Machinery (ZPMC) quay-side container crane at Jeddah Port, Saudi Arabia. This provided the bridge to transition the UWB ranging technology into the Sea Basing environment.

3.2 Task Activities

A potential transition path for the AWINN technologies into the Sea Basing environment was established by successfully installing the VT controller on a Shanghai Zenhua Port Machinery (ZPMC) quay-side container crane at Jeddah Port, Saudi Arabia. The crane has a useable track of 100 meters, with a maximum trolley speed of 4.0 meters per second. The trolley is 45 meters above the pier. The hoist capacity is a maximum of 45 tons of cargo—the spreader bar is 15 tons—for a total of 60 tons, from -20 meters—into a ship-hatch below the pier—to 35 meters above the pier with a maximum hoist speed of 2 meters per second. The crane can lift either a single 8x8x40 ft container or two 8x8x20 ft containers at one time.

The controller has more than doubled the throughput of the average operator from approximately 25 containers per hour to 60 containers per hour. Considering a typical Panamax class container vessel has on the order of 4600 containers, this is a huge increase in performance.

The VT anti-sway controller is a feedback control system designed to reduce spreader-bar/container sway during and at the end of cargo transfer maneuvers. For the control system to work, the "sway angle" or the "pendulation angle" of the container must be accurately measured and fed-back to the control algorithm. Using these measurements, the controller modifies and corrects the operator joystick commands to the trolley motors. In a live, full-scale implementation on a quay-side container crane, a "contact" sway sensor must be rugged and able to withstand very large forces from multiple sources. In the Jeddah installation, cable rider-type sway sensors were used to monitor the spreader-bar/container sway at all times. These "contact" sway sensors measure the cable angles through mechanical linkages attached to the crane hoist cables.

Figure 3-1 shows the VT anti-sway controller installed on the quay-side container crane. The "Main CPU" houses the processing unit: a solid-state computer and power supply. The "Operator Panel" provides an interface to the operator.

Figure 3-1 The "Main CPU" and "Operator Panels" mounted inside of the trolley cabin on the quay-side container crane at Jeddah Port.

The current generation of sensors is cable-rider type as seen in Figure 3-2. They utilize a drop arm attached to an absolute encoder for angle measurements. Due to the fact that the hoist cables are braided steel cables, there is tremendous wear-and-tear on the sensors. There is a pair of sensors per crane.

Figure 3-2 A sway sensor mounted underneath the trolley of the quay-side container crane with hoist cable.

The hoist cable is threaded between spring-loaded pulleys seen in Figure 3-3. The pulleys are parts (1) and (2). Due to the abrasive nature of the braided hoist cable, the pulleys are supported by stainless steel plates at (3) and (4).

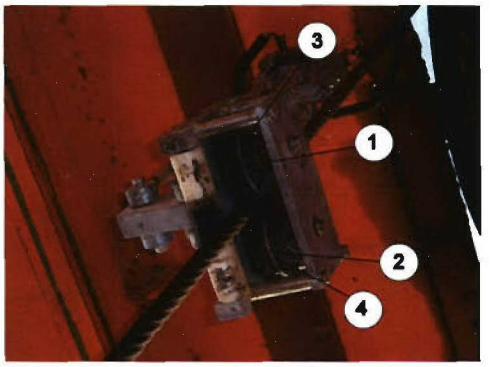

Figure 3-3 A close up view of the sway sensor rider assembly showing the hoist cable and spring-loaded pulleys.

The wear-and-tear is clearly visible in Figure 3-4. The two nylon rollers (4) and (5) are used to keep proper alignment for the sensor-to-cable. Careful examination of (4) shows a deep gouge where the cable has eaten away at the roller. The expected lifetime of each roller is approximately 3 months. The process of replacing the roller requires a person to stand on top of the crane spreaderbar, suspended 45 meters above the ground. Then, nuts at (1) and (2) are removed. Part (3) is then removed. Parts (4) and (5) can now be replaced. Then part (3) is returned and rebolted with nuts (1) and (2).

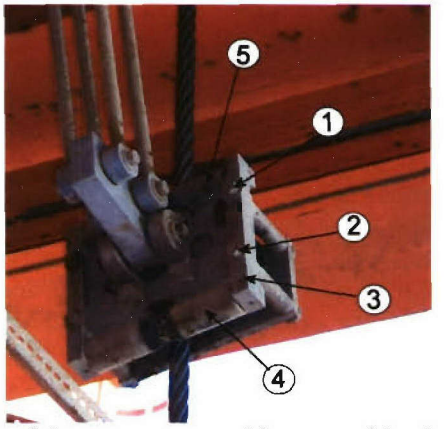

Figure 3-4 A close up view of the sway sensor rider assembly showing the wear-and-tear on the rollers.

3.3 Importance/Relevance

ForceNet is the Navy implementation plan for Network Centric transformation. There are three fundamental concepts in ForceNet: Sea Shield, Sea Strike, Sea Basing. Sea Basing is projecting joint operational independence. There several technological challenges associated with the Navy vision for Sea Basing. The first major challenge is the Close-in command, control, and communication (C3). Currently, ship-to-ship Close-in C3 during UNREP is tedious, time consuming, archaic, and labor intensive. This project will explore, develop, visualize, and integrate the high payoff enabling AWINN technologies for the close-in sea basing environment.

3.4 Productivity

Related Activities: The group responded to the Navy RFP for phase II HICASS RFP.

Honors and Recognition

1. A.H. Nayfeh received the Virginia 2005 Lifetime Achievement in Science Award.
2. A.H. Nayfeh received the Lyapunov Award from the ASME for his contribution to the field of Nonlinear Dynamics.

Publications

1. A.H. Nayfeh, Z. N. Masoud, N. A. Nayfeh, and E. Abdel-Rahman, "Control of Ship-Mounted Cranes," Plenary Lecture, IUTAM Symposium on Vibration Control of Nonlinear Mechanisms and Structures, Munich, Germany, July 28-22, 2005.
2. A.H. Nayfeh, "Nonlinear Dynamics: Phenomena and Applications", Lyapunov Lecture, ASME 20th Biennial Conference on Mechanical Vibration and Noise, DETC2005-84144, Long Beach, CA, September 24-28, 2005.
3. N. A. Nayfeh, Z. N. Masoud, and W. T. Baumann, "A comparison of three feedback controllers for container cranes," Proceedings of the 5th ASME International Conference on Multibody Systems, Nonlinear Dynamics and Control, Long Beach, CA, Sept. 2005.
4. Z. N. Masoud, A. H. Nayfeh, and N. A. Nayfeh, "Sway Reduction on Quay-Side Container Cranes Using Delayed Feedback Controller: Simulations and Experiments," Journal of Vibration and Control. Vol. 11, No. 8, 1103-1122 (2005).

Students Supported

N.Nayfeh – January 25, 2005 to July 2006.
M.Daqaq - January 25, 2005 to July 2006.
O. Marzouk - January 25, 2005 to July 2006.

4. TASK 4 Testing and Demonstrations

4.1 TIP#1 Distributed MIMO UWB sensor networks incorporating software radio

Advances in semiconductor technology have led to an exponential increase in computational power per unit space. Higher processing power implies faster signal processing at the physical layer. This ability to process more information in less time will allow small wireless nodes to coordinate and cooperate with other nodes. This has led to a recent emergence of interest in communication based on cooperation among single antenna wireless nodes to mimic and derive advantages akin to antenna array and MIMO systems. Point-to-point wireless communication systems have been well studied, modeled and perfected over the past four decades. In our research we have attempted to provide efficient ways to analyze and quantify the performance improvements of simple cooperative communication systems under realistic conditions. Figure 4.1-1 shows a representation of cooperative communication.

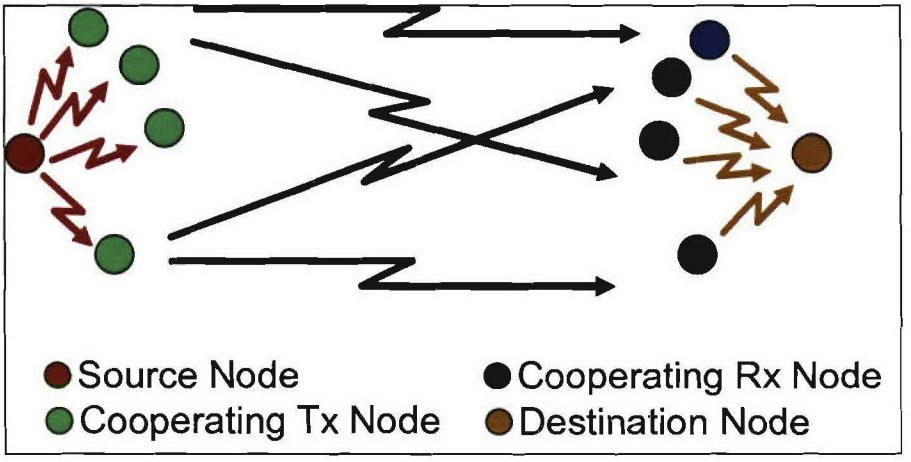

Figure 4.1-1 Representation of cluster-to-cluster cooperative communication scheme.

We presented a computationally efficient method to compute ergodic and outage capacities of distributed MIMO system. We developed a frequency domain method that can be used to analyze the effect of timing error on ABER performance of SISO and cooperative MISO systems. We presented Gaussian approximation approach to analyze the range improvement achievable using cooperative diversity under timing errors. As a special case of application of cooperative communication we examined the use of cooperative relaying over UAVs for extension of range and improving performance for ground based networks.

The following summarizes the final results as the outcome of our investigations on cooperative communication:

1. It was shown that distributed MIMO provides higher capacity than SISO based communication.
2. Cooperative communication based on distributed OSTBC performs better than a SISO system even with 60% symbol timing error when the channels are non-line-of-sight and Rayleigh distributed.

4.2 TIP#2 Close-in UWB wireless application to Sea Basing

Task objective: The objective of this subtask is to develop algorithms that allow UWB technology to provide precision position location, precision ranging, and imaging. With a low duty cycle and wide bandwidth, UWB is naturally suitable to radar and ranging applications. As the time duration of a pulse decreases, it provides finer resolution of reflected signals, such that the system can resolve distances with sub-centimeter accuracy using simple signal processing algorithms.

Accomplishments: The crane demonstration including communications with the crane's control system was successfully carried out.

Description

After investigating the proposed ranging scheme in theory and via simulation, it was desired to put it to a real test. Therefore, a demonstration was planned with the purpose to show that using UWB pulses the range below a cargo crate can be estimated and an automatic crane controller can make use of the ranging information to land the crate on the platform with minimal impact. Furthermore, a real demonstration might give insight to conditions not considered during the theoretical development.

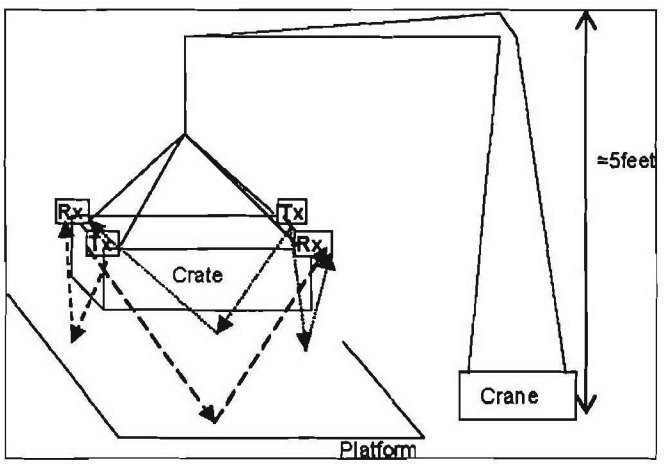

Figure 4.2-1 Demonstration General Layout (not to scale).

The demonstration called for a scale demonstration using a 5 foot boom crane (Figure 4.2-1) in the ESM's Non-linear Dynamics Lab. Originally, the system was supposed to give 10 updates/second for all sides to the crane's control system. However, as it will be explained later, that requirement could not be met with the available equipment.

3. Using cooperative diversity based on randomized OSTBC scheme, the range does not improve linearly with node density under timing error. A maximum of 2X range extension can be achieved with about 50 nodes participating in the scheme.
4. The range of over-the-horizon communication can be improved by about 35 times by applying cooperative beamforming over single-antenna mounted UAVs flying in formation.
5. The average bit error rate (ABER) performance of relay based cooperative diversity systems is better than SISO systems even when the relays decode and forward erroneously. However the above requires proper choice of SNR threshold at the relay for the relay to make decision to forward the received packets. A forwarding protocol was studied and the expression for optimum SNR threshold at the relay was derived.

Setup and Specifications

The demo was based around the major equipment comprising the demo, the transmitter, and the receiver that were already available in MPRG's radio lab. Only the minimal equipment had to be purchased and constructed such as the crate with the antennas, an antenna switch, the four antenna dividers/combiners, a switch driving circuit, a USB Digital I/O interface, and cables.

Equipment List

The following equipment was used to make the demonstration possible:

- Geozondas Pulser, (GZ1106DL1 & GZ1117DN-25)
- HP33120A Function Generator
- Tektronix CSA8000B Digital Sampling Oscilloscope (DSO)
- Tektronix PS280 DC Power Supply
- National Instruments USB 6501 Digital I/O interface
- Custom made Switch Driving Circuit
- Gateway M460 Laptop computer with LabVIEW (2.0GHz Pentium-M, 1GB RAM)
- Crate with UWB antennas made by Randall Nealy (Virginia Tech Antenna Group)
- United Microwave cables Micropore 190 (3x8ft)
- United Microwave cables Microflex 150 (3x10ft)
- Crossover Ethernet cable for direct connection between the laptop computer and the DSO
- 9dB attenuator
- Generic cables for trigger connections

Figure 4.2-2 shows how the equipment was connected, and Figure 4.2-3 and Figure 4.2-4 present actual photos of the equipment. The Geozondas pulser was used as the transmitter generating a -30V 30ps pulse (time width measured at half-amplitude.) The pulser was triggered by the the HP function generator using a TTL signal of 200 KHz. From the pulse the TTL triger signal was attenuated by a 9 dB attenuator in order to safely trigger the Tektronix CSA8000B DSO that was used as the receiver. The DSO and the Switch Driving Circuit (for the antenna switch in the crate) were controlled by the laptop. The laptop communicated with the switch driving circuit and the crane control by the NI USB Digital I/O interface. The only information sent to the crane controller was the current range information. The crane control software was developed by Nader A. Nayfeh.

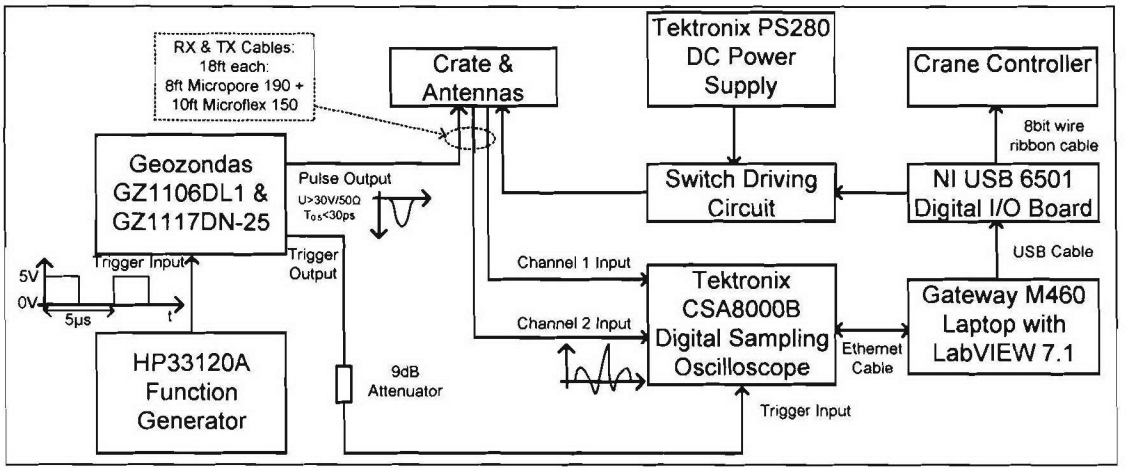

Figure 4.2-2 Demonstration setup block diagram.

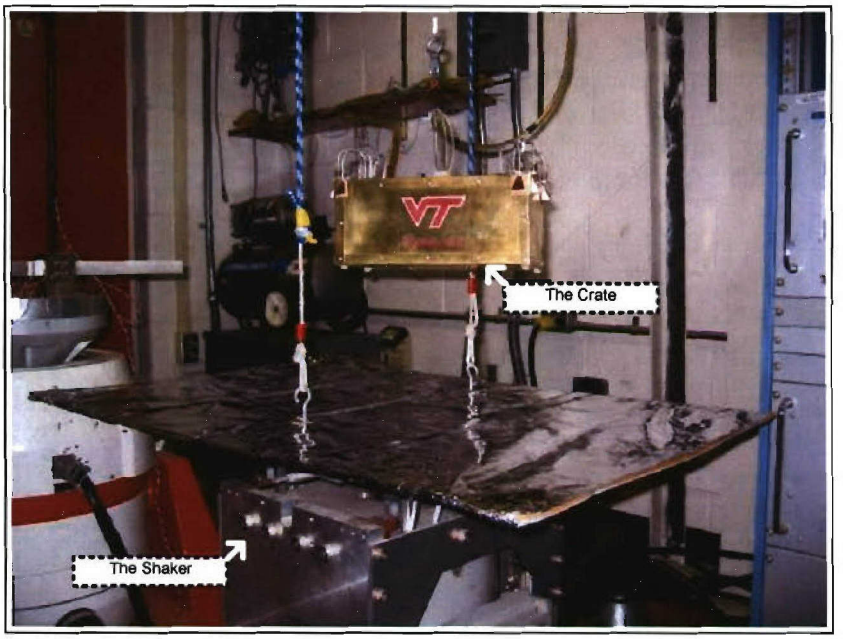

Figure 4.2-3 Demonstration setup photos: Crate and shaker.

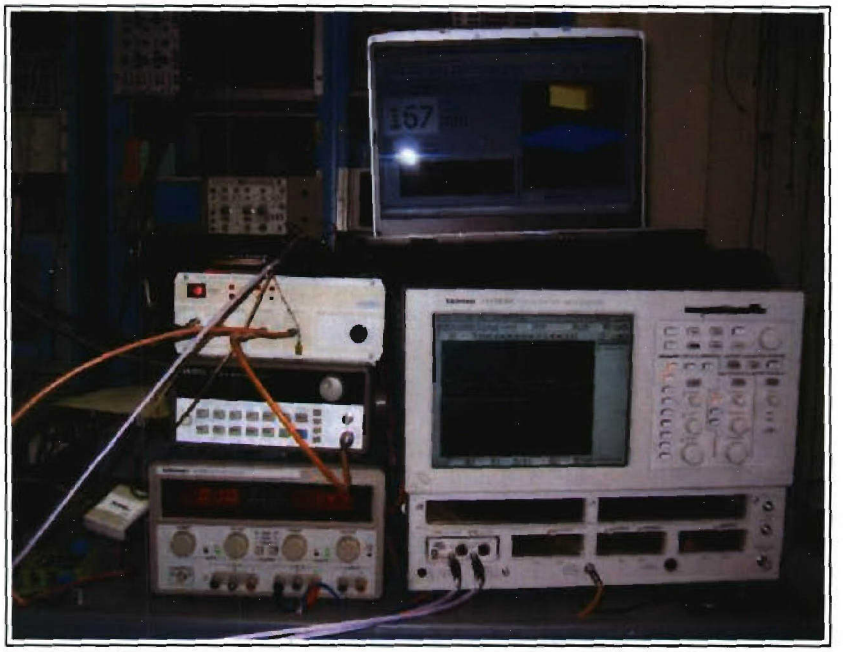

Figure 4.2-4 Demonstration setup photos: Equipment.

Transmitter and Receiver

As was previously mentioned the transmitter was a simple pulser that produces a -30V 30ps Gaussian pulse. Because of the availability of only one transmitter and the fact that the crate had two transmitting sides on the crate, an antenna switch was installed inside the crate in order to switch between transmitting sides.

The receiver was a Tektronix CSA8000B Digital Sampling Oscilloscope, capable of receiving 50, 4000 sample, waveforms per second when triggered with a 200KHz signal. Unfortunately, the DSO was not designed for real time transfer of the acquired data to an external device. The effective rate was at least 16 waveforms when it was continuously receiving the same signal without interruptions or 3 waveforms per second when it was forced to clear the acquired data and start receiving anew (which was required every time the transmission side was changed). This limitation on update rate caused the demonstration to be done in two ways, one with fast update rate using only one side for ranging, and one with the slow update rate fully utilizing the four sides and the orientation estimation algorithm which was developed in the previous chapter.

Crate and Antennas

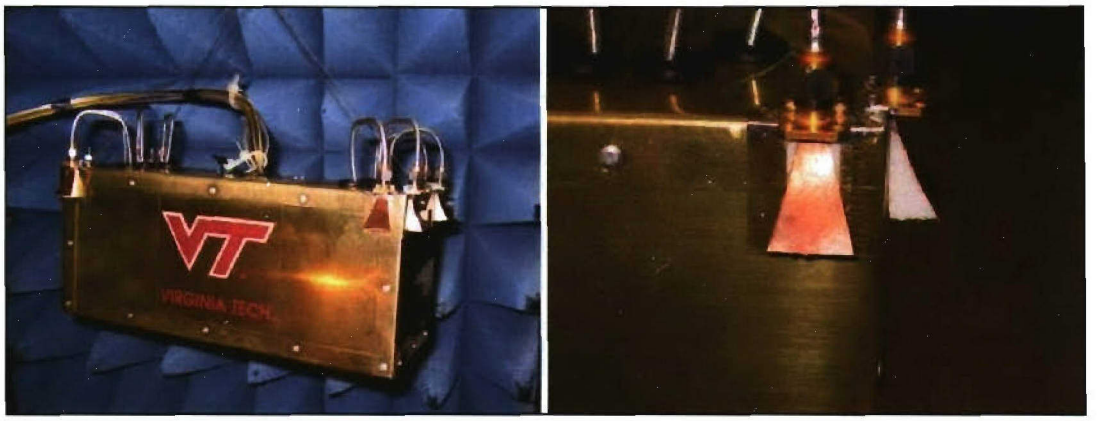

Figure 4.2-5 The crate and the crate antennas.

For the demonstration, one of the major components was the crate with the UWB antennas. Both the crate and the UWB antennas (Figure 4.2-5) were designed and built by Randall Nealy, staff engineer of VTAG. Inside the crate additional components (antenna switch and power dividers/combines) had to be installed; those were installed Haris Volos with the help of Randall Nealy.

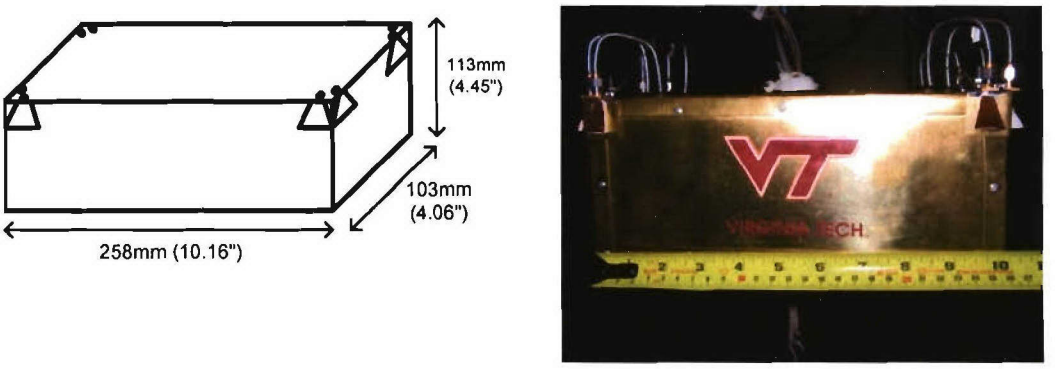

Figure 4.2-6 Crate dimensions.

The crate as shown in Figure 4.2-6 had dimensions of 103 mm (4.06") wide, 258 mm (10.16") long, and 113 mm (4.45") high. The dimensions are approximately 1/24 scale of a real container. Regarding the antennas, an antenna design that will be as directive as possible was desirable. However, due to the size limitations, the actual antennas were most directive and effective in frequencies above 10 GHz. This caused reduced received signal levels because most of the pulse's energy was below 10 GHz. Also, because of the reduced directivity in the low frequencies in some cases unwanted reflections were present. However, with the choice of good quality cables and DSP the only direct effect to the demonstration was to reduce the range from 5ft to 2ft. The sample pulse used for the matched filter detection process is shown in Figure 4.2-8 and was obtained after applying a bandpass filter of 8 to 18 GHz to the received signal.

Antenna Coupling

Due to the small dimensions of the crate, the transmitting and receiving antennas were very close to each other, causing a signal to be directly received from the transmit antenna (coupling). This coupling was very strong compared with the desired reflected signal. The coupling was mitigated by recording it during calibration and subtracting it from the received signal. The received signal and coupling are shown in Figure 4.2-7.

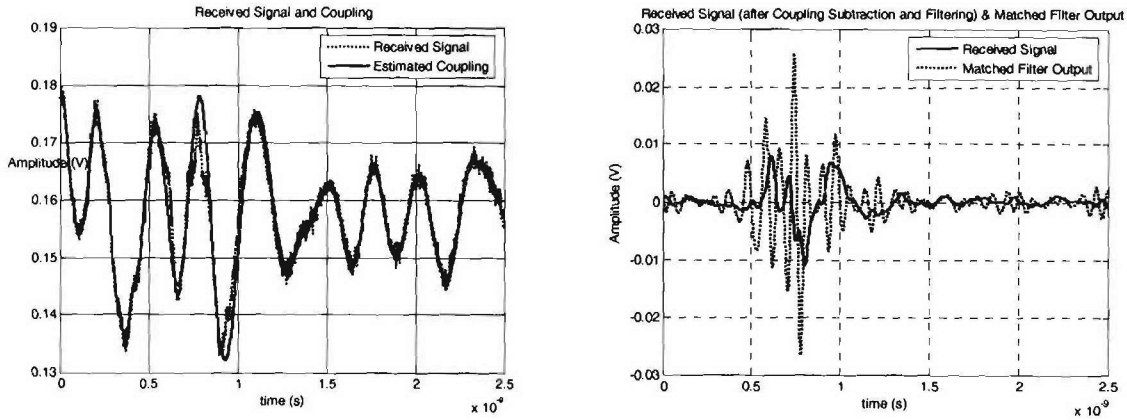

Figure 4.2-7 Received coupling (left) and received signal with coupling subtracted and matched filter output (right).

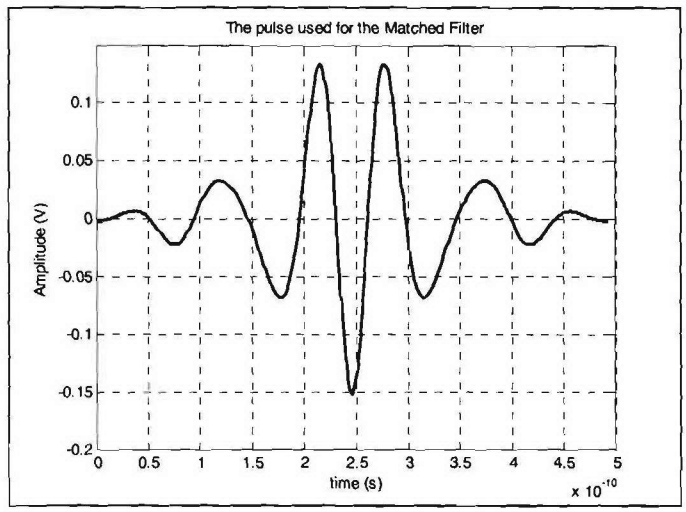

Figure 4.2-8 The pulse used for matched filtering.

Crate Inside Configuration

The crate had four antenna pairs, one pair at each corner. Two of the pairs were designated transmitting pairs and the other two pairs were designated receiving pairs. The transmit and

receive pairs were located on alternate corners as shown in Figure 4.2-9. The signals from the receiving antennas on each corner were added via RF combiners and the signals to the transmitting corner antennas were distributed via RF dividers as shown in Figure 4.2-9.
The parts used inside the crate included:

- 4 Narda 4456-2 2-Way Power Dividers/Combiners 2-18GHz.
- Microwave Communications Laboratories K2-8-LIS/12P Latching Electromechanical Switch, SPDT, DC to 26.5GHz.
- 4 8.5" United Mircowave Microform 139 Cables.
- 4 9.5" United Mircowave Microform 139 Cables.

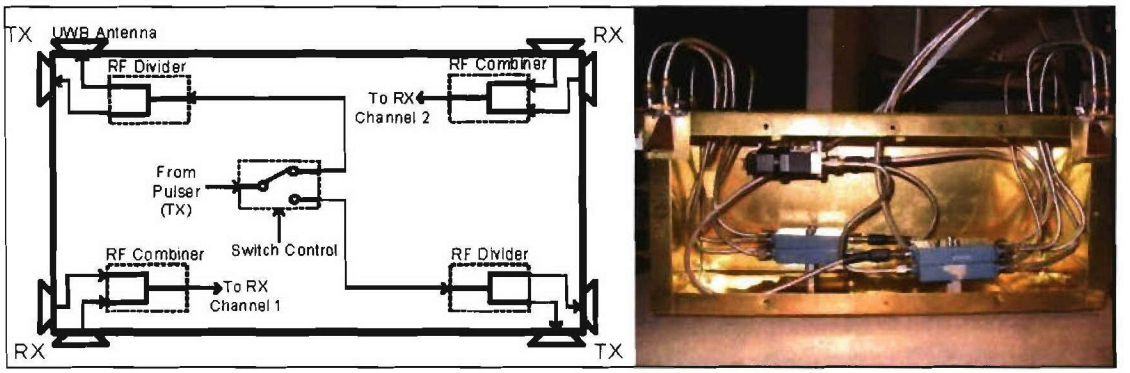

Figure 4.2-9 Crate inside configuration diagram and photo.

Supporting Circuitry

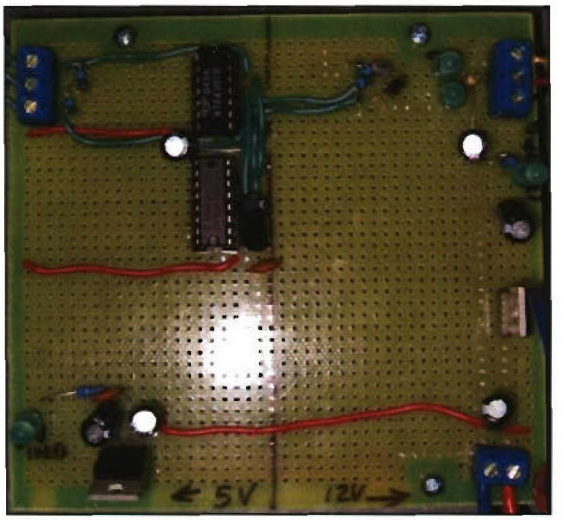

Figure 4.2-10 Switch driver circuit photo.

The antenna switch used inside the crate required a driving voltage of 12 V and 100 mA peak current. The USB I/O card used was not able to meet these requirements. For that reason, a simple driving circuit was designed. The circuit schematic shown in Figure 4.2-11, Figure 4.2-12, and Figure 4.2-13 consists of three parts. First, the power supply's input voltage is regulated to 12 V using a standard regulator IC providing power to the 12 V part of the circuit, and then it is further regulated to 5 V for the 5 V components of the circuit. Second, a simple logic circuit was designed to prevent the combination "1 1" which means both sides are transmitting. That state is undesired and must be prevented to avoid potential damage to the driving transistors and to the switch itself. Third, two high speed switching transistors were used to drive the switch which only draws current when it is changing state (latching switch.) Furthermore, for additional safety the current supplied to the circuit from the external Tektronix power supply was limited to the minimum required for the proper operation of the circuit. The assembled circuit is shown in Figure 4.2-10.

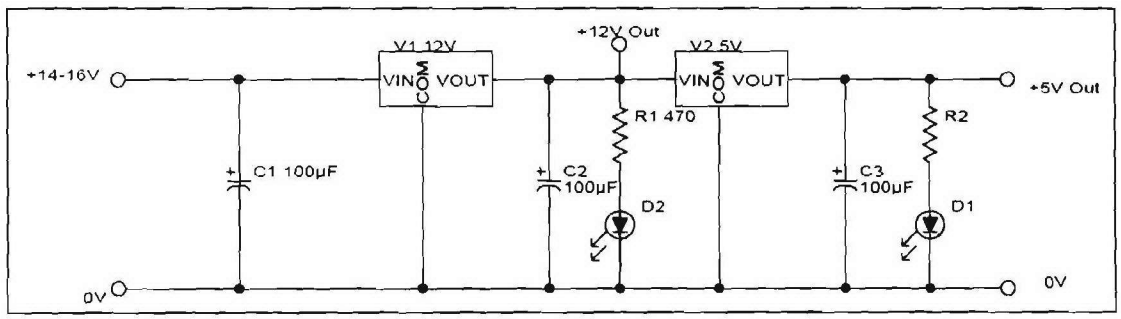

Figure 4.2-11 Power supply schematic.

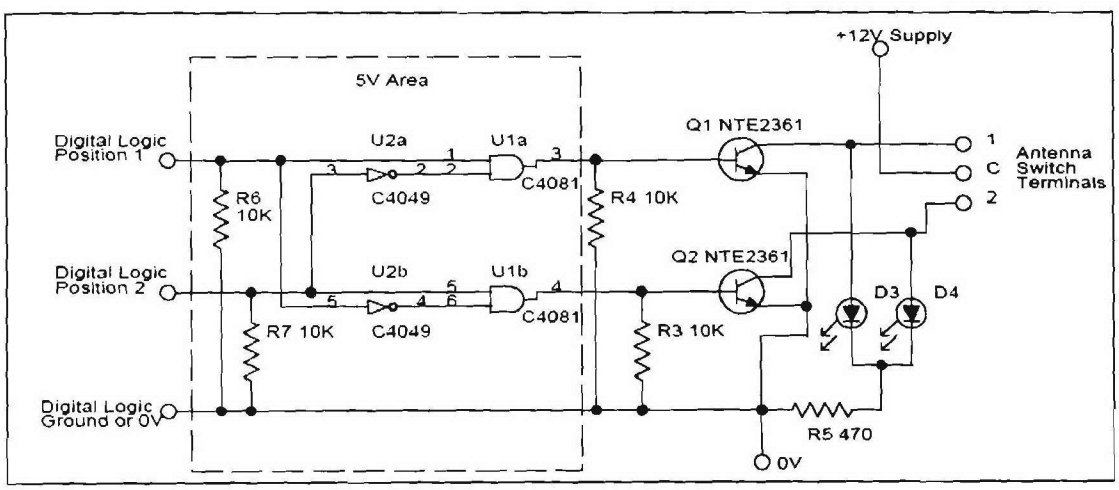

Figure 4.2-12 Logic and driver part schematic.

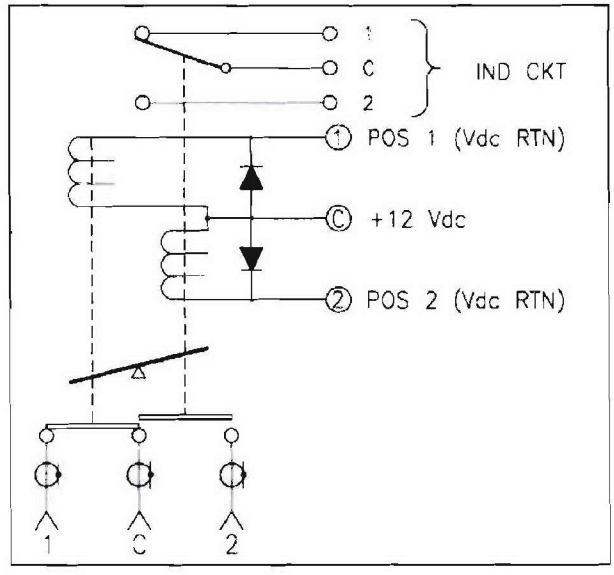

Figure 4.2-13 Switch schematic.

Software Application (LabVIEW)

The application that reads the waveforms, controls the switch, processes and displays the required information was developed in LabVIEW because it provided all the necessary DSP functionality and the ability to connect with external peripherals such as the DSO and the USB I/O interface. Two applications were developed: first, an application utilizing the one side for ranging; and second, after the one side was perfected, the application was expanded to four sides. Figure 4.2-14 shows screenshots from the two applications, one for single-side ranging, and three samples from four-side ranging. As can be seen from the screen shots the results were not limited to numbers, a 3D visual representation was also developed. Figure 4.2-15 shows a sample screen shot of an actual LabVIEW block diagram.

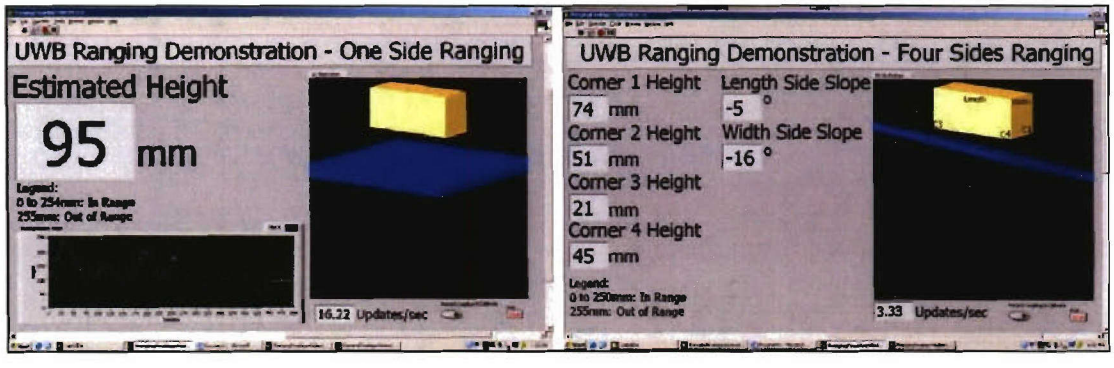

Figure 4.2-14 LabVIEW application screen shots.

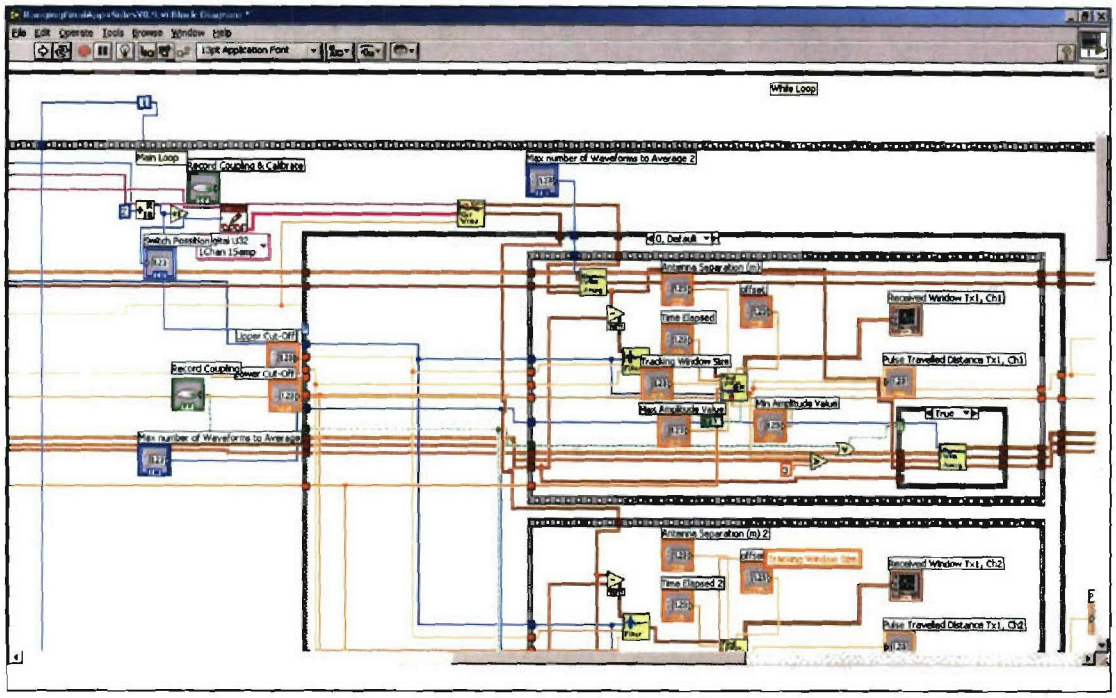

Figure 4.2-15 LabVIEW block diagram sample screen shot.

Single-Side Ranging

This section presents a description of the single-side ranging application referring to the application's block diagram shown in Figure 4.2-16.

The Initialize sub-block establishes connections with the external devices (DSO, USB Digital I/O), reads the reference pulse to be used for the matched filter process, and initializes all the necessary variables. The main program starts with Get waveform that communicates with the DSO and gets the latest acquired waveform. Then, Subtract coupling subtracts the current estimate of the coupling from the received waveform. Furthermore, the Filter waveform sub-block applies a 0.8-20 GHz bandpass filter to remove out-of-band noise in the received signal. Additionally, Find pulse's location and traveled distance applies the acquisition method in order to find the pulse's location and estimate the distance traveled by the pulse (This will be discussed in more detail in its own section). Moreover, Estimate distance applies the Pythagorean theorem to find the height based on the traveled distance assuming a right triangle with a base equal to the half antenna separation and a hypotenuse half the traveled distance. Finally, Non-linear filtering smooths the output by eliminating sudden output changes that might occur due to incorrect estimation. The operation of this block will be also discussed in more detail in its own section.

The Add waveform to coupling database function helps update the coupling database which is being maintained for the coupling estimation. Initially, the database is filled during the calibration process, but later it is continuously updated with new waveforms. When a new waveform is received and the pulse's location is estimated, a half window waveform centered in the pulse's

location is replaced with the current coupling estimation, and the rest of the waveform is included in the database. This allows active coupling estimation without recording the actual pulse.

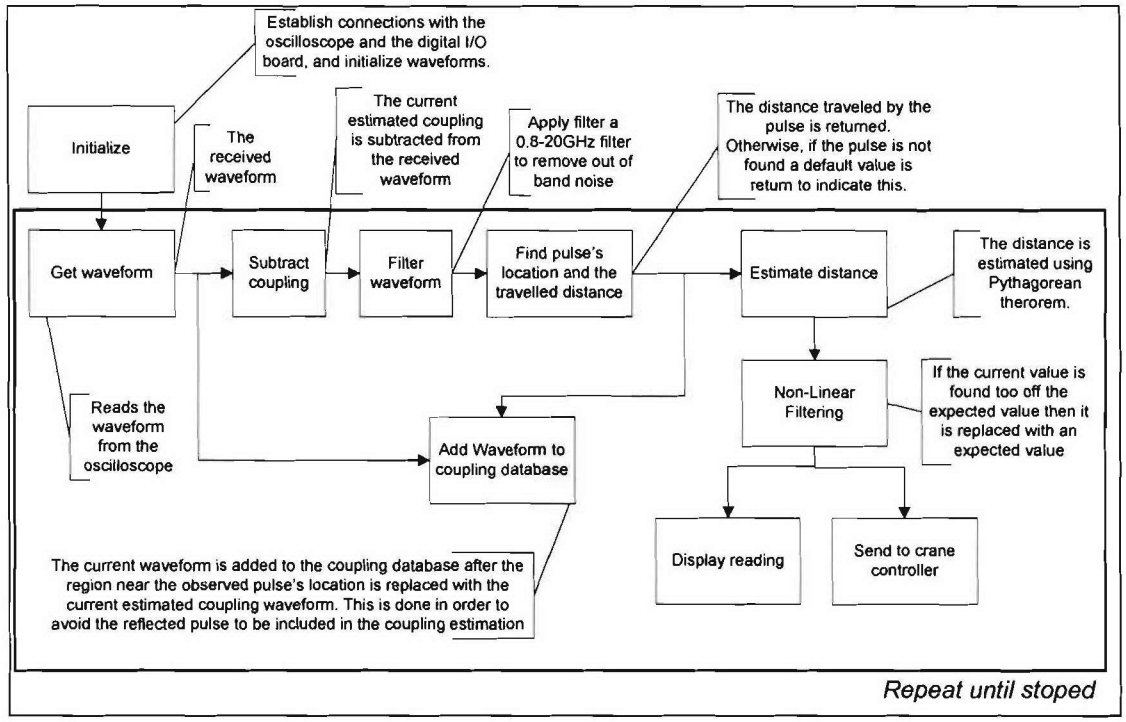

Figure 4.2-16 Single-side ranging application block diagram.

Four-Side Ranging

The block diagram of the four-side ranging application is shown in Figure 4.2-17. The basic components are the same as the single-side application repeated four times, however, there are some differences. First, at each iteration the transmit side alternates. Second, because of the transmit side alternation at each iteration only two waveforms are processed, therefore, only two sides have updated values. For the other two sides, the last known values are used. Third, in this application no data are sent to the crane controller. And fourth, the estimation algorithm for full orientation estimation (which was developed previously for this purpose) is utilized.

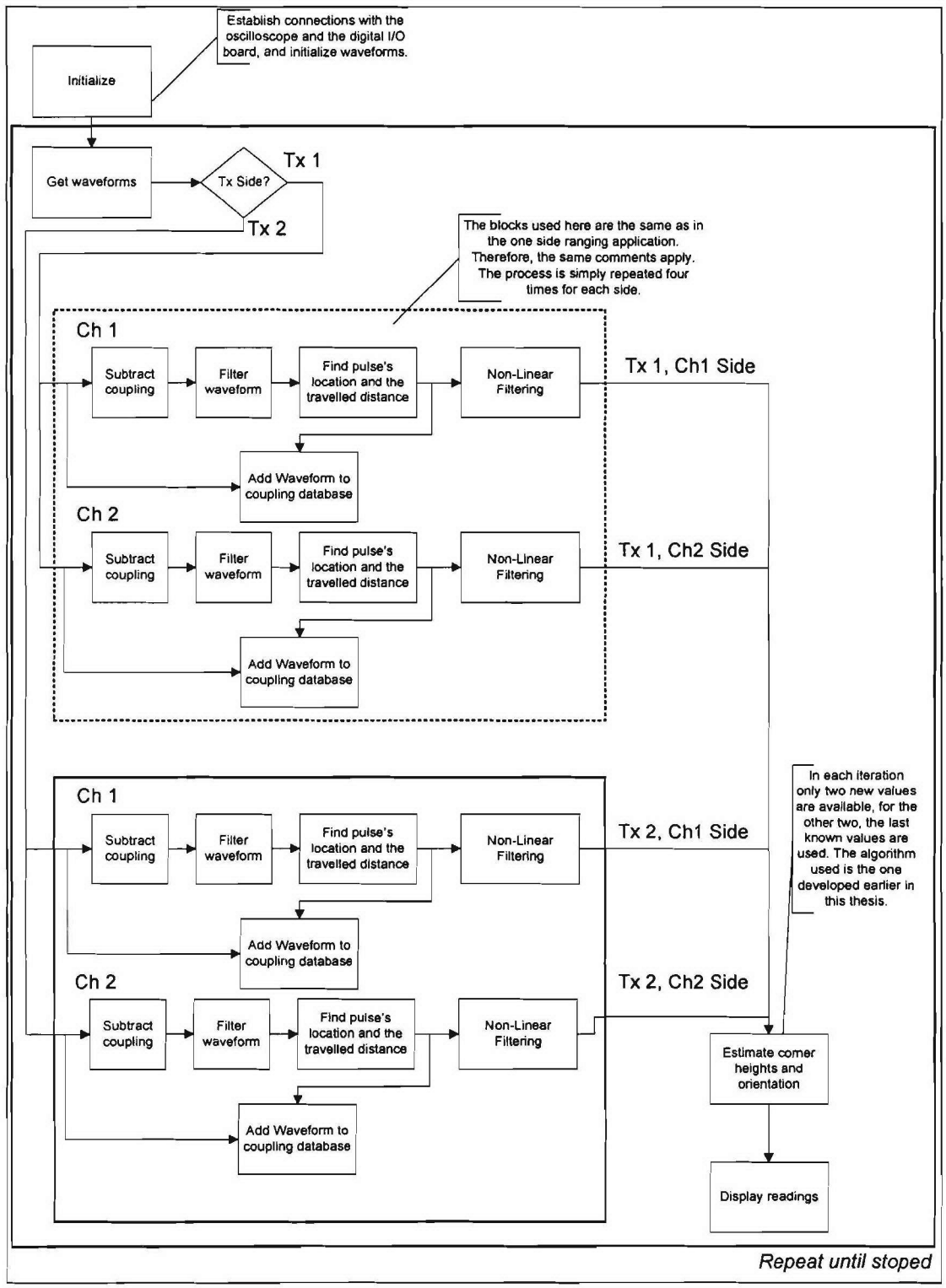

Figure 4.2-17 Four-side ranging application block diagram.

Sub-blocks Used: Record Coupling and Calibrate Procedure--Find Pulse's Location

This sub-block gets the input waveform from the main program, then it applies an exponential threshold to received signal. The exponential threshold is applied knowing that the signal's level decreases exponentially. This was found to eliminate wrong detections due to imperfect coupling cancellation. Furthermore, in parallel a match filter with a threshold is also applied to the received waveform, then both results are combined to get a waveform that will meet both the exponential threshold and the matched filter threshold.

After the above criteria are applied to the received waveform, if the last location of the pulse is known, the detection is limited around the last observed location. This provides a simple tracking knowing the pulse should be near the detected location. However, if no pulse is found satisfying detection criteria, then the whole received window is considered for detection. Finally, if no pulse is found in the whole window then the sub-block returns some default values that indicate that the pulse was not found, and probably was out of range.

If a pulse is found, the second strongest peak is also found and if it is at least 90% as strong as the first peak then it is also considered. It was observed for some cases that near the desired pulse will be another pulse consistently before or after the pulse, depending on the side. For that reason the program was instructed to give priority to one of them. The second pulse was given priority when the pulse was received on the short sides.

The two separate arriving pulses was due different cables inside the crate. The cables on the short side of the crate were in total two inches longer that the cables on the long side (one inch for the receiving antenna, and one inch for the transmitting antenna). This caused the pulse for the long side to be sent earlier and to be received before the intended pulse on the short side. Usually, this pulse was attenuated, but there were cases that caused some instability on the detection, and selecting the second strongest pulse mitigated this problem.

Figure 4.2-18 shows a screen shot of the received window that was used for troubleshooting purposes. On the screen, shot some of the detection features discussed are visualized: the exponential threshold (blue), the matched filter output (yellow), and the matched filter region that was considered for detection (red).

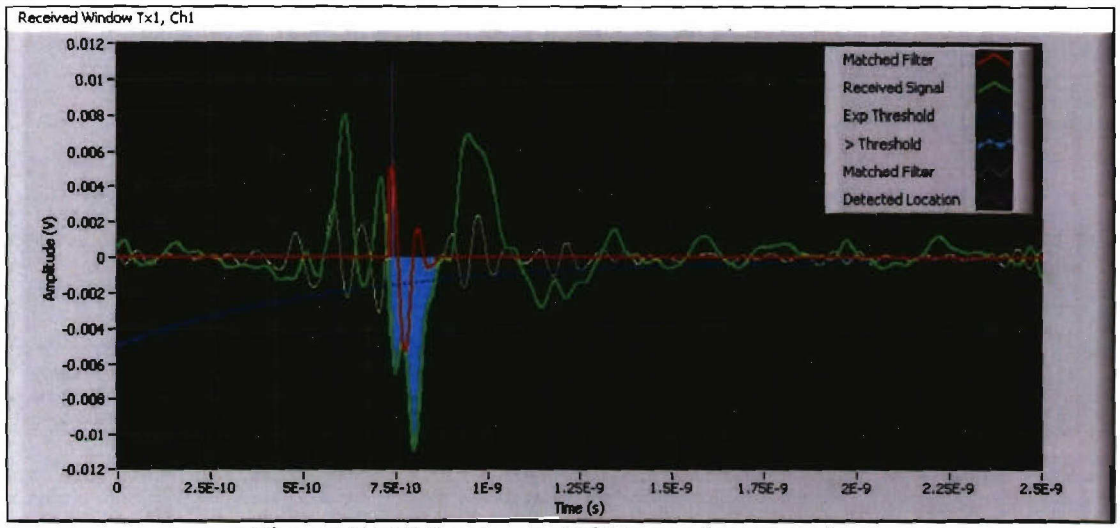

Figure 4.2-18 Received window sample screen shot.

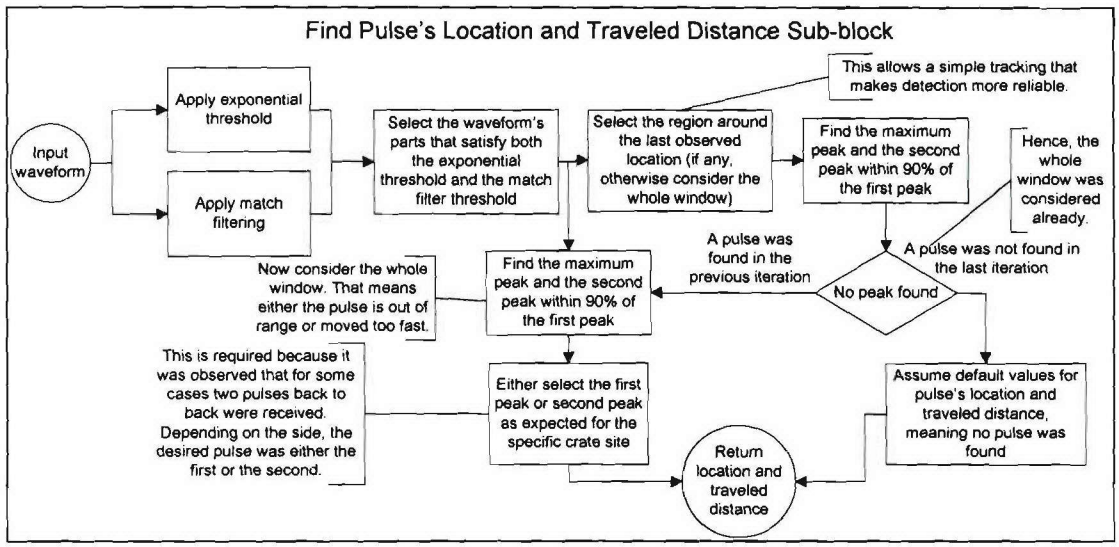

Figure 4.2-19 Find pulse's location sub-block.

Non-linear Filtering

Occasionally, the detector momentarily might assume detection far from the actual pulse's location and then return back to the correct reading. This can cause unwanted spikes on the output of the program. For this reason the program keeps a history of the last two values. Before a value is given for an output, first, the values before and after that value are compared, and if they are found to be within a percentage of each other, then their average is computed. Furthermore, the percentage of the current value is compared to that average value and if it is found to have more than a 40% diffence then it is replaced with the average of its surounding values.

In addition, to the the procedure above, a moving average filter further smooths the output based on a longer history record that is also kept for that reason.

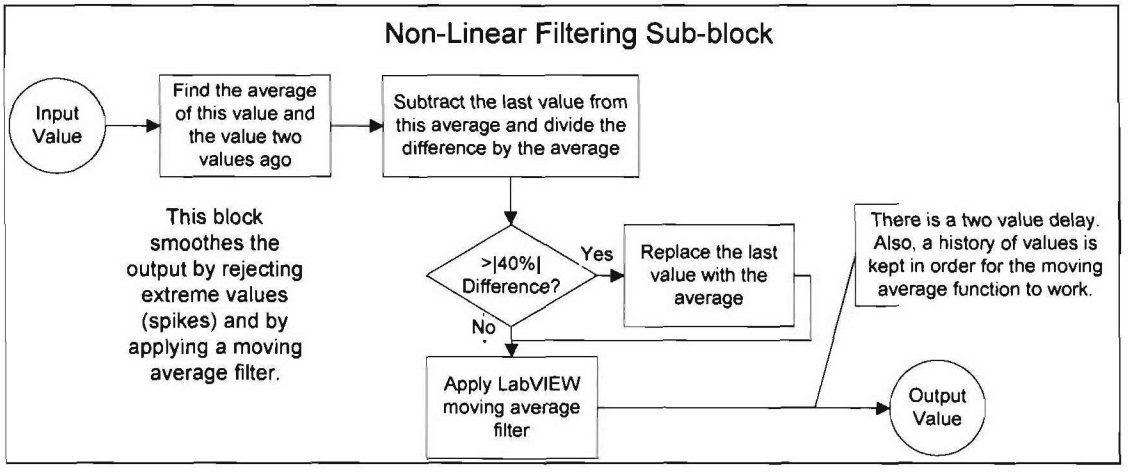

Figure 4.2-20 Non-linear filtering sub-block.

Other Techniques Used

Keeping a waveform database with minimum processing

A waveform database had to be maintained for the coupling estimation. Keeping a number of waveforms requires memory and processor time. The former was not an issue for this application: however, the latter was a problem because whenever a new waveform was added (to the database) and one was removed at the same time, all the waveforms had to be averaged. That caused significant delays. However, a technique was employed that used the minimum processing time: in addition to the waveforms, their sum was maintained as well, and when a waveform was added to the database it was also added to the total sum. Furthermore, the waveform that was removed was subtracted from the sum. This procedure, for the averaging, only required one addition, one subtraction and one division, compared to additions and one division, where is the number of the waveforms kept in the database.

Ethernet: A GPIB replacement

GPIB (General Purpose Interface Bus) is a standard interface for communication between instruments from different sources. The Tektronix CSA8000B DSO is also equipped with a GPIB interface. The problem was that the GPIB's version used has limited data transfer capabilities. The GPIB was successfully replaced by an Ethernet connection between the DSO and the laptop used for the DSP.

The replacement was made possible by installing the updated National Instruments VISA driver (replacing the Tektronix VISA driver) to the DSO. The updated driver provides the NI-VISA server which allowed the laptop to connect using a TCP/IP network connection to the DSO. This allowed faster data transfer and network access to the DSO folders.

Custom GetWaveform Routine Implementation

The DSO had a LabVIEW driver for issuing commands and transferring waveform data from the DSO to the laptop running LabVIEW. However, the GetWaveform implementation of the driver was found not to be optimized for transfer speed. It is speculated that it issues commands that might be redundant and that opens and closes the connection to the DSO each time a waveform is requested which causes some delays. For that reason a new GetWaveform was written in LabVIEW that sends only the necessary commands for obtaining the current waveform. Furthermore, the connection to the DSO was kept open during the acquisition process; therefore no unnecessary time was lost for opening and closing the connection. Finally, the transfer mode was in binary instead of ASCII which yielded fewer bits to be transfered, hence a faster response.

Despite the customization of the GetWaveform the delay introduced by the DSO when clearing the acquired data, required when changing tx sides, could't be overcome. That slowed the transfer rate for the Four-side application.

Demo Outcomes

Single-Side Ranging

The demo was able to provide 1 mm resolution and 16 Updates/second of the estimated height of the the crate. At first the system was demonstrated with a stationary floor. The crate was moved up and down to demonstrate the abilities of the system to accurately estimate the height between the crate and the floor. A sample of the system's output is shown at Figure 4.2-21 where the crate is raised from the floor to the maximum range of the system and then is landed back to the floor. Table 4.2-1 shows a sample set of height measurements. Because of the 1 mm resolution of the system obtaining good estimates of the system's accuracy was a hard task. In order to improve measurement accuracy and minimize measurement errors, the measurements were taken by resting the crate in wooden blocks of known height, instead of the crate being suspended by string wire. Nevertheless, the sample measurements demonstrate that system is accurate in most cases within 1 mm, and the maximum error recorded being 2 mm from 0-191 mm heights. The accuracy for these measurements appears to be independent of height. This is due to the fact that for the heights evaluated the accuracy is within the resolution of the system because of the good SNR observed at these heights. The SNR for these measurements was 29.9 dB and 17.5 dB for the 0 mm and 191 mm case, respectively. For a 250 mm case the SNR was 16.8 dB. The system could potentially range up to 2 ft (600 mm) but for this to happen several changes are needed to the LabVIEW application in order to accommodate for the longer receive time window (more points per waveform) and estimation of good threshold values, furthermore, unlike the first foot (0 - 300 mm), the second foot will experience lower SNR's that will challenge the accuracy of the system. Finally, keep in mind that 1 foot translates to 24 feet in an actual scale system.

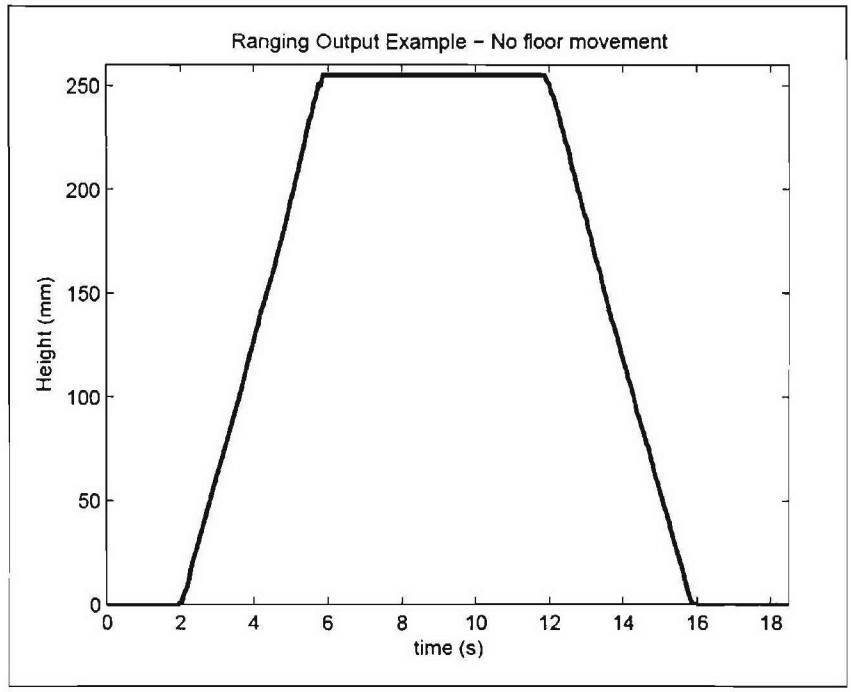

Figure 4.2-21 Sample ranging output: Motion all the way up and then down.

After the ability of the system to provide fast and accurate range information was demonstrated, the floor was set to oscillate with 1 Hz. Then the crate control system successfully landed the crate on the oscillating floor with minimum impact. The range output to the crane control system is shown on the Figure 4.2-22, from which three main regions can be observed: the oscillating region, the landing region, and the landed region.

Table 4.2-1 Single-side sample measurements (mm).

Actual	Measured										σ	mean	Mean % error
	Trial												
	#1	#2	#3	#4	#5	#6	#7	#8	#9	#10			
0	0	0	0	0	0	0	0	0	0	0	0.00	0	0.00
19	20	20	20	20	20	19	19	19	19	18	0.70	19.4	2.11
38	38	38	40	39	39	38	38	38	37	38	0.82	38.3	0.79
57	57	57	58	58	57	57	56	57	57	57	0.57	57.1	0.18
76	77	77	77	77	76	77	76	76	75	76	0.70	76.4	0.53
95	97	96	96	96	95	96	95	95	95	96	0.67	95.7	0.74
115	114	115	115	115	114	115	114	115	114	114	0.53	114.5	-0.43
134	133	135	134	134	134	135	134	134	133	134	0.67	134	0.00
153	153	153	153	153	153	154	153	153	153	154	0.42	153.2	0.13
172	172	173	173	173	173	174	174	173	172	173	0.67	173	0.58
191	191	192	191	192	192	193	192	191	191	192	0.67	191.7	0.37

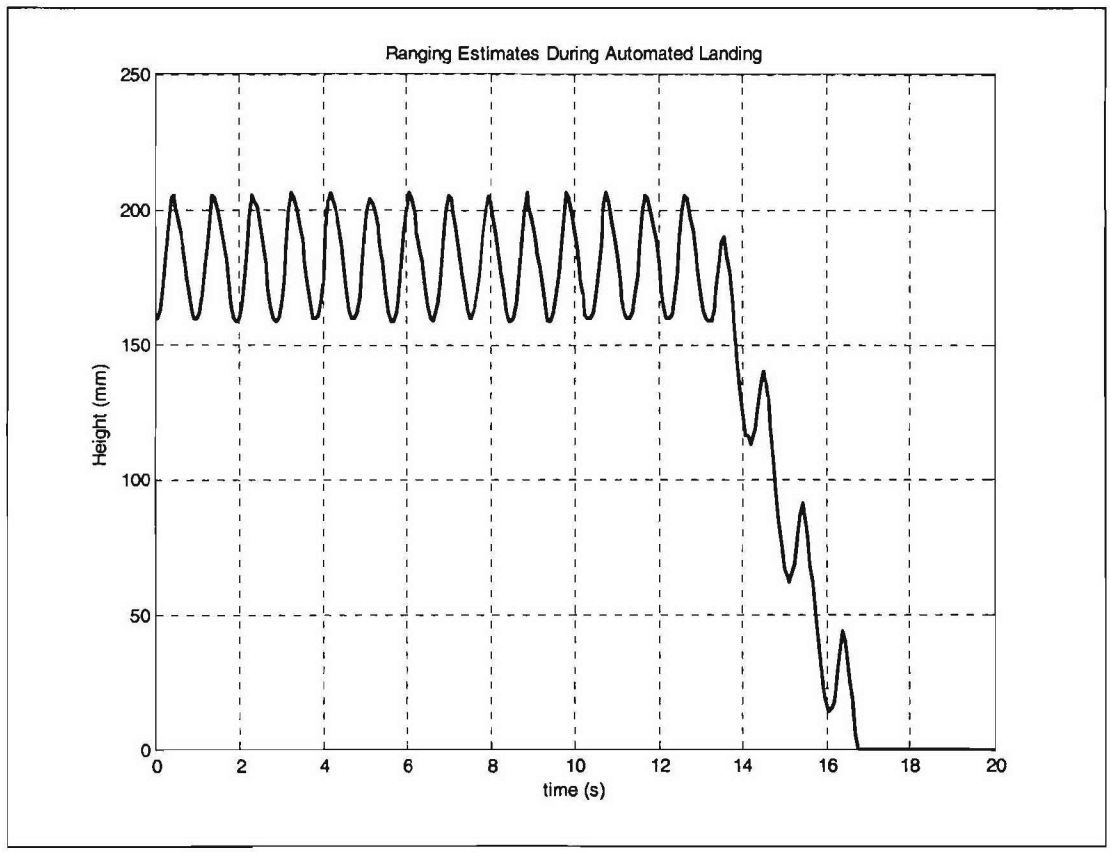

Figure 4.2-22 Height versus time during automatic landing.

Four-Side Ranging

The full implementation of the system was demonstrated in a slow motion manner because of the low update rate of the system (3 updates/second). The orientation capabilities of the algorithm were demonstrated by tilting the floor and by visualizing the tilt on the laptop's screen. Furthermore, because two sides were estimated at a time this caused the effective update rate to be 1.5 updates/second, which further limited the speed of this part of the demo. Also for this case a few sample measurements were taken which are shown in Table 4.2-2. These measurements were taken with the crate suspended using string wire, which makes the measurements subject to measurement errors. The system was found to have the same accuracy as the single-side case.

Table 4.2-2 Four-Side Sample Measurements

	Corner Height (mm)				Slope (°)	
	C1	C2	C3	C4	Length Side	Width Side
Actual	0	0	0	0	0	0
Meas.	0	0	0	0	0	0
Actual	79	78	74	75	0	-2
Meas.	78	78	74	75	0	-2
Actual	48	46	36	39	0	-5
Meas.	49	47	37	38	0	-8
Actual	25	53	55	28	6	-1
Meas.	24	52	54	27	6	-1
Actual	35	59	52	26	6	-4
Meas.	36	61	53	27	6	-5

Conclusions

For the demo, a 1/24 scale crate was used with small UWB antennas. The demo was first performed using a single side for ranging which provided 16 updates/second to the crane controller to test the system with the crate landing algorithm developed by Nader A. Nayfeh. The crate landing algorithm was able to land the crate, using the input from the UWB system developed with minimum impact at an oscillating surface (1 Hz.)

In the second part of the demo, the orientation capabilities of the algorithm were demonstrated at a slower rate. In the demo the algorithm only received the update information of two sides at a time, also limited the update rate of the system by an additional factor of two. It is suggested that the final application will have four receiving channels.

Because the antennas were very close to each other there was a direct received signal (coupling) which was successfully mitigated. This is something that will be a smaller issue in a real-world system in which the antennas will be separated by several meters and the coupling will be attenuated.

For future development an acquisition technique could be employed which will allow more robust acquisition and more sophisticated pulse tracking. Furthermore, pulse shapes might be investigated as some pulses might be more suitable than others for this application because of their different spectrum characteristics. Moreover, the application's environment can be further investigated for making potential suggestions and additions to the system. Finally, the ranging information of the crate can be potentially used for other purposes such as detecting nearby objects to the crate and predict possible collisions.

4.3 TIP#3 Secure Ad Hoc Networks

4.3.1 Project Description

The testing and demonstration of secure ad hoc networks involved integration and testing along three related tracks. Each of these led to a separate demonstration (or coupled set of demonstrations) using a common hardware and software base, as implemented in our test bed network (see discussion of Task 2.1).

(a) Activities within Task 2.1 (Ad Hoc Networks) that support core network services were integrated, tested, and demonstrated. Integrated capabilities included policy-based quality of service (QoS) and resource management using topology control (TC), security based on distributed certificate authorities (CAs) for key management and trust grading, and mobile ad hoc network (MANET) routing support for QoS, security functionality, and accessibility of network information for cross-layer designs. Capabilities were shown operating with Internet Protocol version 4 (IPv4) and, where feasible within the level of effort possible, Internet Protocol version 6 (IPv6).

(b) A cross-layer approach to transporting multiple description (MD) video in ad hoc networks, also a part of Task 2.1, was integrated, tested, and demonstrated. This task utilized application-level routing to use application-specific optimal routes. It was integrated with the MANET routing effort of Task 2.1, e.g., with Optimized Link State Routing protocol with Multiple Channel support (OLSR-MC), to utilize the topology information efficiently obtained by the MANET routing protocol. This information was obtained using the network information (NI) application program interface (API) developed in Task 2.1.

(c) We integrated real-time middleware from Task 2.2 with the combined QoS, security, and routing, as discussed above and as investigated in Task 2.3. Specifically, we developed methods and mechanisms to integrate capabilities at the network level, including use of the NI API, with real-time services offered by middleware.

4.3.2 Demonstration Description

Table 4.3-1 lists the themes, components, and leaders for the three demonstrations. Demonstration (a) focused on core network services. Demonstration (b) involved network support for a video application. Demonstration (c) relates directly to Task 2.3 and involved the integration of network services with an application based on the time-utility function real-time middleware.

The components of the different demonstrations listed in Table 4.3-1 were the same except for the application – or application plus middleware in the case of Demonstration (b) – that was supported. The security, QoS, and routing components are discussed further in Task 2.1. Note that OSPF-MCDS-MC or, more simply, OMM, is a multi-channel version of the Open Shortest Path First with Minimum Connected Dominating Sets (OSPF-MCDS) MANET routing protocol. OLSR-MC, a multi-channel version of the Optimized Link State Routing (OLSR) MANET routing protocol, was the default routing protocol during the demonstrations. The network monitoring tool, TopoView, and topology emulation tools were carried over from the previous NAVCIITI project, but were modified to support new functions in the network and to work in an IPv6 environment as described in Subsection 2.1(f). The OLSR Topology Viewer (OLSR-TV),

an additional performance monitoring tool was also developed as part of Subtask 2.1(f) and used in the demonstrations.

Table 4.3-1 Demonstration Components and Leaders for the Three Demonstrations

Demonstration	Key Components	Leaders
a) Core network services	• Security and key management system • Policy-based quality of service • OLSR-MC routing (or OSPF-MCDS) • TopoView network monitoring • OLSR-TV network monitoring • Topology emulation	• Scott Midkiff • Luiz DaSilva
b) Cross-layer approach to MD video routing	• OLSR routing (or OSPF-MCDS) • TopoView network monitoring • OLSR-TV network monitoring • Topology emulation	• Tom Hou • Scott Midkiff
c) Real-time middleware in an ad hoc network	• Real-time middleware • Security and key management system • Policy-based quality of service • OLSR-MC routing • TopoView network monitoring • OLSR-TV network monitoring • Topology emulation	• Scott Midkiff • Luiz DaSilva • Binoy Ravindran

4.3.3 Cooperative AWINN Elements

This test and demonstration required the inputs from AWINN tasks as listed in Table 4.3-2.

Table 4.3-2 Inputs from Cooperative AWINN Elements

Task (Subtask)	Inputs
2.1(a)	Prototype implementation of a policy-based QoS scheme
2.1(b)	Prototype implementation of MANET security and key management scheme
2.1(c)	Optimized prototype implementation of a MANET routing, specifically OSPF-MCDS-MC and/or OLSR-MC
2.1(f)	OLSR-TV; enhanced TopoView; enhanced topology emulation
2.1(d)	Video sensor application and test bed components
2.2	Real-time middleware

4.3.4 Cooperative Non-AWINN Elements

No non-AWINN components were required, except for tools and equipment carried over from the NAVCIITI project and use of the Naval Research Laboratory implementation of OLSR.

4.4 TIP#4 Integration of Close-in UWB wireless with ESM crane for Sea Basing applications

4.4.1 Overview

Task Objective: The goal of this task is to demonstrate the usefulness of UWB in close-in communications, ship-to-ship cargo transfer for sea-basing operations, and cargo transfer from ship-to-shore and vice versa.

Organization: This task is managed by Dr. A. H. Nayfeh.
Dr. A.H. Nayfeh, Faculty
N.A. Nayfeh, GRA

Summary:
Several experiments demonstrated the usefulness of UWB systems for ship-to-ship cargo transfer:

- Measured an up and down moving object on a shaker. For this purpose, two shakers in the Nonlinear Dynamics Laboratory were used: a shaker with a small stroke and another with a large stroke.
- Measured the orientation of a plate placed on top of a shaker whose head moves up and down.
- Measured the position of a point and the orientation of a plate on top of a shaker head that moves horizontally.
- Measured the position of a point and the orientation of a plate mounted on top of the Stuart platform in the Crane Control Laboratory. This platform has six degrees of freedom: heaving, pitching, rolling, surging, yawing, and swaying.
- Integrated the UWB with the Crane Control System and demonstrated the performance of the total system experimentally.

4.4.2 Accomplishments

Extensive coordination activities with the TIP#2 team positioned us to demonstrate the usefulness of UWB systems for ship-to-ship cargo transfer. The hardware for the demonstration was a 1/24 scale model of the Navy TASC crane. Scaling down of the antennas presents a major challenge, so we included a $1/10^{th}$ scale model of the container crane as a back up.

We worked with the TIP#2 team to determine the range and update rates that need to be provided by the UWB system for the soft-landing experiment. However, some of the range has to be sacrificed for the update rates due to hardware issues. Measurements taken by the UWB system were transferred to the soft-landing system via 8 bit parallel digital I/Os. The UWB periodically updates the outputs at a given rate, while the soft-landing system acquires the data when it needs it.

First tests of the soft-landing experiment with UWB sensors were successfully performed as a single-degree-of-freedom system with a large amplitude shaker as the target in Burruss 115 Fig. 4.4-1. The UWB radar system designed by the MPRG provided excellent ranging information with low noise or error. The UWB system was connected to the soft-landing routine and control system via a 8-bit parallel digital I/O interface. The ranging data was received from 0-255 mm at a sample rate of approximately 16 Hz. The system is approximately a 1:24 scale of a real crane-ship system.

The soft-landing system was demonstrated above a 900-lb shaker, which was excited sinusoidally with amplitudes ranging between 10-30 mm at 1 Hz. Scaling this excitation to a full-size ship gives a sinusoidal motion of approximately 0.25-0.75m at 0.2 Hz. This excitation is within the expected range of a ship at sea state 5.

Several runs of the experiment with the soft-landing system produced consistent impact velocities of less than 8 mm/s. While this value is hard to scale due to differences in motor and inertia, it is a promising value.

Simultaneously, we pursued the golden opportunity of fielding the VT controller on a full-scale container crane at the Jeddah Port in Saudi Arabia. Using the contact sensors, we were able to do 30 moves per hour (more than their skilled operators can do) WITHOUT the memory feature of the SSC controller. We used a container and picked it up from a truck and took it to the sea side to a specific location (55 m distance) and then brought it back on the truck. This operation repeated and we were able to home on the container very easily. We obtained positive responses from the operators.

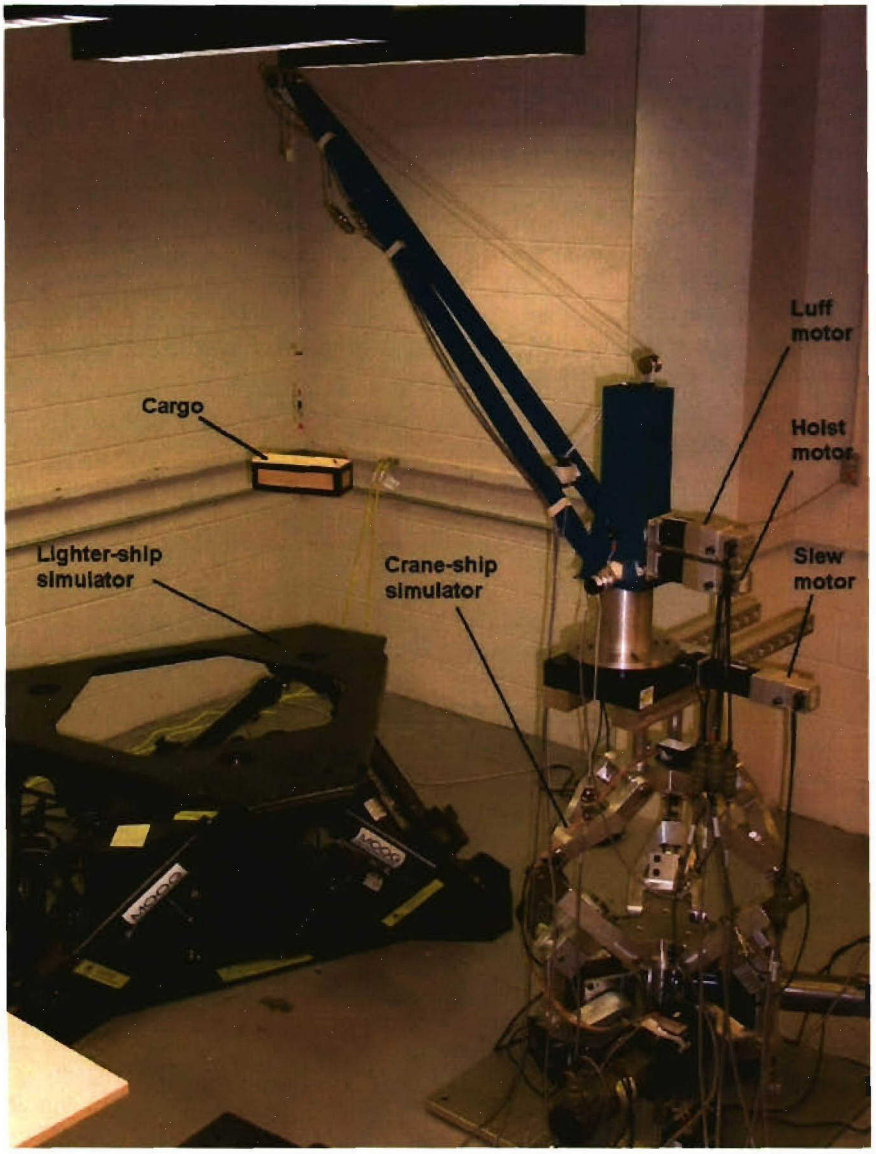

Figure 4.4-1 Experimental setup for demonstrating the full Crane Control System.

4.4.3 Importance/Relevance

The wave-induced motion of a crane ship can produce large pendulations of cargo being hoisted and cause the operations to be suspended. Our work has the potential of being very useful to the Navy's Transformational Sea-Basing System. The success of Sea Basing depends on the ability to sustain logistic operations with significantly reduced reliance on land bases. This requires the development of a high capacity, high reliability at-sea capability to transfer fuel, cargo, vehicle, and personnel in rough seas while underway from commercial container ships to large sea basing ships and then to smaller ships.

5. FINANCIAL REPORT